Observations and insights from a study

of RalGDS in cancer

A dissertation submitted by

Richard Wong

In partial fulfillment of the requirements for the degree of

Doctor of Philosophy

in

Biochemistry

TUFTS UNIVERSITY

Sackler School of Graduate Biomedical Sciences

ADVISOR: Larry A. Feig, Ph.D

Acknowledgements

With great love and respect I thank my family, mentors, and friends for helping me follow my love of science to its fullest.

Abstract

Ral exchange factors are transducers of Ras activation. These exchange factors target the small GTPases RalA and RalB. Four RalGEFs (RalGDS, Rgl 1, Rgl2/Rlf, and Rgl3) have been identified with the ability to bind Ras through a conserved Ras binding domain. Other Ral exchange (RalGPS1, RalGPS2, and Rgr) factors have also been identified which do not have RBDs and are thought to be activated by other signaling pathways

In this thesis we described three major findings that expand the knowledge and understanding of the Ral exchange factor RalGDS. Our studies began with the investigation of structural interactions within the protein. Without the benefit of crystal structure data it is sometimes difficult to glean the relevance of protein interactions and modifications we find in nature. Our characterization of RalGDS through binding assays allowed us to form an understanding about the nature of the N-terminal REM domain's role in regulating the catalytic activity of the Cdc25 domain of RalGDS. With our structural understanding we were able to propose a mechanism for previous and new observations.

Our second major study identified and characterized the c-Met mediated phosphorylation of RalGDS at four sites throughout the protein. This discovery marks the first confirmed and characterized tyrosine phosphorylation of a RalGEF. We will also present the first functional evidence of Ras effector uncoupling through direct phosphorylation of a Ras association domain.

In our final study we identify a novel interaction between 14-3-3σ and RalGDS in response to H_20_2 stimulation. The 14-3-3 family of proteins regulate a variety of cellular

processes and it is provocative that the two proteins have now been shown to directly interact with each other. The elucidation of the biological consequence of this interaction will likely offer interesting new insights into their combined functions both in normal and cancer biology.

Table of Contents

List of Figures

Chapter 1 : Overview

1.1 Ras Superfamily

The Ras superfamily of proteins stands at the foundation of signal transduction biology. These diverse groups of proteins have roles in aspects of cell biology from inception to death. In mammals the breadth of their influence traverses the spectrum of life functions, mediating the interplay of homeostasis all the way to the consolidation of a memory [1, 2]. In line with their importance in normal cell function these proteins have been found to be equally important in the abnormal biology associated with cancer. With over 150 members the Human Ras superfamily is divided into five families on the basis of their sequence and functional similarities. The Ras and Rho subfamilies mediate signal transduction events, the Rab and Arf subfamilies are involved in vesicular trafficking, and the Ran subfamily regulates nuclear to cytoplasmic transport and mitotic spindle organization [3, 4].

Common to the various subfamilies is the binding of guanine nucleotides as a means of modulating the proteins affinities to their effectors. In addition the proteins possess GTPase activity allowing them to hydrolyze bound GTP into GDP. In general the binding of GTP puts the protein into an active state and the binding of GDP an inactive state. The intrinsic GTPase activity allows the switching of an active GTP bound Ras like protein into an inactive GDP bound state. Regulatory proteins that are GTPase activating proteins (GAPs) can act on Ras superfamily proteins to increase their intrinsic GTPase activity and thus the rate at which they are deactivated[5, 6]. A second means of regulation come from guanine nucleotide exchange

factors (GEFs), proteins which destabilize Ras like protein binding to GDP. Once unbound, GDP is rapidly replaced by GTP which is usually at much higher concentration in the cell. Guanine nucleotide dissociation inhibitors (GDIs), which act to stabilize a GTPase in the inactive GDP bound state have also been identified for Rho and Rab subfamilies[4, 7].

1.2.1 Ras subfamily

H-Ras and K-Ras were initially identified by Harvey and Kirsten respectively, from tumor forming retrovirus in rats in the 1960s. Later work identified activated human versions of the proteins in cancer cell lines which sparked an intense study of Ras proteins. The Ras subfamily currently consists of 36 members such as N-Ras, R-Ras, E-Ras, RalA, RalB, Rap, and Rheb [8]. The subject of this thesis we will primarily focus around Ras, RalA, and RalB signaling.

Often associated to membranes, most Ras like proteins are lipidated at their carboxy terminus. The C-terminus contains a prenylation signal sequence of C-a-x-x (a = aliphatic, x = terminal amino acid). Ras proteins with this signal will usually become farnesylated at the Cysteine, exceptions to this are when x = L or F, which instructs geranylgeranylation. Or in the case of the RalA/B proteins which have a C-C-a-a signal sequence which results in geranylgeranylation. After lipidation the terminal three amino acids (a-x-x) are cleaved and the modified cysteine is methylated in the Endoplasmic Reticulum. Variations of the C-terminal lipidation can occur for other subfamily members such as KRas which has a polybasic region rather than palmitoylation site[9].

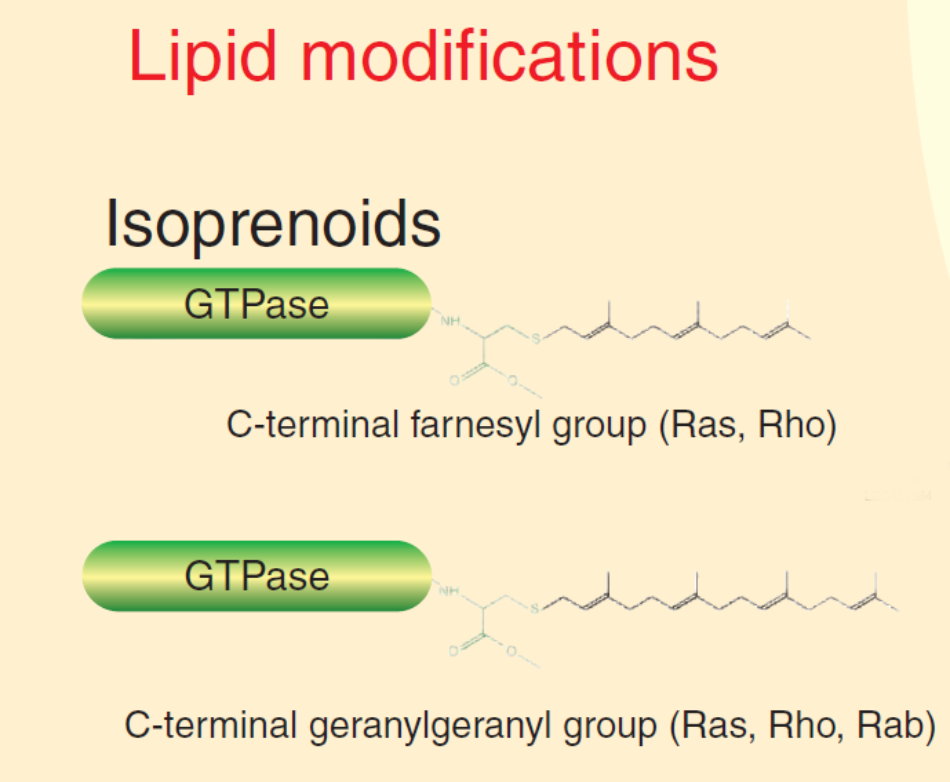

Fig 1.1 Lipid modification at C-terminus of Ras like proteins.

Further study of the structure of Ras proteins identified two specific domains involved in GTP/GDP binding. Termed the switch I (amino acid 30-38) and switch II (aa59-76) domains. The binding of GTP facilitates a conformation change with the switch II domain which creates the surface for effector interaction. GEF binding often acts on these switch domains to destabilize nucleotide binding[10].

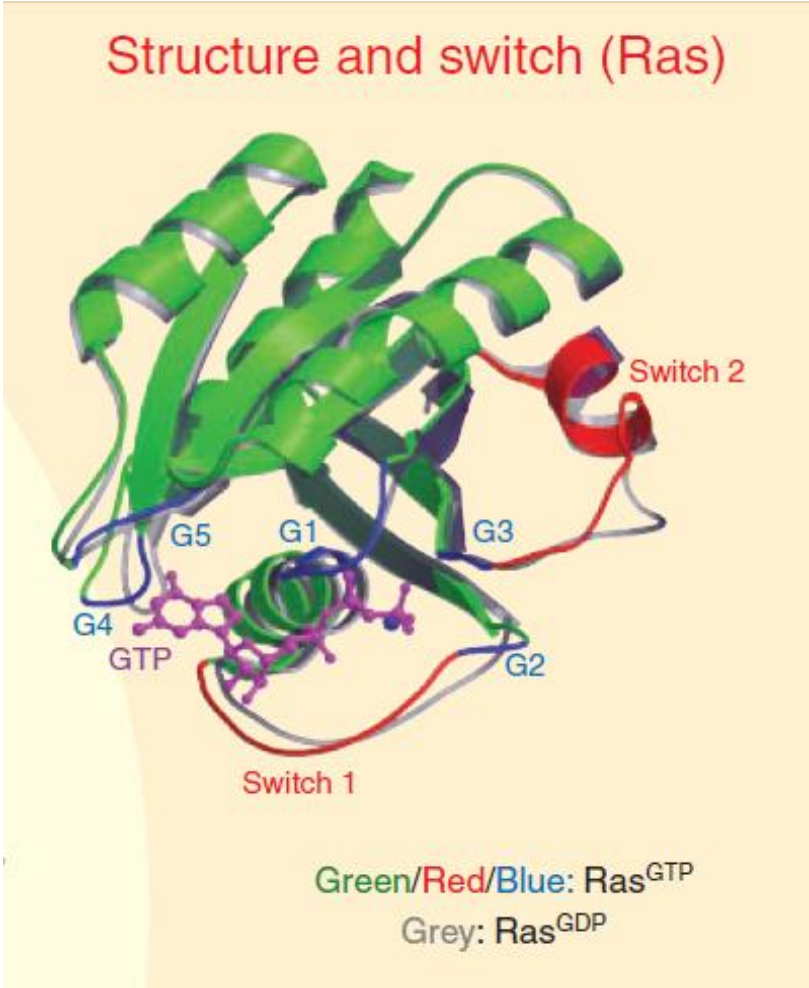

Fig 1.2 Structure of Ras in GTP bound state vs. GDP bound state.

1.2.2 Ras signaling

Initiation of a Ras signaling cascade can come from various upstream activation events. Under normal physiologic circumstances one example of this initiation can be mediated by ligand binding to receptor tyrosine kinases such as EGFR, Met receptor, or PDGFR. Upon ligand biding these receptors homo/hetero dimerize and phosphorylate cytoplasmic facing portions of the receptors. Depending on the sequence of the tyrosine phosphorylated sites they

become targets for SH2 domain containing proteins such as Shc or GrB2. Grb2 is primarily located in the cytoplasm pre-complexed with the Ras GEF Sos (Son of Sevenless). The creation of target SH2 binding sites on the plasma membrane localized tyrosine kinase receptors mediates the translocation of Grb2/Sos complexes to the plasma membrane. This brings Sos in proximity to membrane localized Ras proteins thereby facilitating their exchange of GDP and activation into a GTP bound state[11, 12].

Active Ras then itself becomes a nexus for the binding of effectors that transduce the activation of various biological functions. Three of most well studied effector arms of Ras activation are Raf, PI3K, and the Ral family exchange factors. Other effectors include Tiam-1 (Rac exchange factor), RIN1,2,3 (Rab5 exchange factor) , and Phospholipase C- epsilon to name a few[4, 8].

1.2.3 Ras in cancer

Activated Ras signaling is a key component in promoting tumorigenisis in a variety of cancers types. Mutations inactivating the intrinsic GTPase activity or association to GAP proteins have been identified in the three major Ras family members (H-Ras, K-Ras, and N-Ras). In a survey of malignancies K-Ras mutations were identified in 33% of lung and 44% of colon adenocarcinomas. N-Ras is mutated in 20-60% of analyzed myeloid disorders and H-Ras mutations were found (10-30%) in kidney and liver carcinoma [13]. In tumors that are not found to have specific Ras mutations there is often activation of signaling cascades upstream of Ras that function to activate Ras and its effectors. Examples of this can be found in lung cancers with

EGFR activating mutations, breast cancers with Her2 amplifications, and gastric cancers with c-Met amplifications to name a few [14-16].

With their key role in promoting tumorigenisis intense efforts have been made to develop pharmaceutical regulators of Ras proteins. To date most these efforts have been largely unsuccessful [3, 17-19]. Because of the roadblocks faced in the development of Ras specific inhibitors many studies turned to identify which of the many Ras effector pathways are important in cancer. Fruitful studies have characterized the role of various effectors and work is in progress to develop targeted inhibitors (Table 1.1).

Protein	Function	Substrate or target
Raf-1 A-Raf B-Raf	Serine/threonine kinase	MEK1 and MEK2 serine/tyrosine kinases
p110α p110β p110δ p110γ	Phosphoinositide 3-kinase	Phosphatidylinositol (4,5)-bisphosphate
RalGDS RGL RGL2 (also called Rlf) RGL3	Guanine-nucleotide-exchange factor	RalA and/or RalB small GTPases
Tiam1	Guanine-nucleotide-exchange factor	Rac small GTPase
AF-6	Adaptor	Profilin
RIN1 RIN2 RIN3	Guanine-nucleotide-exchange factor	Rab5 small GTPase
NORE1 (also called RASSF5) RASSF1 RASSF2 FASSF4	Adaptor	MST1 serine/threonine kinase
PLCε	Lipase Guanine-nucleotide-exchange factor	Phosphatidylinositol (4,5)-bisphosphate Rap small GTPase
IMP	E3 ubiquitin ligase	Kinase suppressor of Ras
p120 Ras GAP NF1 GAP	Ras GTPase-activating protein	Ras, R-Ras isoforms

Table 1.1 Summary table of Ras effectors [20]

1.3 Raf effector pathway

The Raf family of kinases in mammals consist of A-Raf, B-Raf, and c-Raf. When Ras is in its GTP bound state it recruits the binding of Raf family members through interaction with their Ras binding domains (RBD) and cysteine rich zinc binding domains. The localization to the plasma membrane is essential for the activation of Raf kinases which is achieved in part through tyrosine phosphorylation of the kinase. Once activated Raf then phosphorylates MEK1/2 (MAPK/Erk Kinase), a dual specificity tyrosine/threonine kinase. MEK1/2 in turn phosphorylates a tyrosine and threonine on the TEY motif in the activation loop of ERK1/2 (Erk kinase). ERK1/2 are serine/threonine kinases with various substrates in the cytoplasm and nucleus which effect a wide range of biological activities. Examples of which include transcription factors such as c-myc which regulates cell cycle progression, other kinases such as RSK1 which can regulate mTOR activity, cell cycle regulation with the induction of Cyclin D accumulation, and regulators such as RNA pol I upstream binding factor which is important for facilitating ribosomal RNA production[21, 22].

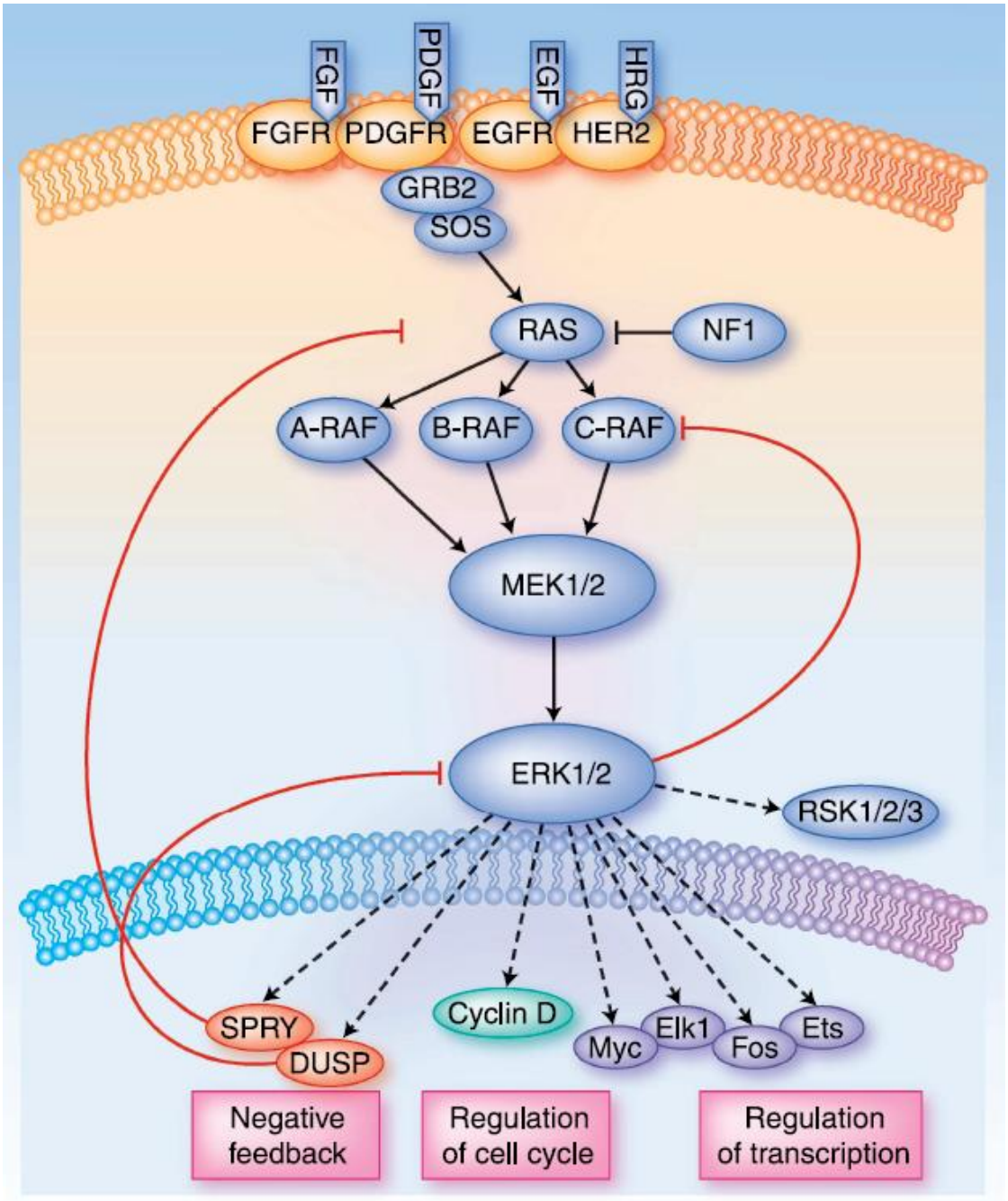

Fig 1.3 Raf effector pathway

1.4 PI3K effector pathway

Phosphoinositide kinases (PI3K) are involved in transducing signals involved in mitogenic upregulation, cell survival, and vesicular trafficking to name a few. PI3K is made up of p85 regulator subunit and a p110 catalytic subunit[23]. The multi subunit kinase complex of class 1A and 1B PI3Ks have the ability to bind active Ras thereby localizing it to the plasma membrane. There it is brought into proximity with its substrate phosphatidylinositol-4,5-bisphosphate (PIP2) to generate phosphatidylinositol-3,4,5-trisphosphate (PIP3). PIP3 is the binding target of Pleckstrin homology domains within the kinases PDK1 and its substrate AKT. The co-localization of the two kinases propagates PI3K signaling through PDK1 activation of AKT. AKT activation initiates a cascade of pro survival (FOXO1,3a,4 and BAD inactivation) , pro growth (upregulation of mTORC1 via inhibition of TSC2), and proliferation signaling (inhibition of p27, p21 , and FOXO transcription factors) [23, 24].

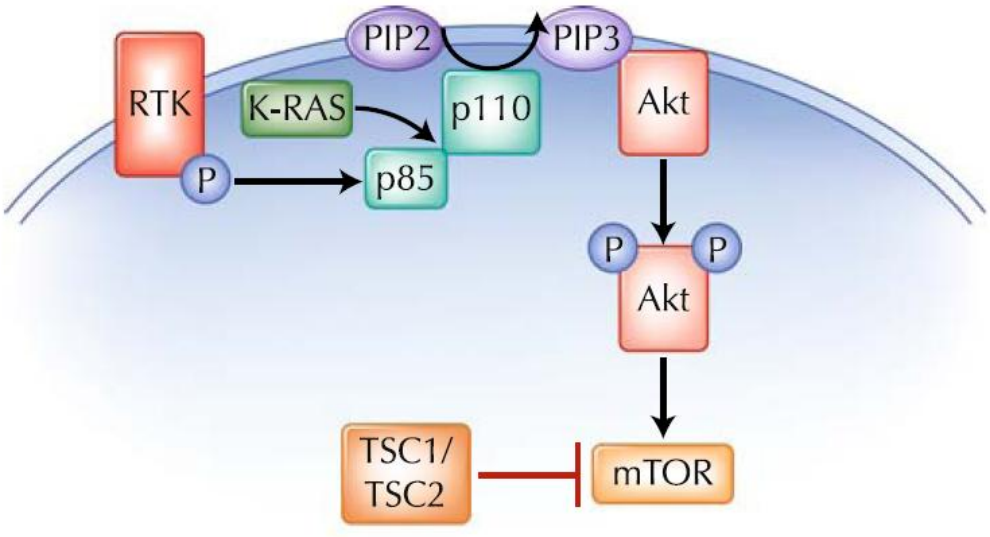

Fig 1.4 PI3K effector pathway [23]

1.5.1 Ral exchange factors

Ral exchange factors represent the transducers of the third major Ras effector pathway. These exchange factors target the small GTPases RalA and RalB. Four RalGEFs (RalGDS, Rgl 1, Rgl2/Rlf, and Rgl3) have been identified with the ability to bind Ras through a conserved Ras binding domain. Other Ral exchange (RalGPS1, RalGPS2, and Rgr) factors have also been identified which do not have RBDs and are thought to be activated by other signaling pathways [25, 26].

1.5.2 RalGDS structure

The RalGEFs downstream of Ras all share a common structural layout and have a high degree of homology. The proteins begin with an N-terminal Ras Exchange Motif (REM). REM domains are found in a variety of Ras subfamily GEFs. In the RasGEF Sos1 the REM domain has been shown to regulate the catalytic activity of the exchange factor. Studies presented in this thesis will characterize in detail how the REM domain of RalGDS regulates its catalytic activity. Centrally located in RalGEFs is a Cdc25 homology domain. This domain is the catalytic core of the protein and directly facilitates Ral exchange activity. The Cdc25 domain contains a catalytic helical hairpin which binds to the Switch domains in the target Ral proteins to displace GDP. Studies of Cdc25 domains of the exchange factors Sos1, Epac2, and RalGPS1 have shown that the orientation of the catalytic hairpin with respects to the rest of the Cdc25 domain regulates the ability of the domain to bind to its target GTPase [27]. The C-terminus of RalGEFs contains the Ras binding domain. As the name suggests this region of the protein mediates binding to the

Switch domain of active Ras proteins. A crystal structure has been published for RalGDS RBD bound to Ras and will be discussed in Chapter 2 of this thesis.

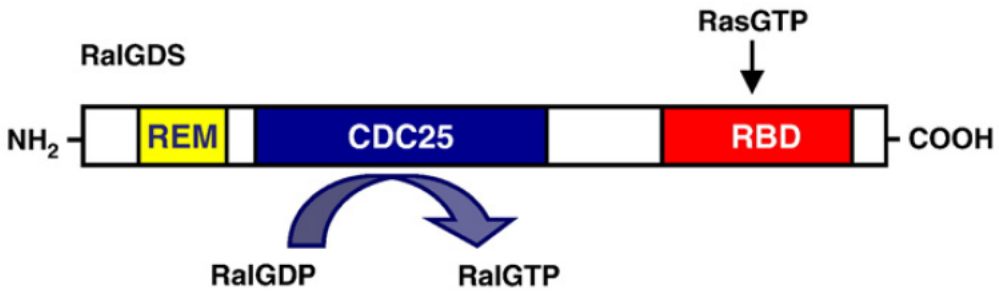

Fig 1.5 RalGDS structure

1.5.3 RalGDS regulation

RalGDS activation is regulated by various intrinsic and extrinsic mechanisms. The canonical mechanism of activation is through spatial localization to its substrate Ral proteins. Active Ras presents a high affinity binding site for the RBD of RalGDS. Binding to Ras functions to co-localize RalGDS to membrane where Ral proteins are found thereby facilitating their interaction. Localization can also serve to negatively regulate RalGDS as shown in studies of RalGDS interaction with beta arrestin [29]. In these studies RalGDS formed a complex with beta arrestin in the cytoplasm restricting it from Ral proteins at the membrane. fMLP (formylated tripeptide) receptor binding stimulates the release of RalGDS from beta arrestin allowing its localization to the membrane to then activate Ral. ERM (ezrin, radixin and moesin) like protein Merlin has also been shown to negatively regulate RalGDS mediated Ral activation.

Merlin was shown to bind RalGDS in the cytoplasm presumably preventing its localization to the plasma membrane although the mechanism of this action is currently unknown [30].

RalGDS intrinsic regulation had been heavily studied both in our lab and others. Previous work done in our lab found the N-terminal REM domain negatively regulated the exchange activity of the protein. Truncation of this domain led to an increase in exchange activity when compared to wildtype protein. Binding of PDK1 to the N-terminus of RalGDS was also found to relieve the inhibition of the REM domain in a non phosphorylation dependent manner. Our lab also found PKC phosphorylation to a site in the N-terminus down regulated the exchange activity of RalGDS, possibly through modifying the interaction of the REM domain with the Cdc25 domain [31, 32]. Other groups have found RalGDS could interact with calmodulin during thrombin-induced exocytosis of Weibel-Palade bodies. Calmodulin was found to bind to an IQ-like binding site located upstream of the REM domain and this interaction was shown to increase Ral activation cells [33]. Groups studying the RalGEF Rgl2 found PKA was able to phosphorylate the protein possibly to a site within its Ras binding domain. This theoretically could affect the Ras binding ability of Rgl2 although functional studies were unable to confirm this in the full length protein [34].

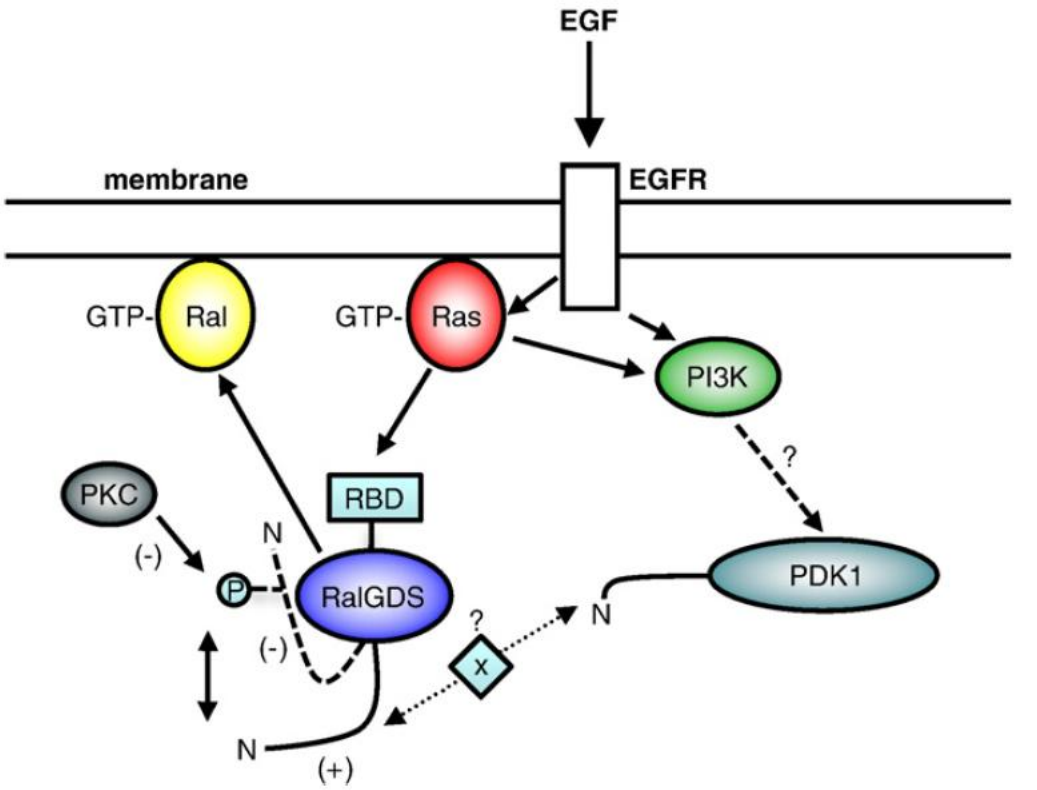

Figure 1.6 Modes of RalGDS regulation

1.5.4 Ral independent RalGDS interactions

Recent studies done in our lab have identified a completely Ral independent role for RalGDS. It was discovered that RalGDS was able to facilitate EGF and insulin mediated activation of Akt. MCF10A breast cells with RalGDS knockdown showed diminished Akt phosphorylation in response to EGF or insulin stimulation. Previous studies have shown that RalGDS is able to bind PDK1, the kinase responsible for Akt activation. New work showed

RalGDS was also able to bind the scaffolding protein Jip1. Jip1 was found to also bind Akt and the complex was found to localize to PDK1 through RalGDS [35].

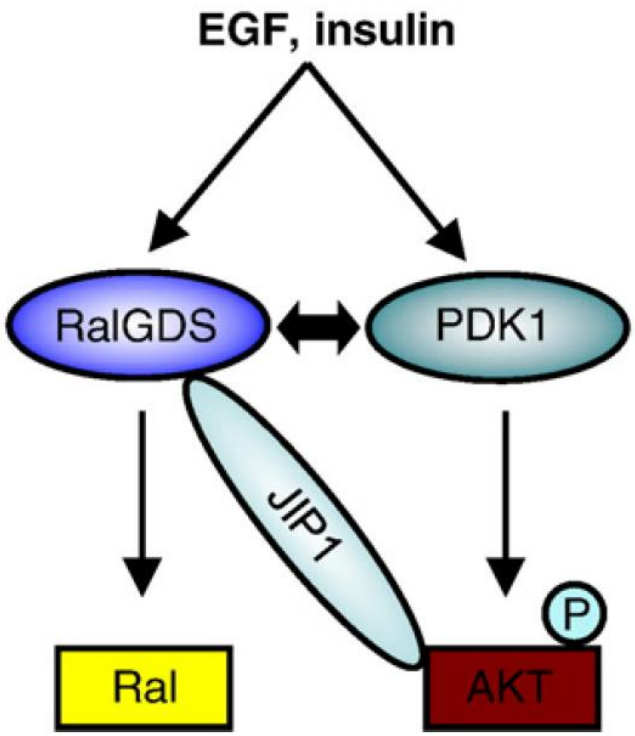

Figure 1.7 RalGDS scaffolding of Akt to PDK1 through Jip1

1.5.5 RalGDS in cancer

There is ever growing evidence of the importance of RalGEFs in cancer progression. Experiments with RalGDS knockout mice impaired tumor formation of Ras driven skin carcinomas from DMBA/TPA treatment [36]. Cells derived from these knockout mice were found to have diminished JNK signaling, suggesting that they were anti-apoptotic. This findings corroborated earlier studies showing Ral regulation of JNK [37] . Other studies using effector

selective mutant H-Ras12V showed that the RalGDS effector pathway, mediated bone specific metastasis of DU145 prostate cancer cells [38]. A study that sequenced the genomes of various human breast cancer samples identified mutations in the REM domain (Y209S) and RBD (V734M) of RalGEF family member Rgl1 [39]. The biology of these mutations will be discussed in Chapter 2.

Although there are many studies highlighting the specific role of Ral proteins in cancer biology there is also growing evidence of the importance of the RalGEF itself. A study of mutant K-Ras driven pancreatic ductal adenocarcinoma (PDAC) cells found Rgl2 to be elevated and important in promoting soft agar growth. When Rgl2 was knocked down soft agar growth could not be rescued by the overexpression of active Ral proteins, suggesting a role for the exchange factor outside Ral activation [40].

1.6 Ral GAPs

Recent identification of the first RalGAPs has opened new avenues of investigation into the biology of Ral regulation. Named RalGAP1 and RalGAP2 they are a large heterodimeric complex, each consisting of a catalytic α1 or α2 subunit and a common β subunit. The RalGAP complex shares structural and catalytic similarities with the tuberous sclerosis tumor suppressor complex [41]. A second RalGAP dimer (RGC1, RGC2) has also been recently identified with 83% homology to RalGAP1 and RalGAP2. It was found that Akt2 mediated phosphorylation of this complex was able to negatively regulate its GAP activity in insulin stimulated adipocytes [42].

1.7.1 Ral GTPase

RalA and RalB are small Ras like GTPases that are regulated by the RalGEFs and RalGAPs discussed in earlier sections. Like Ras these proteins have a defined set of effectors that bind to the GTP bound active state. RalA and RalB share 82% sequence homology with a highly conserved GNP binding and hydrolysis site.[43]. Unlike Ras proteins that are farnesylated, Ral proteins are prenylated by geranylgeranyl- transferases at their *CAAX* motif for the addition of a geranylgeranyl lipid structure [44].

Despite their high degree of homology the Ral proteins have structural variations that mediate their functional differences. RalA and RalB are the most different in their C-terminal hypervariable tails. This region is responsible for the determination of membrane association and therefore subcellular location [44, 45]. In studies done in our lab immunofluorescence staining of MDCK cells revealed that RalA accumulated in the plasma membrane and the perinuclear recycling endosomes, while RalB was found in punctuate foci throughout the cytoplasm. Activating mutations of both RalA and RalB enhanced their respective accumulation in the membrane. Exchanging the C-terminal domains between RalA and RalB failed switch their localization or secretory/membrane delivery functions. This suggested that both effector binding and localization is critical for normal Ral GTPase function [45].

The Ral proteins are important in a variety of cellular functions. In regulating mitotic progression, RalA is required to tether the exocyst to the cytokinetic furrow in early cytokinesis. RalB is then required for recruitment of the exocyst to the midbody of this bridge to drive abscission and completion of cytokinesis [46]. In studies of laminin induced neurite branching of rat sympathetic neurons, Ral A was found to be important in promoting branching through

interactions with its effector the exocyst complex. Ral B was found to promote branching through the interaction with Phospholipase D [47].

The Ral proteins are important in the process of phagocytosis. Studies in murine macrophages found RalA knockdown negatively affected FcgammaR-mediated phagocytosis. RalA was found to promote phagocytosis through its interactions with phospholipase D. RalB knockdown on the other hand was shown to increase phagocytosis through an unidentified mechanism [48]. In the study of macroautophagy, RalB was found to localize to nascent autophagosomes and is activated during nutrient deprivation. RalB and its effector Exo84 were found to be necessary for nutrient starvation-induced autophagocytosis and directly engaged autophagocytosis. RalB activation alone was also sufficient to promote autophagosome formation [49].

In cellular migrations assays, normal rat kidney (NRK) cells knocked down for RalB showed a decrease in the ability to close scratch wounds. Migration was also decreased in Boyden Chamber assays towards a chemoattractant. RalA knockdown of wildtype cells showed no change, but when Ral A was knocked down in the RalB knockdown cells normal migration was restored [50].

1.7.2 Ral GTPases in cancer

RalA and RalB, sometimes serving seemingly opposing roles, have been shown to be important in numerous aspects of cancer biology. Studies in T-antigen and telomerase expressing rat kidney cells found that a constitutively active RalGEF (Rlf-CAAX) as well as

activated RalA, but not RalB, was sufficient to replace Ras in promoting anchorage independent growth. In the same study knockdown of RalA by shRNA in the HT-1080, J82 and SW-620 cancer cell lines inhibited their ability to form tumors in the flanks of immunocompromised mice [51].

Attempts to knockdown RalB in HeLa, MCF-7, and SW480 cancer cell lines were found to result in cell death. Knockdown of RalA in these same cells was not found to affect their viability. When investigators knocked down RalA and then RalB, cell did not die as they did in the RalB single knockdown. The RalB mediated survival effects were later found to be mediated by its effector the exocyst and its interaction with the innate immune response protein TBK1 [52-54].

In a study using a panel of 10 human pancreatic cell lines it was observed that RalA knockdown inhibited the ability of these cells to grow in soft agar and form tumors in mice. RalB knockdown had no effect in these assays. When the knockdown cells were tested in Matrigel invasion assays RalA and RalB knockdown had an effect in decreasing invasion. When the cells were tested in tail vein injection metastasis assays both RalA and RalB were found to have decreased metastasis. Double knockdown cells had an even greater effect in preventing metastasis. These results suggest to investigators that RalA was important in tumor cell initiation and RalB was important in invasion and metastasis [55].

In recent studies done in our lab the role of RalA in both the tumor and stroma highlighted new and expected roles for the protein. Using oncogenic H-Ras driven keratinocytes and human foreskin fibroblasts, we generated a 3 dimensional skin model for squamous cell carcinoma. In this model we could assay the invasiveness of the transformed keratinocytes into a stromal layer created by the fibroblasts. In contrast to other studies that found RalA promoted

tumor progression, researchers found RalA was preventing invasiveness. RalA knockdown in the keratinocytes resulted in an increase in the invasive potential of those cells. The mechanism of this action was shown to be through the regulation of E-cadherin recycling to the membrane mediated by the RalA effector Exo84 [56].

When studying the stromal layer made from the human fibroblasts, knockdown of RalA was shown to decrease the invasive ability of the transformed keratinocytes. Knockdown of RalB in the stromal cells did not have any effect on invasiveness in these studies. It was found that RalA mediated secretion of the c-Met receptor ligand HGF was important in driving keratinocyte invasiveness. The secretion was likely mediated through the RalA effectors Sec5/Exo84 as knockdown of these proteins mimicked the effect of RalA knockdown [57].

1.8. Ral effectors

RalA and RalB mediate the diverse range of their activities through binding of a set of four known effectors RalBP-1, the Exocyst, PLD, and ZONAB.

1.8.1 RalBP-1

RalBP-1 (also called RLIP76) was the first Ral effector to be identified. The protein contains a Ral binding domain, a CDC42 GAP domain, and a Reps binding domain [58, 59]. RalBP-1 GAP activity has been demonstrated against Rac and CDC42 *in vitro* and CDC42 GAP function was found in *Xenopus* embryos as a regulator of actin cytoskeleton stability during gastrulation [60].

Studies done in our lab found RalBP-1 bound Reps-1. This protein was phosphorylated in response to EGF stimulation and had the ability to bind Crk or Grb2 through their SH3 domains [61]. Further studies found Reps-1 could bind Rab11-FIP2 to mediate EGF receptor specific internalization [62].

RalBP-1 has also been linked to the extrinsic death pathway though its suppression of FLIPs protein. Knockdown of RalBP-1 caused an increase in FLIPs proteins levels and a decrease in TRAIL sensitivity in human astrocytes. Over expression of RalBP-1 cause the opposite to occur with an increase in TRAIL sensitivity and decrease in FLIPs proteins levels. RalBP-1 served as a RalA effector in these studies, with RalA activation and supression mediating similar affects[63].

1.8.2 Exocyst

The exocyst, also known as the Sec6/8 complex, is a Ral-regulated, evolutionarily-conserved octameric protein complex containing Sec3, Sec5, Sec6, Sec8, Sec10, Sec15, Exo70 and Exo84. It functions to tether protein-containing secretory vesicles during transport from the trans-Golgi network to the basolateral plasma membrane in epithelial cells [64]. Of the many subunits in the exocyst complex Ral proteins have been shown to bind Sec5 and Exo84.

Studies done in our lab found that RalA mediated E-cadherin delivery to the basolateral membrane of MDCK cells through binding of the Sec5 and Exo85. A mutant protein unable to bind these effectors lost the ability to traffic E-cadherin. RalB was found to not to have an effect on E-cadherin delivery. This result was due to a diminished ability of RalB in binding the exocyst components. Even though the Ral family members have identical effector binding

Switch domains it was found that differences in the proximal hypervariable C-terminus had an effect on exocyst binding preference under conditions of secretion [65]. The role of RalB in migration has been shown to be mediated in part by the Sec5 exocyst protein. Scratch wound assays found RalB bound Sec5 and localized the exocyst complex to the leading edge of migrating cells. RalA was not found to be involved in this process [66].

1.8.2 ZONAB

ZONAB (ZO-1 interacting Y-box transcription factor) interacts with RalA. In MDCK cells it has been observed that RalA-ZONAB complex increases as epithelial cells become more dense and increase cell contacts [67]. In reporter assays, ZONAB was also found to functionally interact in the regulation of the ErbB-2 promoter in a cell density-dependent manner. Paracellular permeability in MDCK cells could also be regulated by ZONAB [68]. Overexpression of ZONAB in retinal pigment epithelium was found to cause the cells to undergo epithelial-mesenchymal transition and increase their proliferiatve capacity. These observations suggest that some aspect of Ral activation may be able to drive EMT through ZONAB [69].

1.8.4 PLD

Phospholipase D is found in two isoforms (PLD1 and PLD2) and can bind to both RalA and RalB. PLD activity is facilitated by the recruitment of the small GTPase Arf6 and Ral proteins in a complex with PLD. PLD at the plasma membrane hydrolyzes phosphatidylcholine to produce choline and phosphatidic acid; a downstream byproduct of phosphatidic acid is

diacylglycerol, a robust protein kinase C (PKC) activator [70]. PLD1 is predominantly localized under steady-state conditions at the Golgi complex, endosomes, lysosomes, and secretory granules, whereas PLD2 is found at the plasma membrane, suggesting different cell biological roles for the PLDs [71].

Elevated phospholipase D activity and a driver mutation in PLD2 have been reported in malignant breast cancer biopsy samples. PLD expression levels also correlate with tumor size and survival in progression of colorectal carcinoma, and increased expression of PLD2 is found in gastric carcinoma and renal cancer [71, 72]. PLD activity may also play an important role in cell motility and migration, a critical step in the spread of cancer. Increased PLD activity enhances the ability of MDA-MB-231 human breast cancer cells to migrate and invade matrigel [71, 73].

1.9 Met

Met tyrosine kinase receptor (also known as the HGF receptor) promotes tissue remodelling, which underlies developmental morphogenesis, wound repair, organ homeostasis and cancer metastasis. The promiscuous docking motif in the C-terminal tail of Met binds numerous SH2 domain containing effectors, such as PI3K, the non-receptor tyrosine kinase Src, the growth factor receptor-bound protein 2 (GRB2), and SH2 domain-containing transforming protein (SHC) adaptors, SHP2, phospholipase Cγ1 (PLCγ1) and the transcription factor STAT3. MET also associates with GRB2-associated-binding protein 1 (GAB1), a multi-adaptor protein that, upon phosphorylation by the Met receptor, provides extra binding sites for SHC, PI3K, SHP2, CRK, PLCγ1 and p120 [74]. Depending on the cellular context Met is known to regulate multiple signaling pathways, a summary of which are listed in Fig 1.9.

With this myriad of possible binding partners Met receptor activation in response to hypoxia and inflammatory cytokines or pro-angiogenic factors has been shown to aggravate the intrinsic malignant properties of already transformed cells by conveying proliferative, anti-apoptotic and pro-migratory signals [74, 75]. Amplification or upregulation of Met has been identified in a variety of cancer cell types, including breast, lung, head/neck, and gastric [76-78] .

Studies described in Chapter 3 will characterize RalGDS as a novel downstream target of Met activation in oncogene addicted gastric cancer cells, and suggest its possible role in antagonizing Met driven cancers.

52

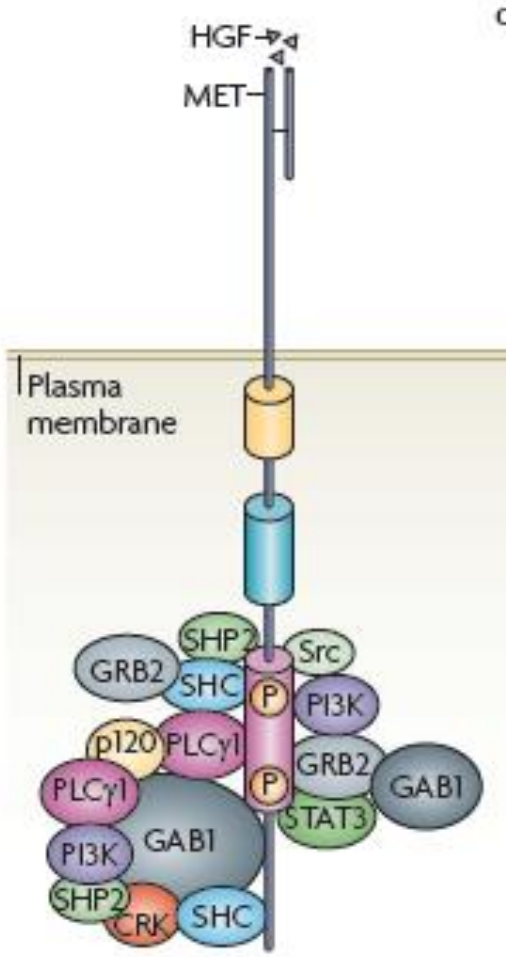

Figure 1.8 Met docking motif binding partners [74]

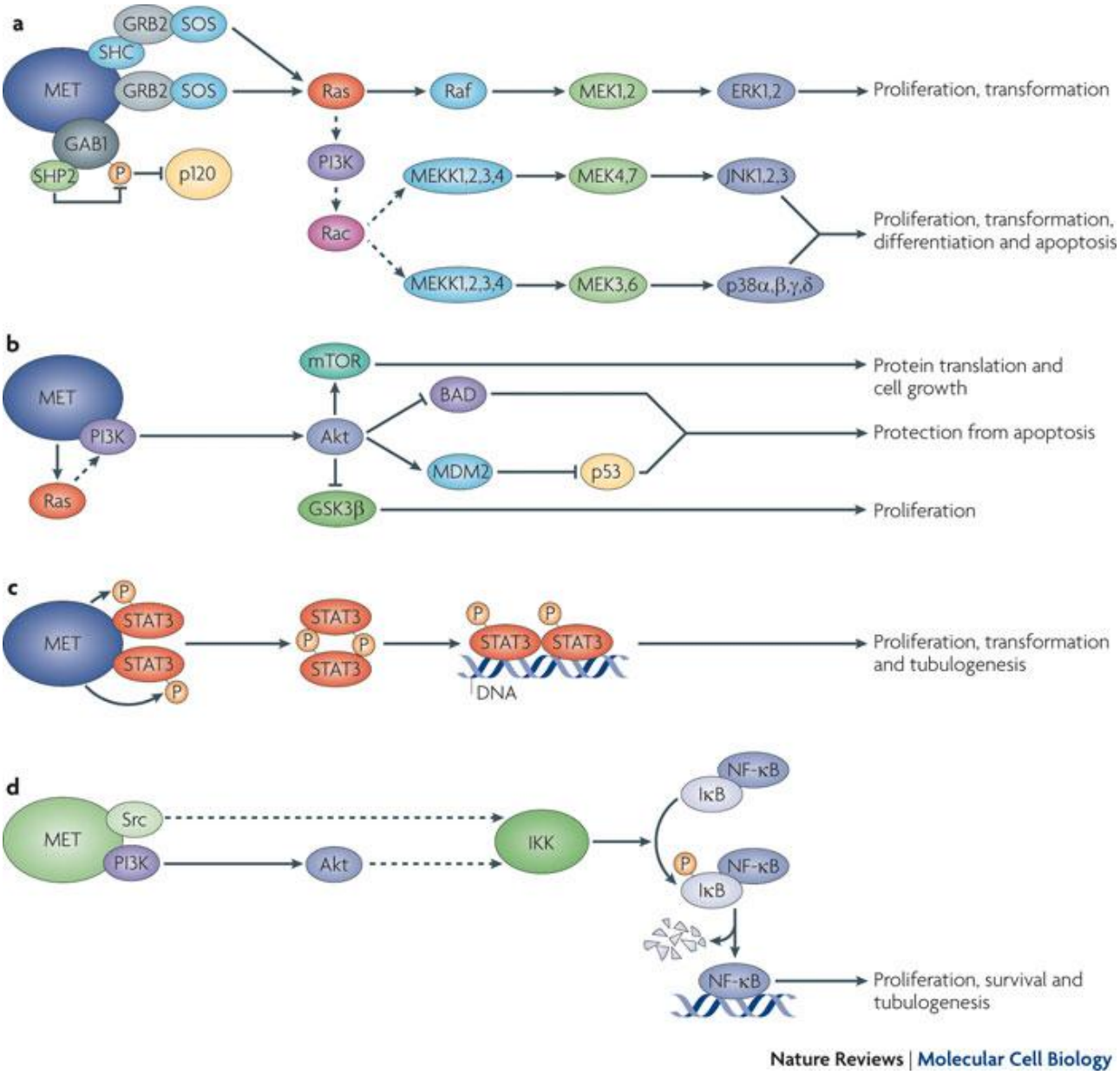

Figure 1.9 Met regulated signaling pathways [74]

Chapter 2 : Insights into the intramolecular auto inhibition of RalGDS

2.1 Introduction

The importance of Ras family GTPases in cancer biology is without question. K-Ras mutations have been associated with 33% of lung, 80% pancreas, and 44% of colon adenocarcinomas, N-Ras with myeloid cancers, and H-Ras with Kidney and liver carcinomas [13, 79-81]. Intense efforts have been made to develop pharmaceutical regulators of these molecules. To date these efforts have been largely unsuccessful. Unlike with the success of ATP analogue inhibitors of protein kinases, which can act at nanomolar affinities against micromolar affinities to ATP, the picomolar affinities of small GTPases in the presence of millimolar concentrations of GTP make the same strategy unlikely to succeed [3, 17-19]. Moreover, an ideal Ras inhibitor would restore the defective GTPase activity of the mutant forms found in tumors. The disruption of membrane targeting of the GTPases through inhibition of key lipidation steps has also hit roadblocks in specifically inhibiting Ras, partially because gernanyl-geranylation of some Ras proteins can compensate for defective farnysylation [82, 83] .

With the problems inhibiting the GTPases themselves it becomes necessary to look at other targets of regulation such as the downstream effectors of Ras. One class of Ras effectors are exchange factors for Ral GTPases. To this end greater understanding needs to be achieved about specific GEF structure and biology. In this chapter we will present data on aspects of intramolecular interactions of the RalGEF RalGDS which give insight into the regulation of its catalytic activity.

Many Ras superfamily GEFs have a common theme of intramolecular inhibition of catalytic activity that can be relieved by various binding or phosphorylation events. The Ras GEF Sos is a prime example of this. With the benefit of crystal structure data investigators were able to show that the Sos Cdc25 catalytic domain is positively regulated by binding of RasGTP to a distant allosteric site. It was shown that an upstream REM domain was associated with the Cdc25 domain and that binding of RasGTP to a linker region between the two domains increased catalytic activity possibly through stabilization of the catalytic domain in an active conformation. When RasGTP was not bound to the allosteric site the REM domain inhibited exchange activity by holding the catalytic domain in an inactive orientation [84, 84-86]. There are many other examples of GEFs with intramolecular inhibition systems. The Rap GEF EPAC has a cAMP binding domain that blocks the catalytic domain until it is relieved b[87]

y cAMP binding. In the Rho GEF Kalirin an upstream SH3 domain inhibits the catalytic DH domain via an intramolecular association until it is relieved by binding of other SH3 containing proteins to the internal ligand site [87]. Tim, yet another RhoGEF has a short upstream helical motif that blocks the catalytic site until the helix becomes phosphorylated by Src [88]. In various GEF studies it has been noted that truncating residues upstream of the Cdc25 catalytic domain often results in increased catalytic activity [3].

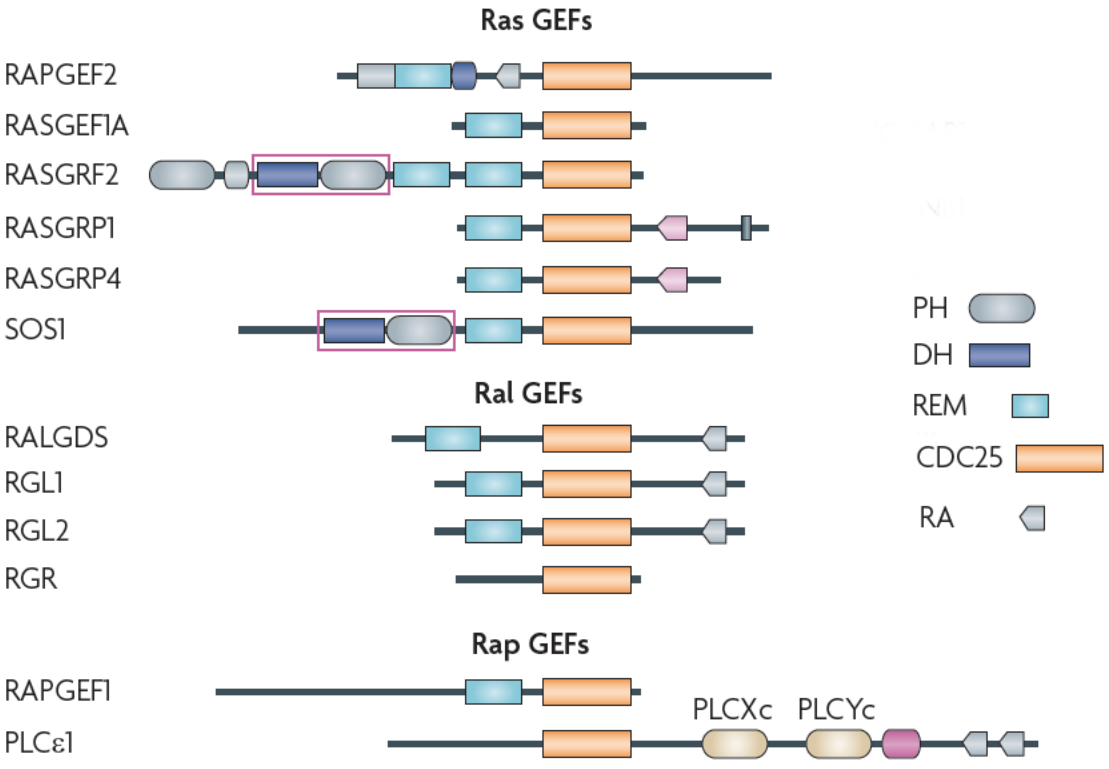

Fig 2.1 Predicted domains of various Ras subfamily exchange factors [3]

Previously studies in our lab showed that truncating the REM domain containing N-terminal 300 amino acids of RalGDS increased exchange activity. Further work showed that binding of PDK1 to this 300aa region also increased exchange activity in a manner not dependent on PDK1's kinase activity, consistent with the idea that binding relieved the inhibitory activity of the N-terminus [89].

To date there is a solved crystal structure for the Ras binding domain of RalGDS bound to Ras [90]. Findings in Chapter 3 will take advantage of this information to give insights into the

biology of the RalGDS : Ras interaction. With no crystal structure for the remainder of the protein we took advantage of the ability of the isolated N-terminus to bind the catalytic domain of RalGDS to devise assays to elucidate the nature their interaction.

2.2 Results

2.2.1 The N-terminal REM domain of RalGDS associates with the Cdc25 domain.

In the hopes of identifying regulators of RalGDS that bind to the N-terminus, a yeast two hybrid assay was performed using the first 300aa as bait. Sequence analysis of hits from the screen showed that the N-terminus could bind three RalGDS fragments. Common to the three hits was the region containing the Cdc25 catalytic domain. Other domains such as the N-terminal REM and C-terminal Ras Binding Domain could be lost and binding was still preserved (Fig 2.2). These results suggested to us that the N-terminal region may be forming an association with elements of the Cdc25 catalytic domain *in vivo*.

To confirm an *in vivo* interaction, we made an HA tagged expression construct of the 300aa fragment (HA-1-300aaGDS) used as bait for the screen. Next we made a Myc tagged construct consisting of an N-terminal truncation of RalGDS similar to the sequence of Hit 1 from the yeast screen (301aa-852aa, Myc-301-852aa-GDS). When Cos-7 cells were co-transfected with both constructs we found that HA-1-300aaGDS was able to form an *in vivo* association with Myc-301-852aa-GDS (Fig 2.3). This confirmed to us the yeast two hybrid results and suggested that in the context of the full length protein an intramolecular interaction may be occurring.

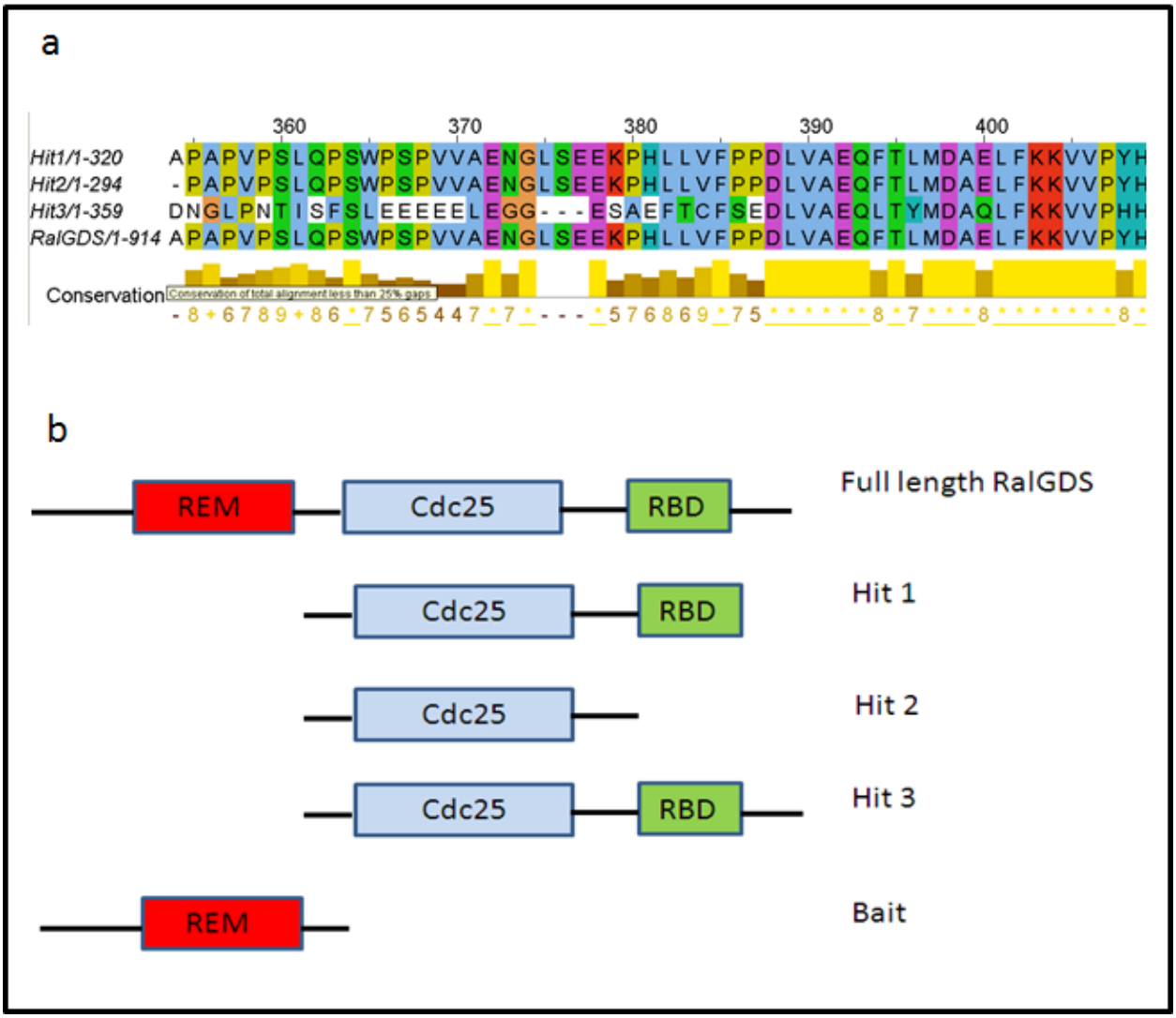

Fig 2.2 Yeast Two Hybrid screen identifies RalGDS as binding partners to REM domain.

The N-terminal 300aa of RalGDS was used as bait in a yeast two hybrid screen looking for binding partners to this domain. Of the six hits that resulted from the screen four were identified as fragments of RalGDS [Hit 1 and Hit 2 (identified twice)] or the RalGDS family member Rgl1 (Hit 3). a) Sequence of Yeast two hybrid hits aligned to RalGDS. b) Schematic of RalGDS region represented by each Hit.

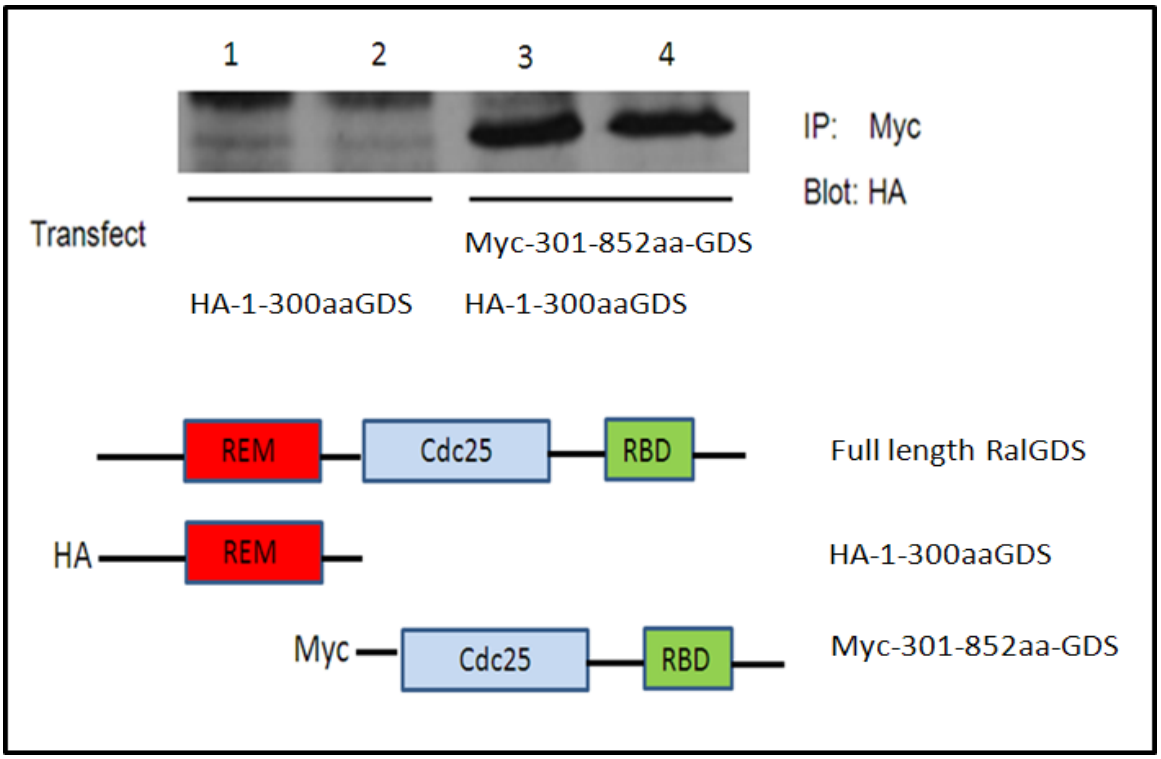

Fig 2.3 N-terminal 300aa of RalGDS forms an association with Myc-301-852aa-GDS.

An HA tagged expression construct of the 300aa used as bait for the yeast two hybrid screen (HA-1-300aaGDS) was transfected into Cos7 cells alone or with a Myc-301-852aa-GDS construct containing the region of RalGDS shown in the diagram above. Transfected cells were lysed and immunoprecipitatied with Myc antibody. Cells transfected with HA-1-300aaGDS alone did not show any co-immunoprecipitation of the HA construct with Myc antibody pull down (Lane 1+2). Cells transfected with both constructs showed that HA-1-300aaGDS co-immunoprecipitated with Myc-301-852aa-GDS when cell lysate was subject to Myc antibody pull down (Lane 3+4). .

Having confirmed an *in vivo* interaction we next wanted to narrow down the minimal region of the N-terminal sequence needed for association. To accomplish this four truncation constructs were made of HA-1-300aaGDS (Fig 2.4) and each was tested to see if they were still able to maintain an association with Myc-301-852aa-GDS. The only fragment that lost the ability to bind to Myc-301-852aa-GDS was one in which the first 50aa of the REM domain were

deleted (Fig 2.5). This showed us that the first half of the REM domain is essential for the intra-molecular association we believe is occurring within the full length protein.

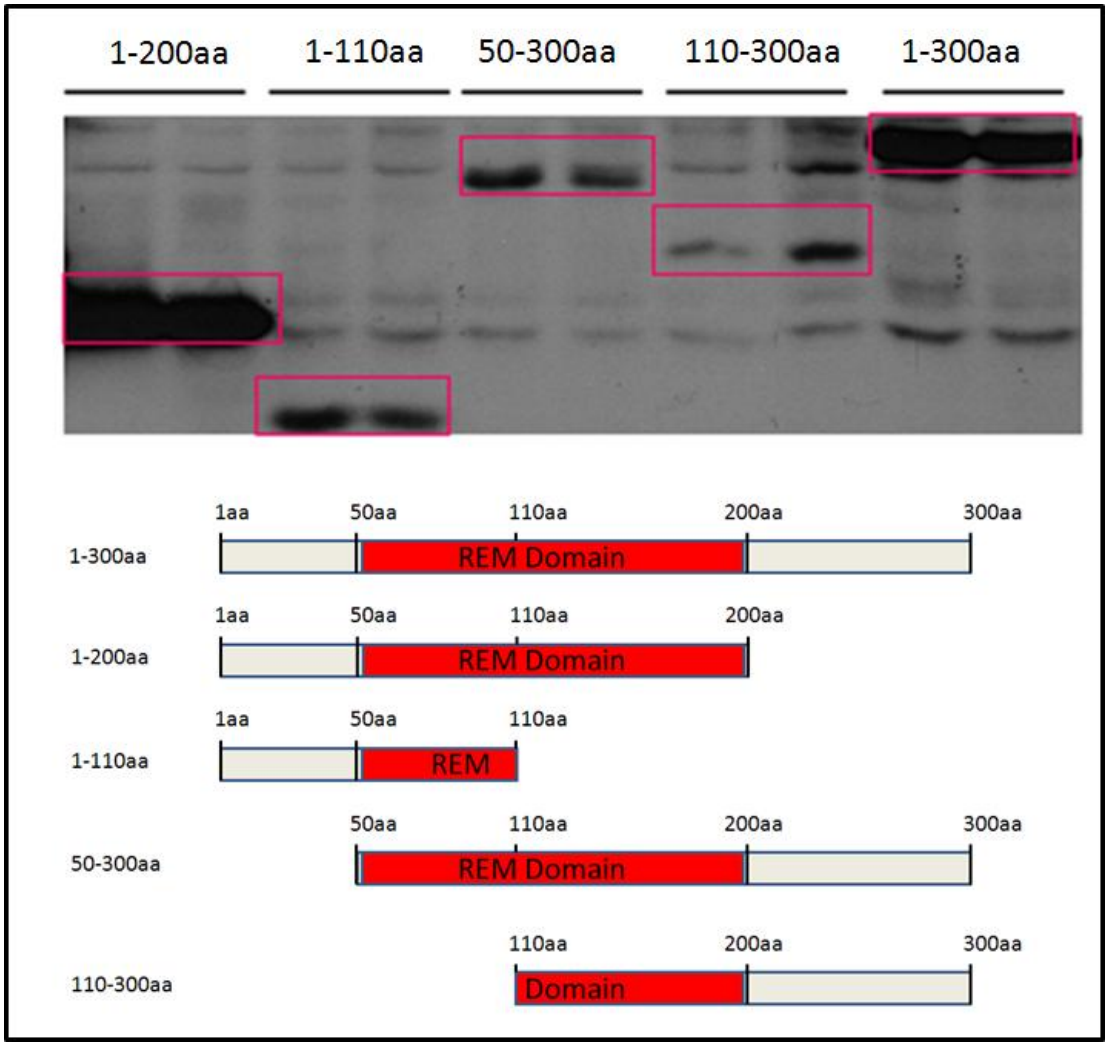

Fig 2.4 Expression of truncation constructs of N-GDS.

Four HA tagged truncation constructs of full length HA-1-300aaGDS were created using regions diagramed in the figure above. The tagged constructs (labeled 1-200aa, 1-110aa, 50-300aa, and 110-300aa) were expressed in Cos7 cells and lysate was immunoblotted to confirm expression and compare size to full length 300aa N-GDS

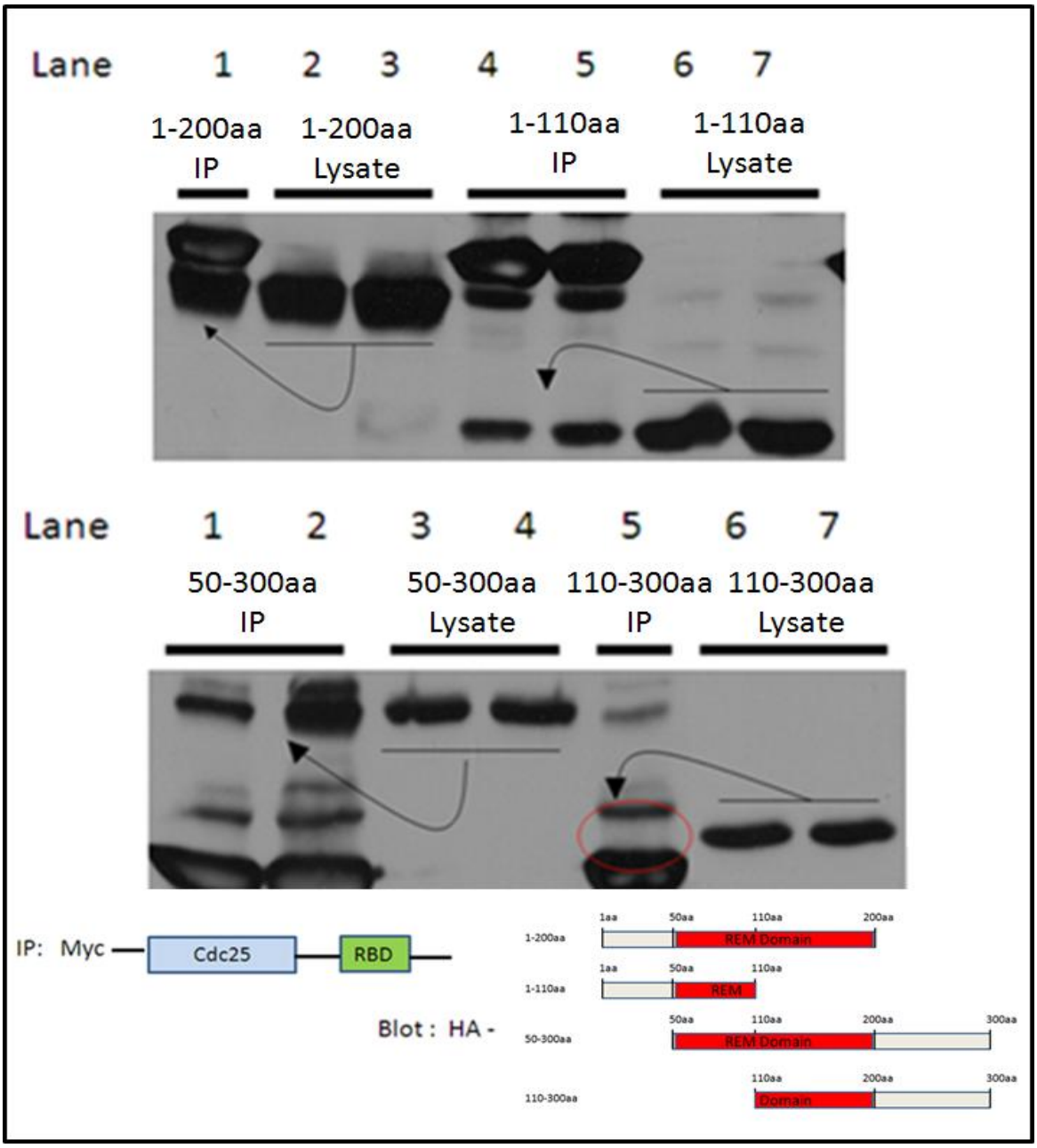

Fig 2.5 First 50aa of the REM domain essential for RalGDS intramolecular association.

HA-truncation constructs were co-transfected with Myc-301-852aa-GDS to map the portion of the N-terminus essential for the association with Myc-301-852aa-GDS. Immunoprecipitation of Myc-301-852aa-GDS showed an association to all but the HA-110-300aa construct (Lower lane 5). Association of the other truncation constructs was intact [HA-1-200aa (Upper lane 1), HA-1-110aa (Upper lane 4+5), HA-50-300aa (Lower lane 1+2). Expression of each HA- construct was confirmed by HA blot of the lysate [HA-1-200aa (Upper lane 2+3), HA-1-110aa (Upper lane 6+7), HA-50-300aa (Lower lane 3+4), and HA-110-300aa (Lower lane 6+7)].

We next determined where within Myc-301-852aa-GDS the REM domain bound. Relevant hits from the yeast two hybrid screen all contained the Cdc25 domain, suggesting that this was the region of interaction. Two expression constructs consisting of the first 160aa (1-160aa) and last 100aa (160aa-260aa) of the 260aa long RalGDS Cdc25 domain were made (Fig 2.6). Then each was co-expressed with HA-1-300aaGDS. We found the 1-160aa construct was unable to bind to HA-1-300aaGDS, while the 160aa-260aa and full length Myc-301-852aa-GDS maintained binding (Fig 2.7). These results told us that in RalGDS there was an association occurring between the REM domain and Cdc25 domain with the essential regions of this interaction in the first 50aa of the REM domain with the last 100aa of the Cdc25 domain. Noting that a similar situation is the case in Sos1 we next conducted to a detailed comparison between the two proteins in the hopes of gaining insight into the nature of the RalGDS intra-molecular interaction [83,84].

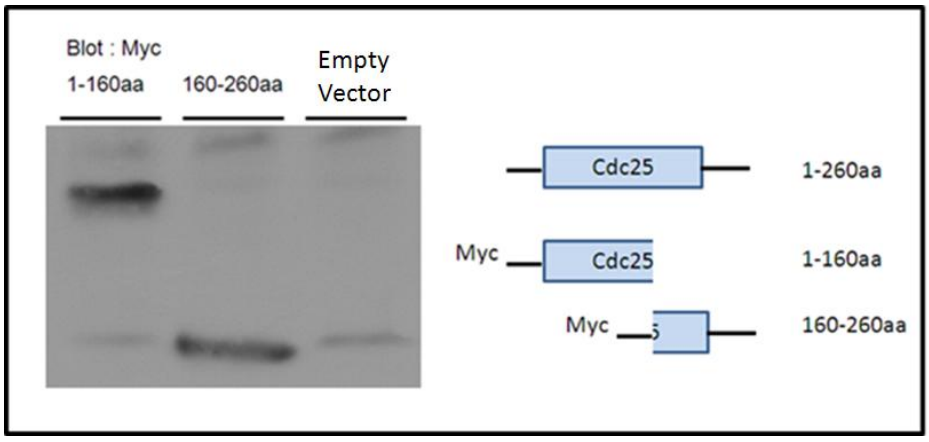

Fig 2.6 Expression of truncation constructs of RalGDS Cdc25 domain.

In order to map the region within the Cdc25 domain of RalGDS responsible for the intramolecular association to the REM domain, two Myc tagged truncation constructs were created using regions diagramed in the figure above. The tagged constructs (labeled 1-160aa and 160-260aa) were expressed in Cos7 cells and lysate was immunoblotted to confirm expression.

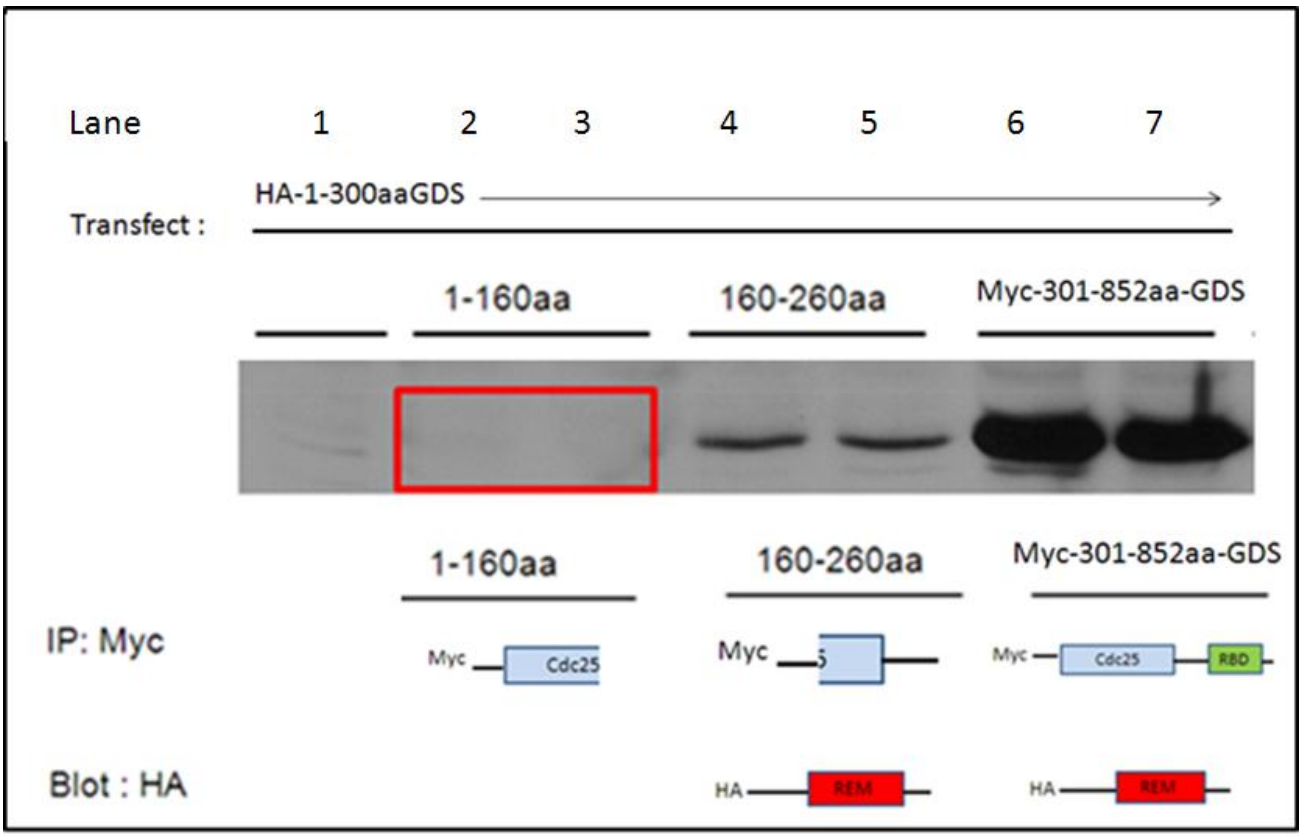

Fig 2.7 Last 100aa of Cdc25 domain essential for RalGDS intramolecular association

Myc tagged Cdc25 domain truncation constructs (diagramed above) were co-transfected into Cos7 cells with an HA-1-300aaGDS expression construct. Cells were lysed and subject to Myc antibody immunoprecipitation and HA antibody blot. Lane 1 shows the negative control of only HA-1-300aaGDS transfected Cos7 cells. Lanes 2+3 Myc 1-160aa construct was not able to pull down HA-1-300aaGDS, showing that the truncated C-terminal 100aa of the Cdc25 domain was needed for association. Lanes 4+5 show that the Myc 160aa-260aa construct was able to pull down HA-1-300aaGDS. Lanes 6+7 show that the Myc-ΔN-GDS construct was able to pull down HA-1-300aaGDS.

2.2.2 Using the crystal structure of Sos1 as a template for insights about RalGDS

Having shown that the REM domain associates with the Cdc25 domain in RalGDS, we looked to the structure of Sos1 for insights into how this might affect catalytic activity. First we aligned the sequences of the REM and Cdc25 domains of RalGDS with Sos1 (Fig 2.8). Then analyzing the crystal structure of Sos1 at the aligned 50aa in the REM domain and 100aa in the Cdc25 domain critical for intramolecular association in RalGDS, we found an interface of interaction (Fig 2.9). We found the sites corresponded to a region critical to the catalytic activity and regulation of Sos1. In the Cdc25 domain, the 100aa region mapped to the catalytic helical hairpin directly responsible for Sos1 exchange activity. In the REM domain, the 50aa mapped to residues that form a hydrophobic interface with the catalytic helical hairpin necessary for stabilizing it in an active orientation. Other investigators have shown that mutations to charged residues on either the Cdc25 or the REM side of the hydrophobic interface decreased the exchange activity of Sos1. The Sos1 allosteric regulation is thought to mediate interactions that twist the catalytic hairpin in and out of active confirmations via the REM domain [84, 85]. The sites making up the hydrophobic pocket are well conserved in RalGDS, with highlighted beige and green sites denote similar substituents or exact matches, respectively (Fig 2.9).

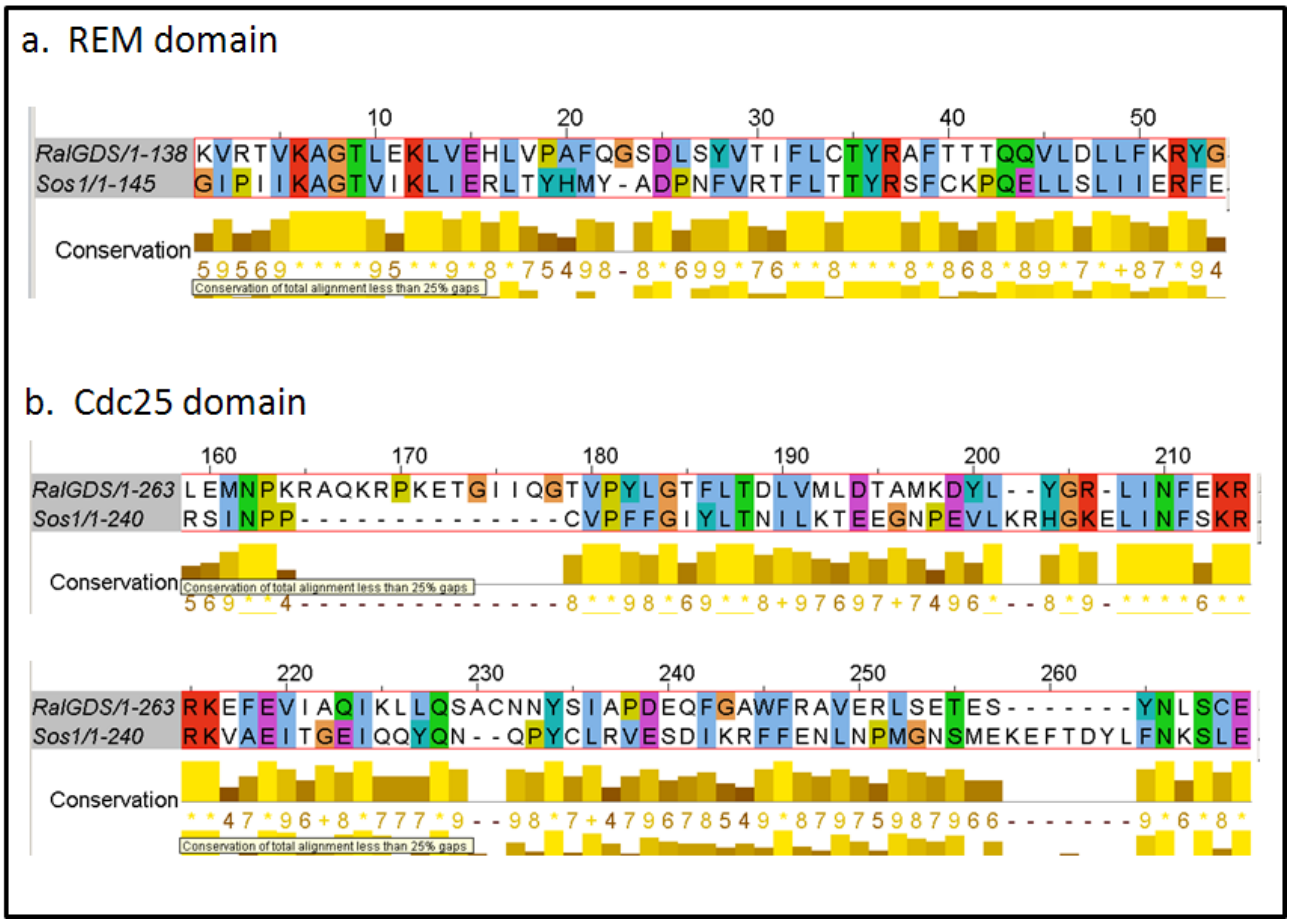

Fig 2.8 Sequence comparisons of the REM and Cdc25 domains of Sos1 and RalGDS.

The sequences of the (a) REM domains and (b) Cdc25 domains from Sos1 and RalGDS were analyzed using a **MU**ltiple **S**equence **C**omparison by **L**og- **E**xpectation (MUSCLE) proteomics tool. Conservation at each residue between the two proteins was determined and scored by similarities in physic-chemical properties [91] . Highlighted in this figure are the alignment of the (a) 50aa of the REM domain and (b) 100aa of the Cdc25 domains that form the basis for the RalGDS intramolecular association.

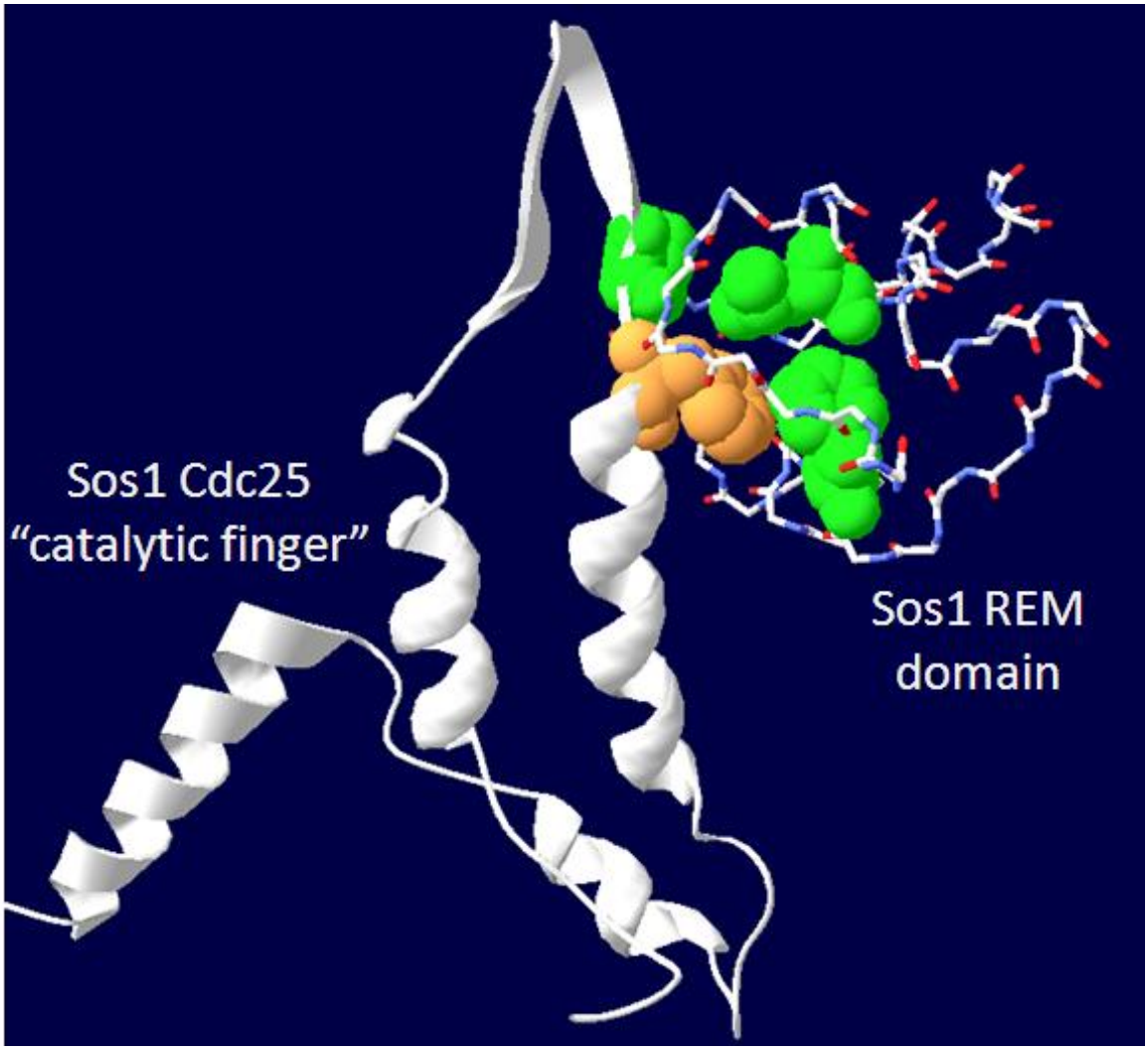

Fig 2.9 Crystal structure of Sos1 at the REM: Cdc25 domain site of association.

Analysis of the crystal structure of Sos1 reveals that the homologous sites to the mapped regions of association in RalGDS correspond to the catalytic helical hairpin of the Cdc25 domain (ribbon structure) and a hydrophobic pocket of interaction to REM domain (stick structure) in Sos1. The highlighted green Van der Waals force residues represent critical hydrophobic amino acids conserved between Sos1 and RalGDS. The highlighted beige residue represents a phenylalanine in Sos1 that is a tyrosine in RalGDS, both residues maintain the hydrophobic nature of the pocket.

2.2.3 A single amino acid substituion in the REM domain of RalGDS, that is analogous to a Rgl1 mutation found in breast cancer, blocks its binding to the catalytic domain.

A study that sequenced the genomes of various human breast cancer samples identified a tyrosine to serine mutation in the REM domain of RalGEF family member Rgl1 [39]. We asked if a comparable mutation in the REM domain of RalGDS could affect its interaction with the catalytic CDC25 domain of RalGDS. To this end we generated the mutation in HA-1-300aaGDS (HA-1-300Y172S) and tested its ability to associate with Myc-301-852aa-GDS in cells. We found that the binding activity of the mutant construct was dramatically reduced (Fig 2.10). Because this mutation was not in the 50 amino acid segment that we found was critical for binding, we hypothesized that this mutation indirectly affected binding by the REM N-terminal 50 amino acids to the catalytic domain.

To gain insight into how this mutation disrupts REM binding to the CDC25 domain, we again turned to the Sos1 structure. Sos1 contains a phenylalanine rather than a tyrosine at this residue (Fig 2.11 highlighted in blue) which contributes to the hydrophobic pocket that is formed by REM association with Cdc25. Thus a mild change from non-polar to polar side chain in a tyrosine to serine mutation could destabilize the association between the two domains in both Sos1 and RalGDS. This mutation was generated in the full length protein and tested for effects on exchange activity. When expressed in Cos7 cells, we found no change in activity as compared to wildtype protein (data not shown). The mutation was also tested in the context of Rgl (the GEF it was identified in) and no difference in activity was found for this mutant as well. It is possible that this mutation may not have a direct effect on exchange activity, but may act to modulate allosteric regulation of the protein.

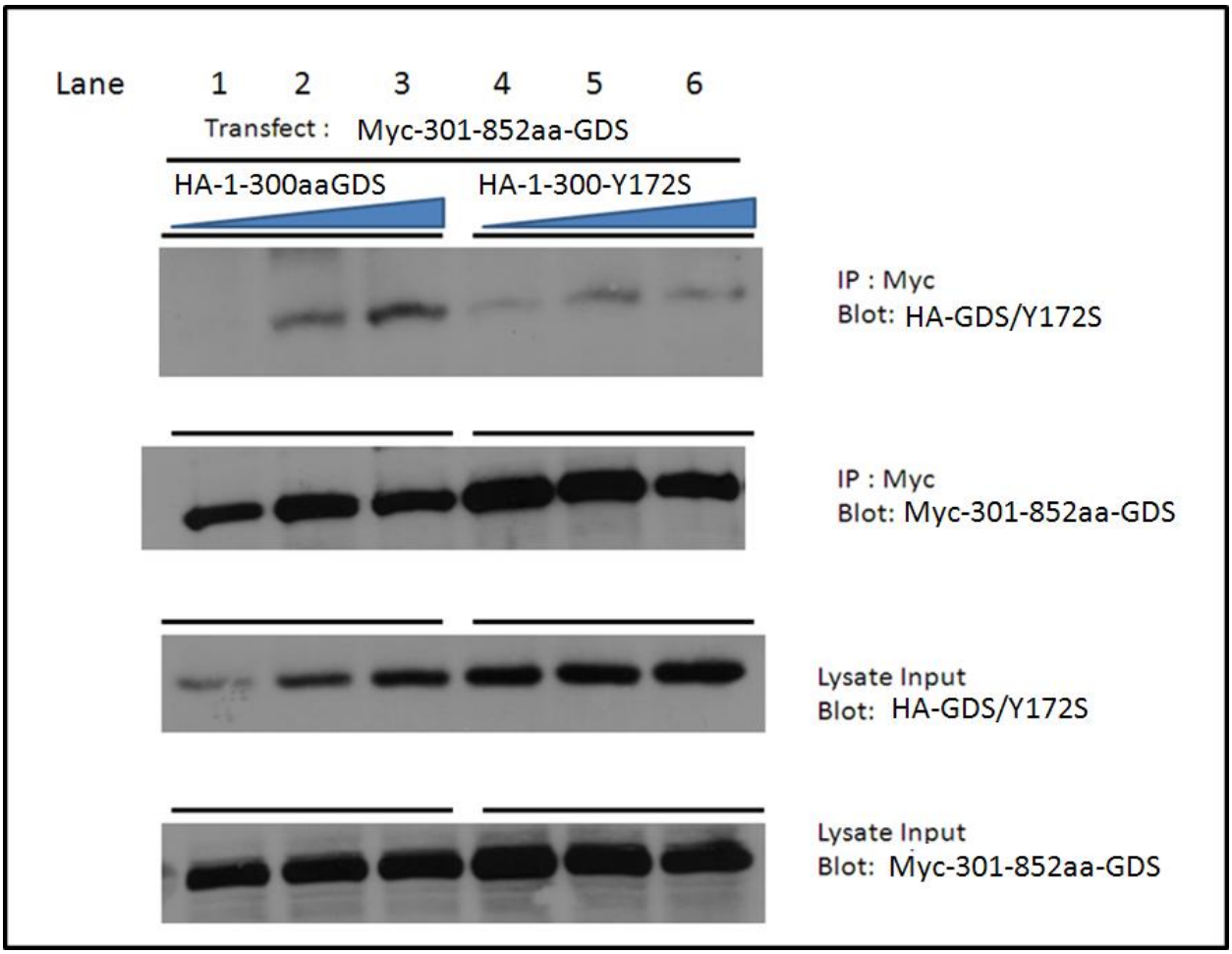

Fig 2.10 Cancer associated mutation in the REM domain of RalGDS decreases Rem: Cdc25 binding.

Wildtype HA-1-300aaGDS and a construct mimicking a mutation found in a cancer genomics screen (HA-1-300-Y172S) were co-transfected with Myc-301-852aa-GDS. Increasing concentrations of the HA constructs were transfected with a single concentration of the Myc-301-852aa-GDS construct in order to establish data point in which a similar amount of HA construct was expressed between the wildtype and mutant samples (Lane 3 vs. Lane 4 HA blot of the lysate input). Immunoprecipitation of Myc-301-852aa-GDS showed that for an equal amount of the wildtype HA-1-300aaGDS vs. mutant expressed in the cell, the mutant HA-1-300-Y172S had a greatly diminished association capacity (Lane 3 vs Lane 4 IP: Myc Blot: HA).

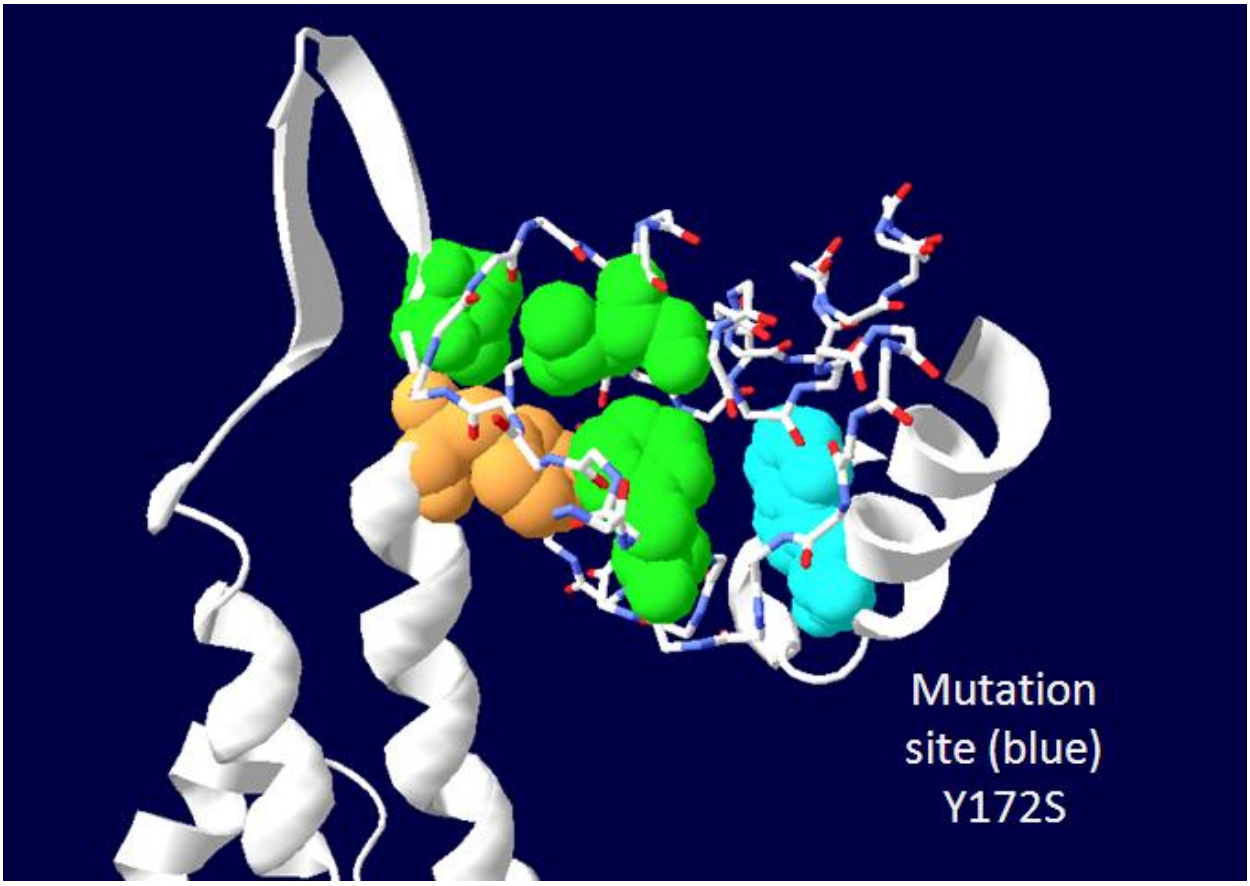

Fig 2.11 Mapping of the RalGEF mutation site to the Sos1 crystal structure.

Mapping the location of the identified mutation site found in Rgl1 (highlighted in blue) shows its proximity to the hydrophobic pocket at the center of the REM: Cdc25 association. The highlighted green Van der Waals force residues represent critical hydrophobic amino acids conserved between Sos1 and RalGDS. The highlighted beige residue represents a phenylalanine in Sos1 that is a tyrosine in RalGDS, both residues maintain the hydrophobic nature of the pocket.

2.2.4 Tyrosine phosphorylation site may also impact REM: Cdc25 interaction

In a study that is the subject of the next chapter we found that RalGDS becomes tyrosine phosphorylated at multiple sites in response to sustained c-Met signaling. One of the sites of phosphorylation (RalGDS Y52) mapped to a tyrosine a few residues upstream of the REM domain. The Sos1 structure suggests that this site (a methionine in Sos1) is in close proximity to the hydrophobic pocket (Fig 2.12). Thus, the negative charge created by a phosphorylation at that site might change the catalytic activity of the Cdc25 domain. In fact mutating a Sos1 site (beige) on the helical hairpin to a Glutamic acid has been shown to decrease Sos1 exchange activity [92].

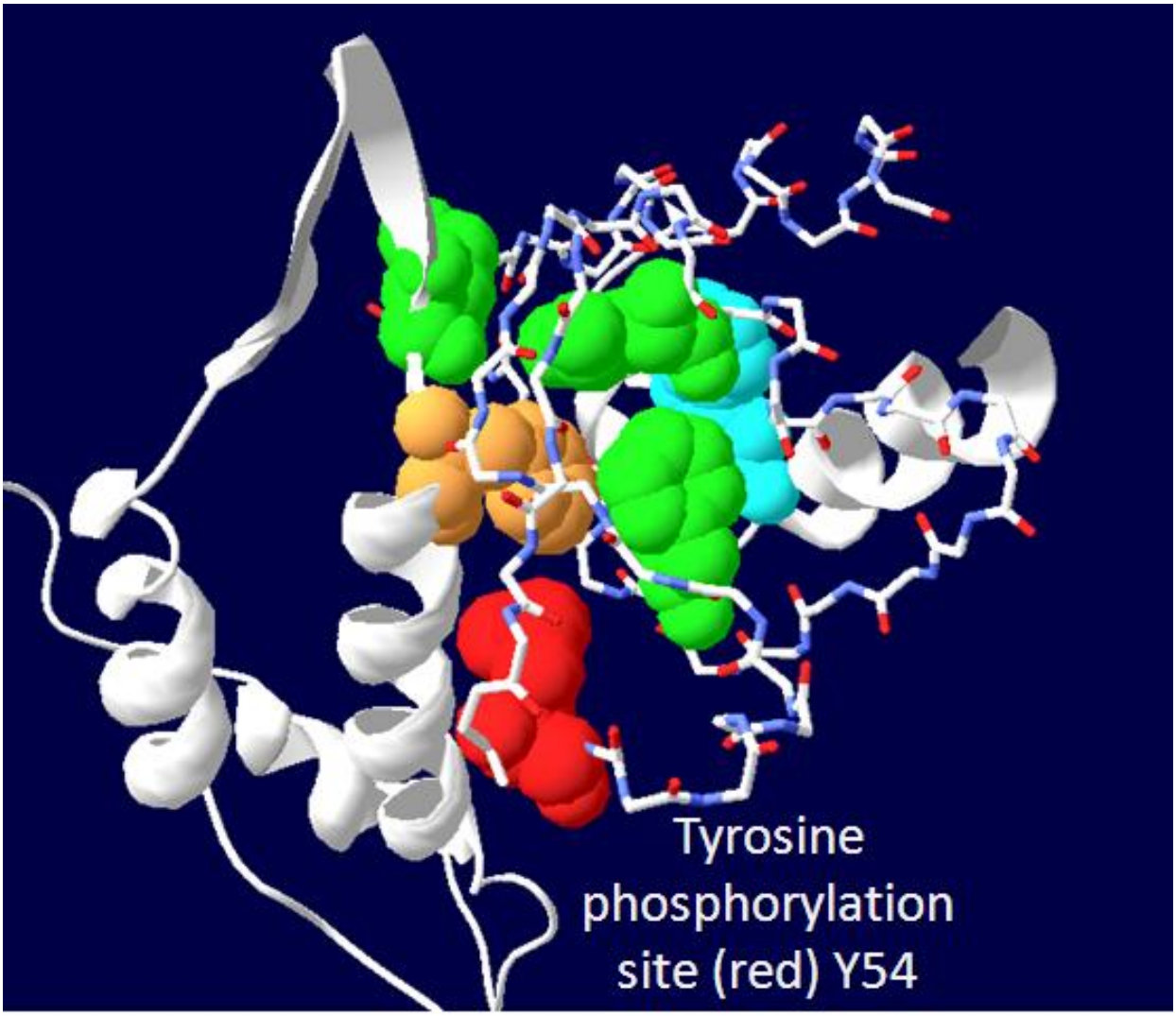

Fig 2.12 Mapping of a RalGDS tyrosine phosphorylation site to the Sos1 crystal structure.

Mapping the approximate location of an identified tyrosine phosphorylation site found in RalGDS (highlighted in red) in response to c-Met activation shows its proximity to the hydrophobic pocket at the center of the REM: Cdc25 association. The highlighted green Van der Waals force residues represent critical hydrophobic amino acids conserved between Sos1 and RalGDS. The highlighted beige residue represents a phenylalanine in Sos1 that is a tyrosine in RalGDS, both residues maintain the hydrophobic nature of the pocket. The highlighted in blue residue represents an identified mutation site in Rgl1.

2.3 Discussion

A greater understanding of RalGEFs is essential for future development of pharmacological inhibitors. In this chapter we presented evidence for an intramolecular association between the REM and Cdc25 catalytic domains of RalGDS. This association is of a similar nature to that found in Sos1. Using the crystal structure of Sos1 as a template, we are able to make predictions about the possible consequences of mutations and modifications to this region of RalGDS found in nature [83,84].

It was previously shown that the truncation of the REM domain of RalGDS allowed for an increase in exchange activity in *in vitro* studies [89]. This lead us to believe that the REM domain may act in an inhibitory manner on the protein. With the results in this chapter we are now able to propose a possible mechanism of this inhibition. Acting in a similar manner as Sos1, the RalGDS REM domain forms hydrophobic pocket with the helical hairpin of the Cdc25 domain responsible for exchange activity. In Sos1 the REM: Cdc25 interaction holds the hairpin in an orientation that affects its ability to interact with the switch two region of Ras. Upon binding at an allosteric site by RasGTP, the REM domain is shifted, pulling along with it the helical hairpin into a sterically favorable orientation to interact with Ras (Fig 2.13).

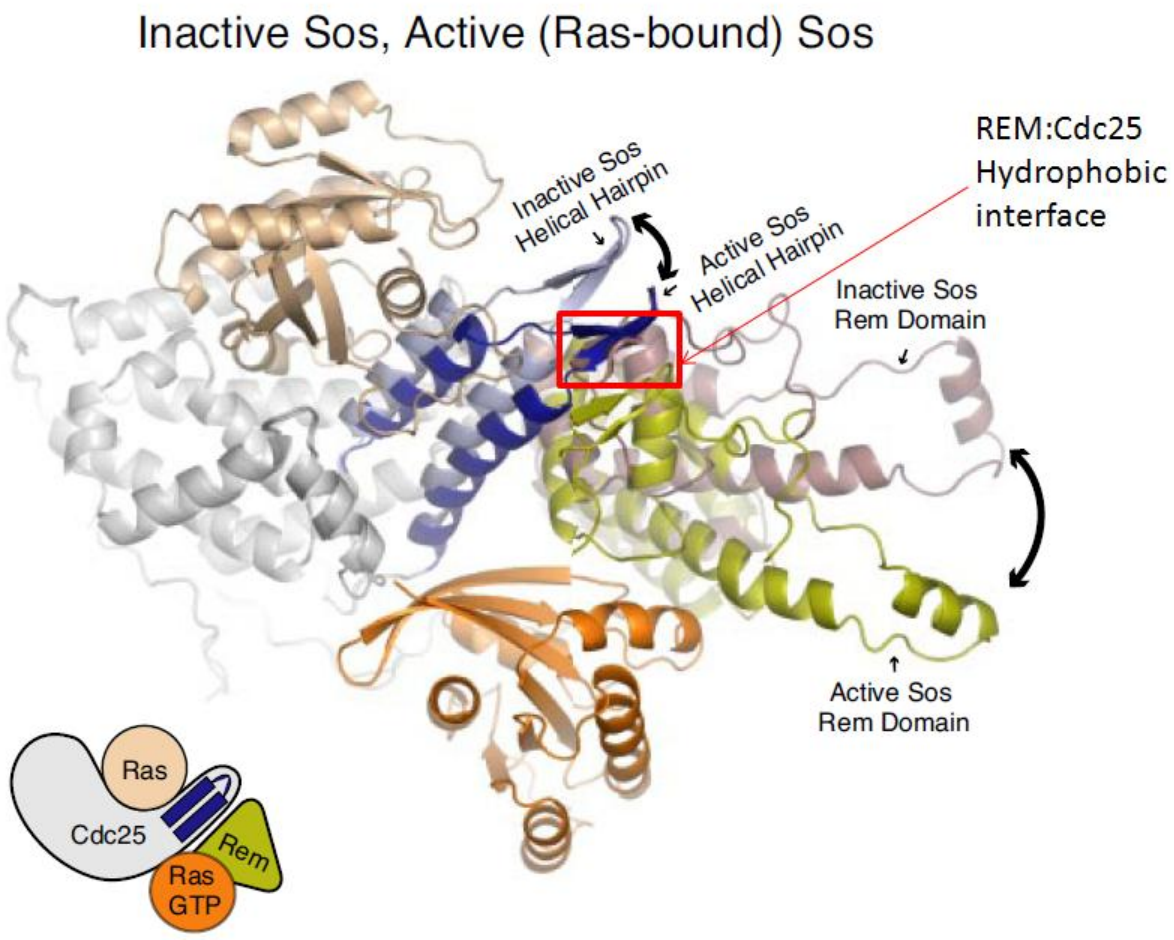

Fig 2.13 Crystal structure of Sos1 Cdc25: Rem in and out of active orientation due to allosteric RasGTP binding. [27]

It is known that the association of PDK1 to the REM containing N-terminus of RalGDS acts to increase the exchange activity of the protein. This is true even when the kinase activity of PDK1 is removed. With the information presented in this chapter, we can now propose that PDK1 may act in a similar fashion as the allosteric binding of RasGTP does in Sos1.

In this chapter, we also looked at two modifications in the region of REM: Cdc25 association found in nature. The first was a mutation of a tyrosine to serine in the REM domain of a RalGDS family member. We found this mutant decreased the association between the domains. When this mutation was tested for effects on exchange activity we found no change as compared to wildtype protein. It is possible that this mutation may not have a direct effect on exchange activity but may act to modulate normal allosteric regulation of the protein. The second modification to this region of interaction that we identified was the phosphorylation of RalGDS in the REM domain as a consequence of sustained c-Met signaling. The effects of this modification and reasoning in the greater context of c-Met signaling will be discussed in detail in the next chapter.

With the goal of identifying a targetable means of regulating small GTPases we have highlighted one possible site within RalGDS and possibly other GEFs. In Sos1 the REM: Cdc25 association has been shown to dictate allosteric regulation of exchange activity. Targeted charge mutations within the hydrophobic pocket created by the association have been shown to decrease Sos1 catalytic activity. A similar type of association and regulation is found in the Rap GEF EPAC2 [88]. For RalGDS we also find this REM : Cdc25 interaction effecting catalytic activity. In nature we have found at least three modifications or interactions to this region in RalGDS (mutation, phosphorylation, PDK1 regulation) suggesting that site may be an evolutionarily selected and physically accessible point of regulation for RalGDS. A large variety of small GTPase GEFs have predicated REM domains, further study will likely reveal regulatory roles for these as well. With growing structure and function data as to the nature of REM domain regulation of GEFs, they may one day be a standard target of pharmaceutical regulation.

2.4 Future Directions

To further characterize the dynamics of the intramolecular association in RalGDS we will mutate sites within the REM: Cdc25 hydrophobic pocket to disrupt the association and look for changes in exchange activity. Although the identified cancer mutation did not affect exchange activity, changes to residues at the core of the pocket may have a more direct effect on activity.

We will also do mapping studies to identify the region of the N-terminus with which PDK1 interacts. Initial studies localized the site to within the N-terminal 300aa of RalGDS. If PDK1 is acting as an allosteric regulator (like RasGTP for Sos1), we expect the site of association to be in the linker region between the REM and Cdc25 domain. Characterizing GEF regulation from allosteric sites may also prove useful when selecting targets for pharmacological inhibition

Chapter 3: Tyrosine phosphorylation of RalGDS by Met uncouples RalGDS from active Ras.

3.1 Introduction

Ras effectors consist of an ever increasing roster of players. The regulation of effector selection is important to the biology of Ras signaling because of the diverse set of cellular programs they initiate. Effector selection is partially attributed to temporal and spatial segregation mediated by the location of upstream activation and scaffold proteins recruited to the site of activation. Under normal circumstances these activation complexes are created and dissolved to trigger a defined biological event. In many cancer settings however, these complexes are created and sustained, locking the cell in an abnormal state of activation.

Classic examples of this can be seen with Her2 activation in over 20% of breast cancers [15, 93], c-Met amplification in gastric cancers [76-78], and EGFR activation in various subsets of lung, prostate, and colorectal cancers [14, 94, 95] to name a few. In these complexes, Ras and its effectors are often a key component of the aberrant signaling cascade. Over the course of the cancer's evolution some effector pathways become down-regulated while others key to proliferative and anti-apoptotic signaling are maintained [96, 97]. In this chapter we will discuss a novel mode of regulation for the Ras effector RalGDS, which uncouples the GEF from active Ras signaling complexes in c-Met amplified gastric cancer cells.

While investigating the role of Ral signaling in the gastric cancer cells lines MKN45 and KATOII/III we found exogenously expressed RalGDS to be tyrosine phosphorylated. The cell lines have in common c-Met amplification and the MKN45 line is often cited as a prime example of c-MET oncogene addition [78, 98, 99]. We found RalGDS phosphorylation to be dependent on c-Met signaling and mass spectrometry analysis identified four phosphorylation sites. They were found in the REM domain, Cdc25 domain, and two in the Ras binding domain (RBD). Characterization of one of the Ras binding domain sites showed phosphorylation at this location blocks the ability of RalGDS to bind Ras *in vivo*. The location of the other phosphorylation sites map to regions predicted to be critical for RalGDS activity. Structural correlations suggest a mechanism by which exchange activity would be negatively affected by these phosphorylation events. Taken together, these findings suggest that in the context of amplified c-Met signaling RalGDS and consequently Ral activation is actively down-regulated

3.2 Results

3.2.1 Exogenous RalGDS is tyrosine phosphorylated in gastric cancer cell lines KatoII and MKN45

Studies by other labs on c-Met "oncogene addicted" cell lines found that only a subset of the downstream pathways are sustained and required for cell survival. Introduction of mutationally active Ras or its effectors Raf or AKT could rescue growth arrest from c-Met inhibition [16]. Active Raf or AKT could not rescue inhibited cells as efficiently as Ras, suggesting a role for other effectors. Not mentioned in these studies was an analysis of RalGEFs so we initiated work to examine their role in c-Met oncogene addiction.

First we attempted to overexpress RalGDS in MKN45 and Kato III cells through lipofection, lentiviral and retroviral delivery vectors. Problems arose when we noted the protein expression was lost over the span of weeks when compared to GFP which was stably maintained (data not shown). This suggested the possibility that c-Met addicted cells don't tolerate a functional Ral signaling cascade. Then, analysis of Myc-tagged RalGDS immunoprecipitated from early passage KatoIII cells revealed that it was being tyrosine phosphorylated. Myc-RalGDS from MKN45 cells was also positive for tyrosine phosphorylation (Fig 3.1).

Knowing that both cell lines were amplified for c-Met lead us to hypothesize that RalGDS was phosphorylated in response to c-Met to suppress its activity. To test this theory, we co-transfected Cos7 cells with a Myc-RalGDS and c-Met expression vector. RalGDS was phosphorylated only in cells co-transfected with c-Met (Fig 3.2). We also obtained a c-Met specific inhibitor and found that treated early passage RalGDS expressing MKN45 cells lost RalGDS phosphorylation (Fig 3.3). The notion that the RalGEF effector arm of Ras signaling is being specifically modified in c-Met oncogene addiction suggests it may play an important role in the biology of c-Met driven cancers.

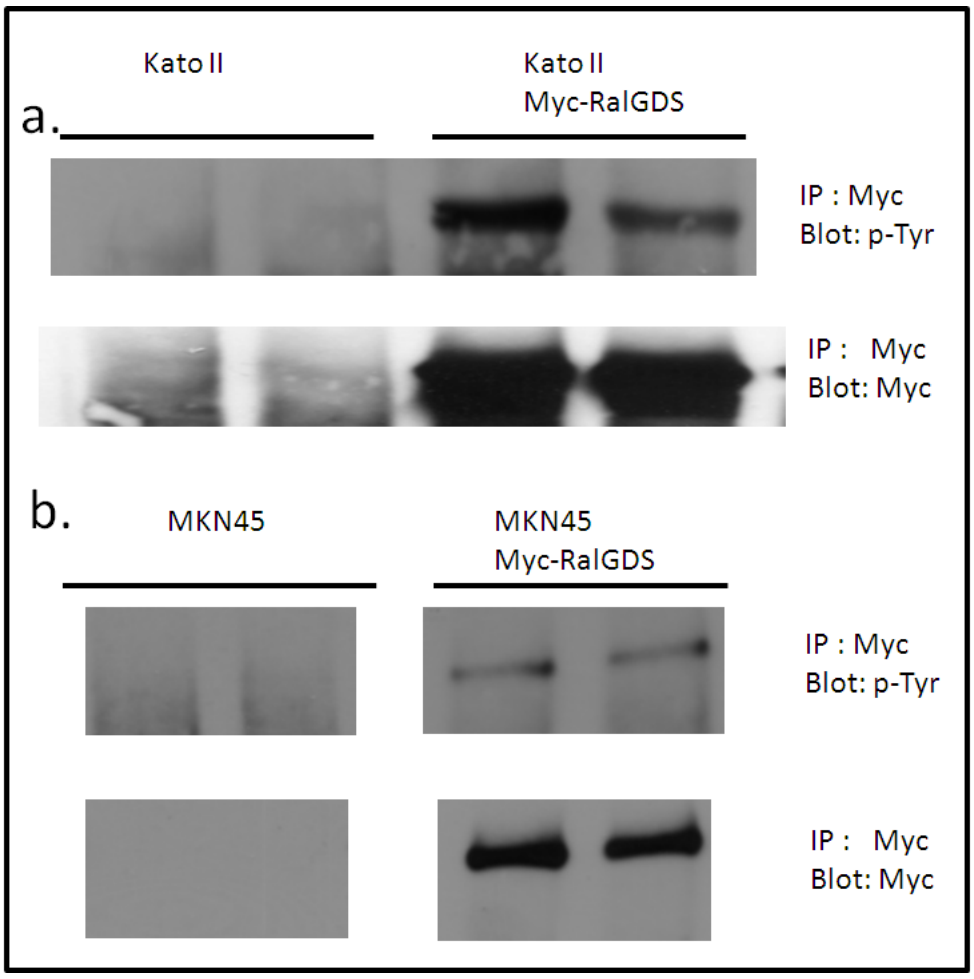

Fig 3.1 Exogenously expressed RalGDS is tyrosine phosphorylated in MKN45 and KatoII cells.

a) KatoII cells transfected with a Myc-RalGDS expression construct and (b) MKN45 cells stably infected with a Myc-RalGDS expression construct were lysed, subject to Myc immuno precipitation, and blotted with a total phospho-tyrosine antibody. Phospho-tyrosine blots were stripped and re-blotted with Myc antibody to assess Myc-RalGDS pull down.

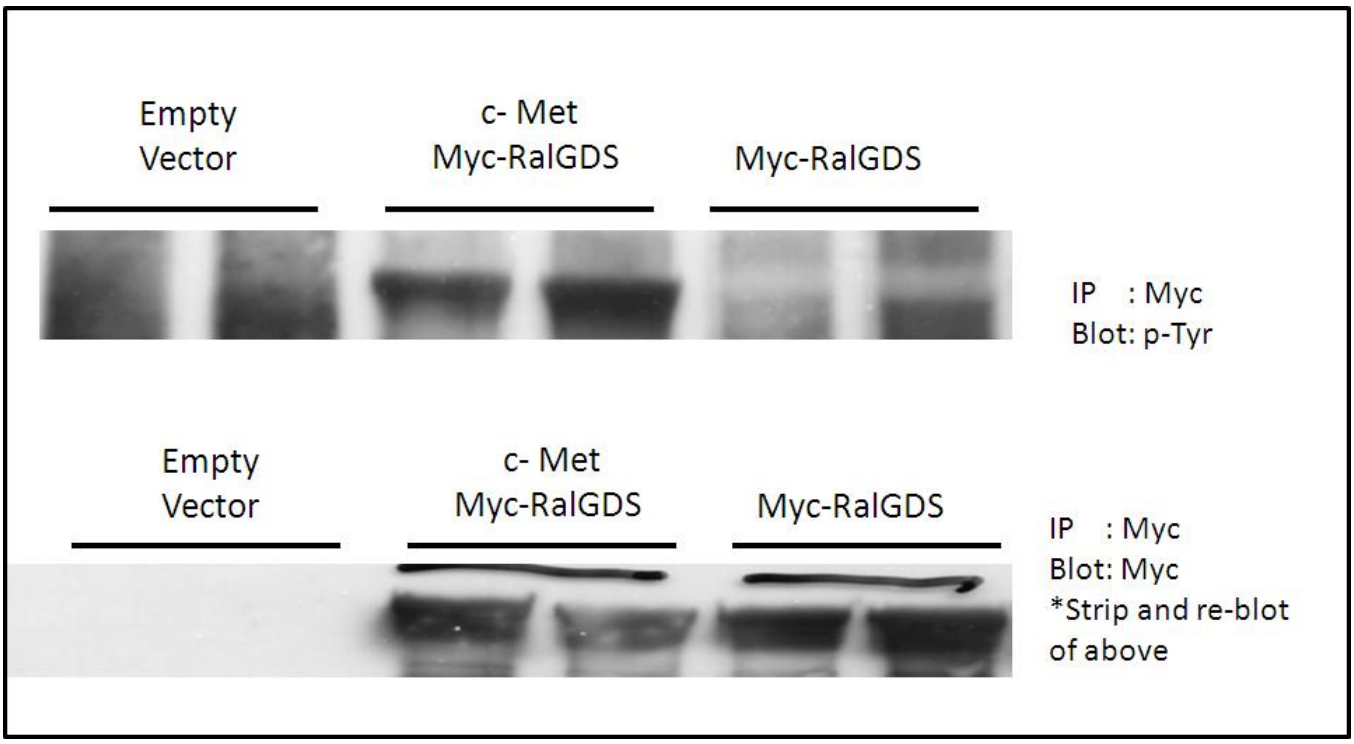

Fig 3.2 c-Met alone can mediate RalGDS phosphorylation

Cos-7 cells were co-transfected with Myc-RalGDS and wildtype c-Met expression constructs. Cells were lysed, subject to Myc immuno precipitation, and blotted with a total phospho-tyrosine antibody. Phospho-tyrosine blots were stripped and re-blotted with Myc antibody to assess Myc-RalGDS pull down.

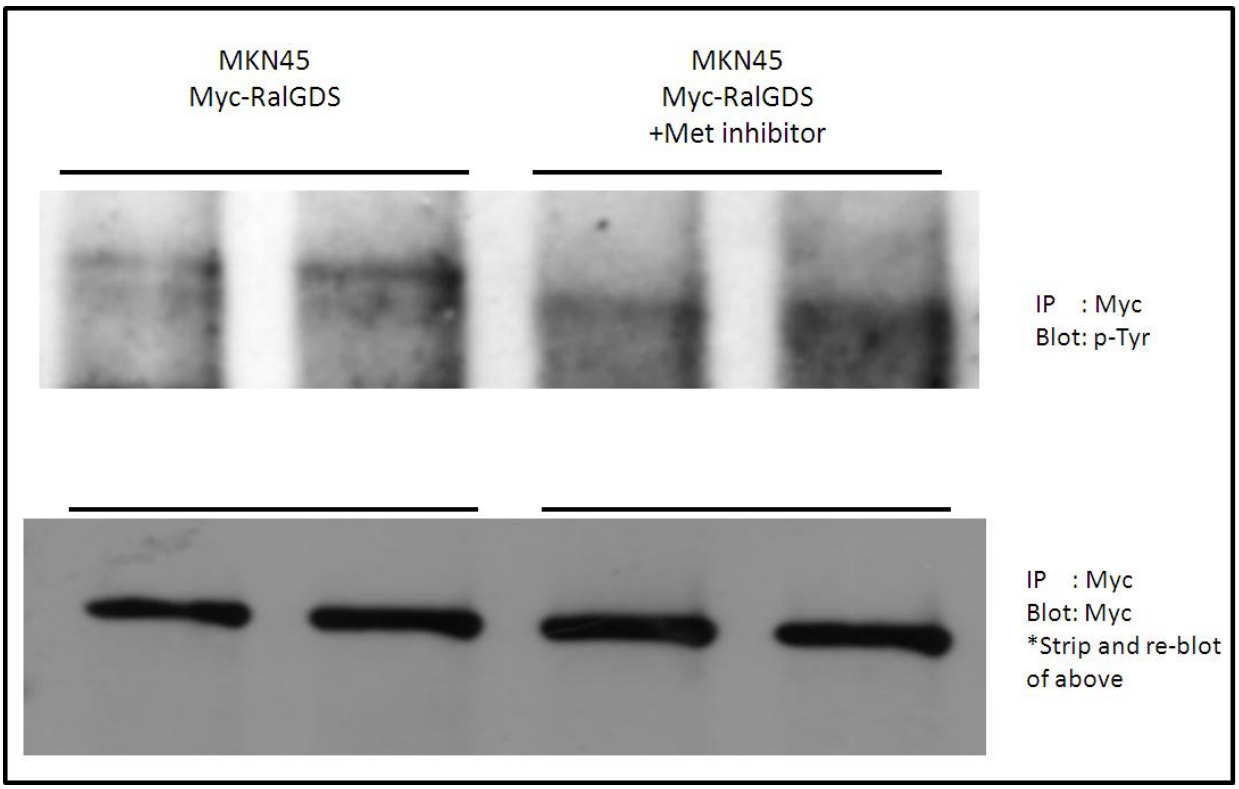

Fig 3.3 c-Met inhibitor blocks RalGDS phosphorylation

MKN45 cells stably infected with a Myc-RalGDS expression construct were treated with 2uM c-Met Kinase inhibitor II (Calbiochem) for 4 hours, lysed, subject to Myc immuno precipitation, and blotted with a total phospho-tyrosine antibody. Phospho-tyrosine blots were stripped and re-blotted with Myc antibody to assess Myc-RalGDS pull down.

3.2.2 RalGDS is phosphorylated at four sites in response to c-MET signaling

Initial attempts at mapping the c-Met mediated phosphorylation site by deletion analysis lead us to believe there was more than one site being modified (data not shown). To expedite the identification of all the sites, we turned to mass spectroscopy analysis. Results from this survey identified four tyrosine phosphorylation sites (Fig 3.4) [RalGDS sequence Accession ID Q03385]. The site at Y752 was identified in initial mass spectroscopy screens before optimization of protocols lead to the identification of the remaining three sites. Subsequently the majority of our characterization studies revolve around the Y752 site and only recently have we begun to study the other three phosphorylation sites.

One site (Y463 in the Cdc25 catalytic domain) was also found in RalGDS samples isolated from cells not transfected with c-Met. We were able to show that c-Met increased the amount of phosphorylation at this site when we co-expressed the isolated RalGDS Cdc25 domain with c-MET (Fig 3.5).

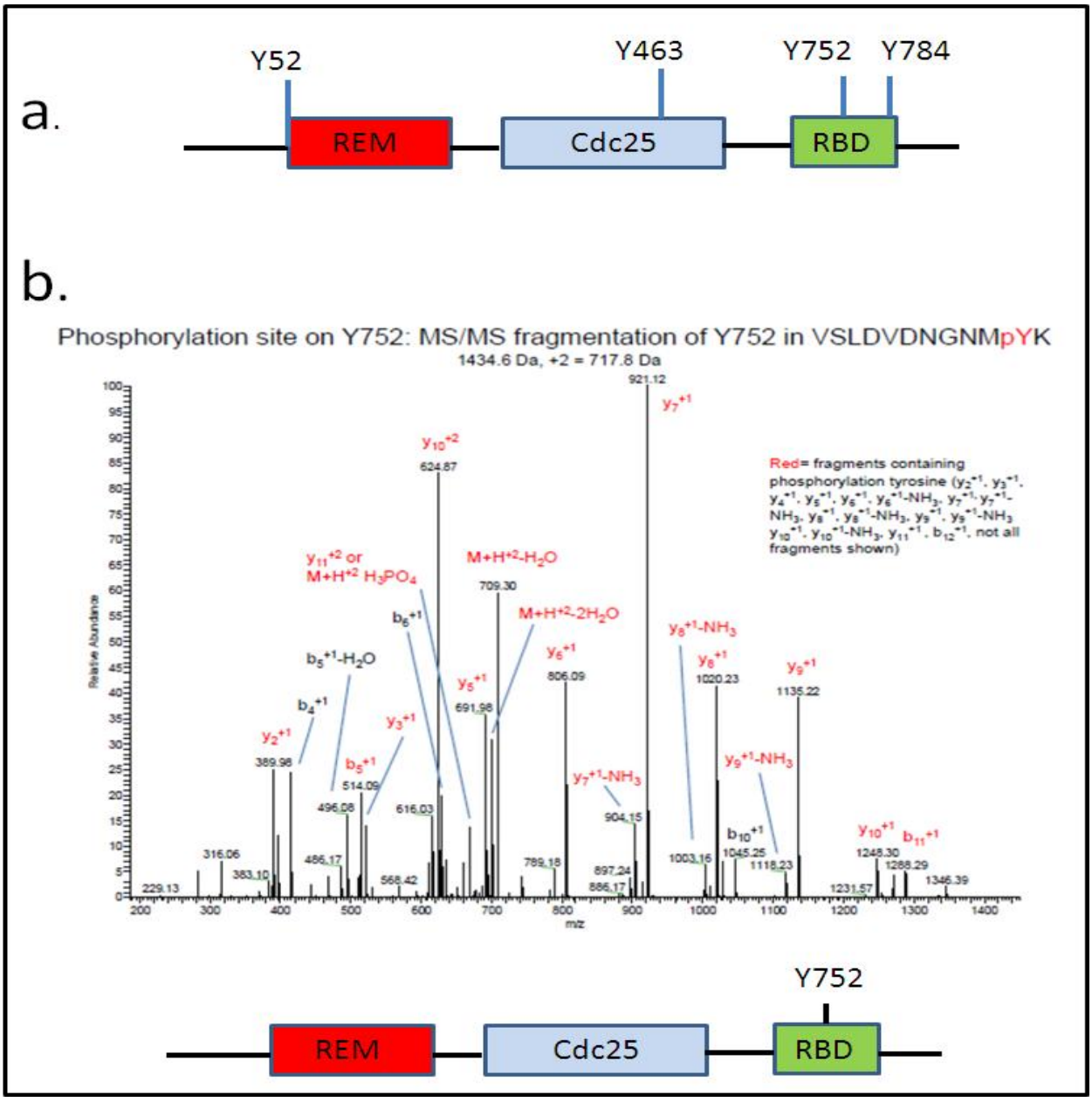

Fig 3.4 Mass spectroscopy identifies four tyrosine phosphorylation sites.

Cos-7 cells transfected with Myc-RalGDS alone or with c-Met expression vectors were lysed and immuno precipitated with Myc antibody. Isolated Myc-RalGDS was sent for mass spectroscopy identification of tyrosine phosphorylation sites. This survey identified four sites (a) Y52, Y463, Y752, and Y784. (b) Initial surveys could only confirm the Y752 site. Optimization of protocols lead to confirmation of the remaining three sites.

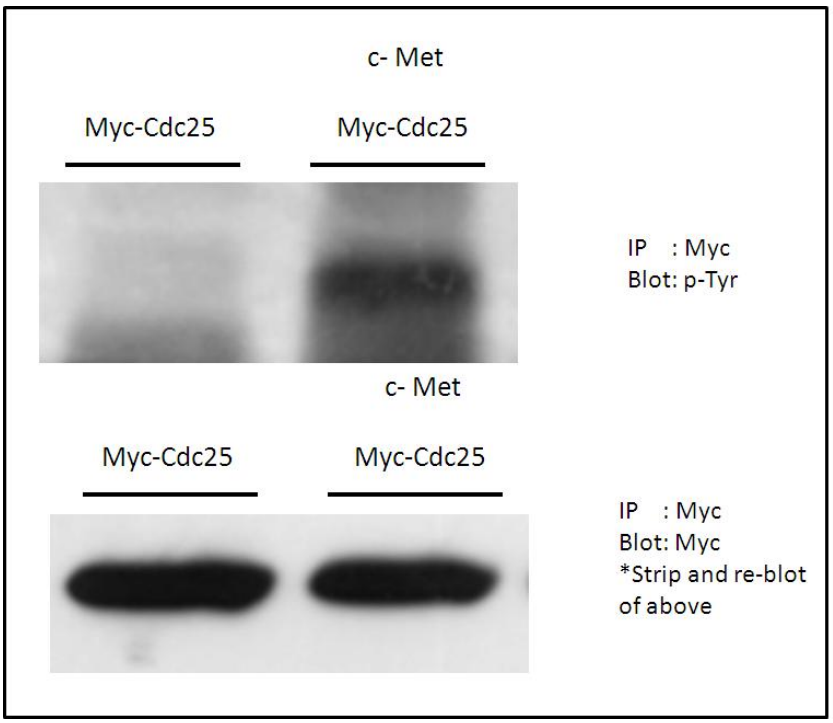

Fig 3.5 c-Met increases tyrosine phosphorylation at the Cdc25 Y463 site.

To asses if c-Met mediates an increase in phosphorylation at the Y463 site Cos-7 cells were transfected with a Myc-RalGDS-Cdc25 domain construct alone or with a c-Met expression construct. Cells were lysed, subject to Myc immuno precipitation, and blotted with a total phospho-tyrosine antibody. Phospho-tyrosine blots were stripped and re-blotted with Myc antibody to assess Myc-RalGDS pull down

Two sites, Y752 and Y784 map within the RalGDS Ras binding domain (RBD). Using the solved crystal structure of the RBD bound to Ras we modeled the two tyrosine locations for insights into possible consequences of phosphorylation (Fig 3.6). The Y752 site mapped to a critical region for RBD: Ras binding. Residues in the RBD at this location make a highly conserved positively charged ridge (highlighted in blue) which forms the basis for binding to a negatively charged pocket (highlighted in red) in the Ras Switch I region. Phosphorylation at the Y752 site (highlighted in green) would place a large negative charge in the positive interface and

would be expected to disrupt Ras binding. Data presented later in this chapter confirms this. The Y784 site (highlighted in orange) maps in close proximity to the positive ridge. It is possible that the charge shift from phosphorylation at this site may also disrupt Ras binding, studies to confirm this have yet to be performed.

Sequence analysis of the other known RalGEF family members which have RBDs show both tyrosines are conserved. A majority of other RBD containing proteins surveyed did not have tyrosines at similar locations although they did contain uncharged amino acids (Fig 3.7). Conservation of the RBD phosphorylation sites in all the RalGEFs but not in other Ras effectors suggests a means of uncoupling Ral activation from Ras while not affecting other Ras pathways.

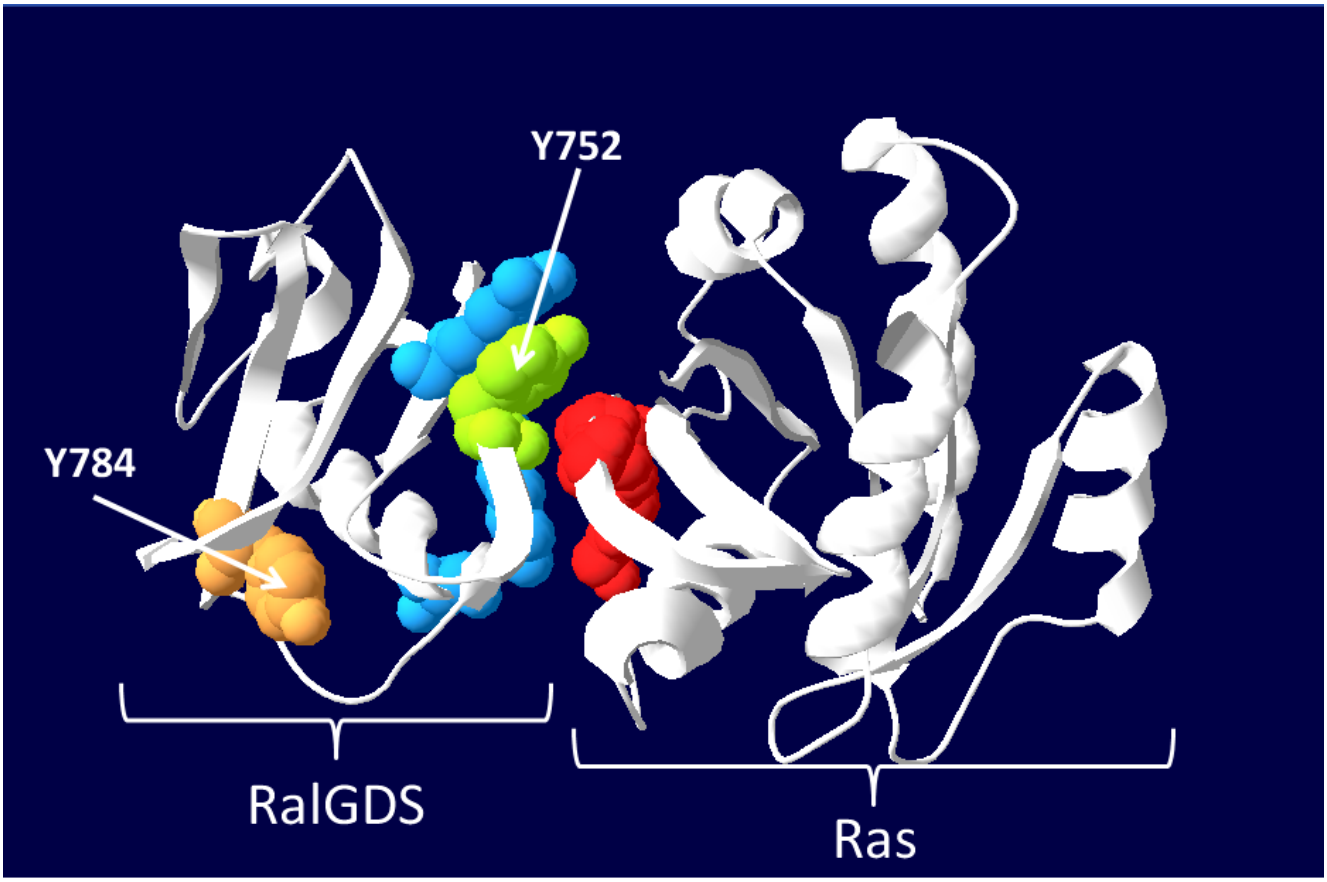

Fig 3.6 Mapping of the RalGDS tyrosine phosphorylation sites Y752 and Y784 in the RalGDS-RBD:RAS crystal structure.

Using the solved crystal structure for RalGDS RBD bound to Ras we modeled the location of the Y752 (highlighted in green) and Y784 (highlighted in orange) phosphorylation sites. Y752 resides in a highly conserved positive charged ridge (residues highlighted in blue) which forms an interaction with a negative charged pocket (highlighted in red) in the Ras Switch I domain.

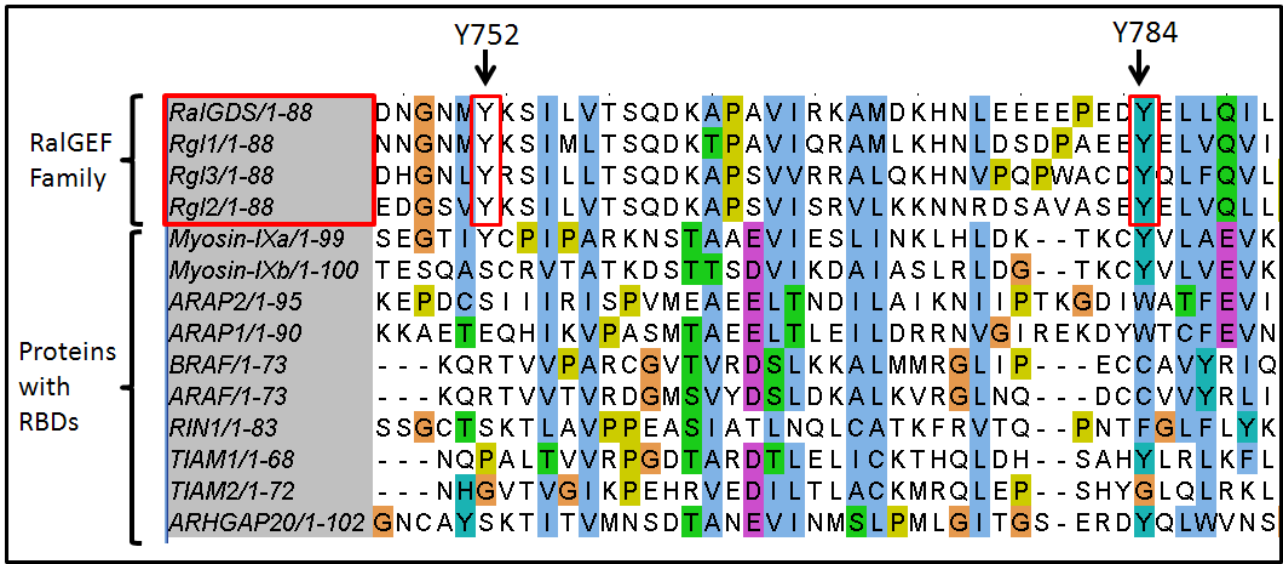

Fig 3.7 RBD phosphorylation sites are conserved among RalGEF family members

Sequence alignment of RalGEF family members which contain RBDs show conservation of the Y752 and Y784 phosphorylation sites. A survey of other RBD containing proteins shows little conservation at similar locations. [RalGDS sequence Accession ID Q03385]

A third phosphorylation site (Y463) mapped within the Cdc25 catalytic domain of RalGDS. Although there is no crystal structure for this Cdc25 domain there are solved structures for the RalGEF RalGPS1a and RasGEFs Sos1 and RalGRF1 Cdc25 domains. Using the Sos1, RasGRF1, and RalGPS structures as templates, we localized the Y463 site to the Flap2 region of the Cdc25 domain (Fig 3.8). Flap1 and Flap2 are conserved structural regions that serve to buttress the catalytic helical hairpin of the Cdc25 domain. Studies in RalGPS1a and RasGRF1 find the interaction with the Flap regions important in maintaining the catalytic hairpin in an orientation optimal for facilitating exchange [100, 101]. In RasGRF1 and RalGPS1a the flap regions are tightly associated with the catalytic hairpin maintaining it in an active orientation (Fig 3.9). In Sos1 the Flap2 region has a wider gap with the catalytic hairpin and it is speculated the

movement of the hairpin relative to the flaps allows for the shifting of the hairpin in and out of an optimal exchange orientation. The Y463 site is provocative in that it sits in between the residues Asn462 and Arg467 which are conserved among the RalGEF family members. The two amino acids help form a positively charged interface at the center of the Flap 2 region which is the basis of a tight polar interaction with the catalytic hairpin in RalGPS1a. The charge shift as a result of phosphorylation at Y463 would most likely destabilize Flap2 association with the catalytic hairpin and possibly have a negative impact on the catalytic activity of the hairpin. Studies to confirm this hypothesis are in progress.

The fourth phosphorylation site (Y52) mapped to the REM domain of RalGDS (Fig 3.10). The association of the REM domain with the Cdc25 domain and its possible consequences on catalytic activity was discussed in Chapter 2. Briefly, the REM domain associates with the catalytic hairpin in a manner similar to the same domains in Sos1. In Sos1 this association helps keep the hairpin in orientations that increase or decrease catalytic activity based on allosteric binding. Charge mutations to the region of association have been shown to decrease catalytic activity in Sos1. A phosphorylation at Y52 would put a negative charge in close proximity to the region of association and would be expected to negatively impact exchange activity. Studies to confirm this hypothesis are in progress.

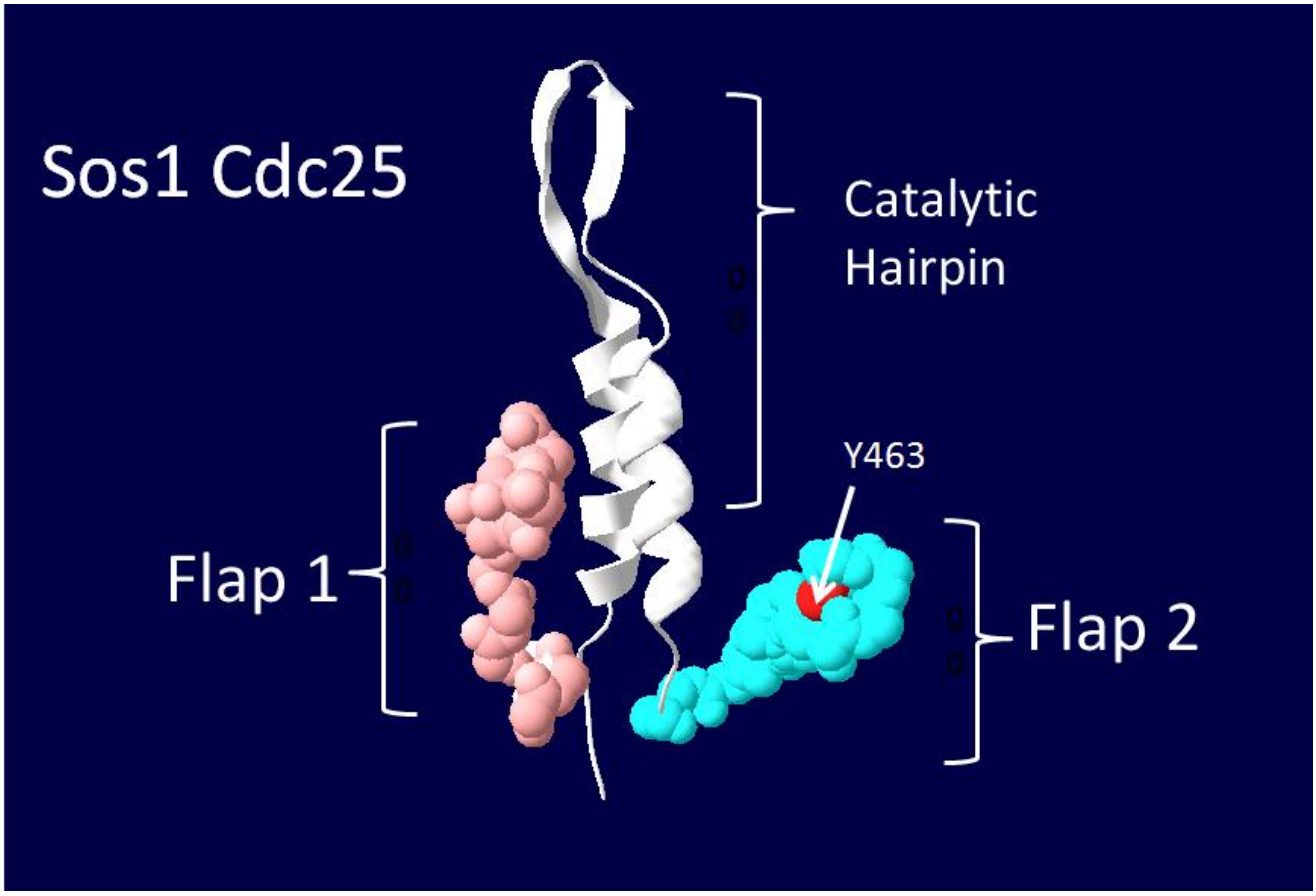

Fig 3.8 **Mapping of the RalGDS tyrosine phosphorylation site Y463 to the Sos1 crystal structure**.

The approximate location of the Y463 site found in RalGDS (highlighted in red) was mapped to the Sos1 crystal structure. The site resides in the Flap2 region of Cdc25 domain (highlighted in blue). Both Flap1 and Flap 2 regions have a role in buttressing the catalytic hairpin of Cdc25 regions.

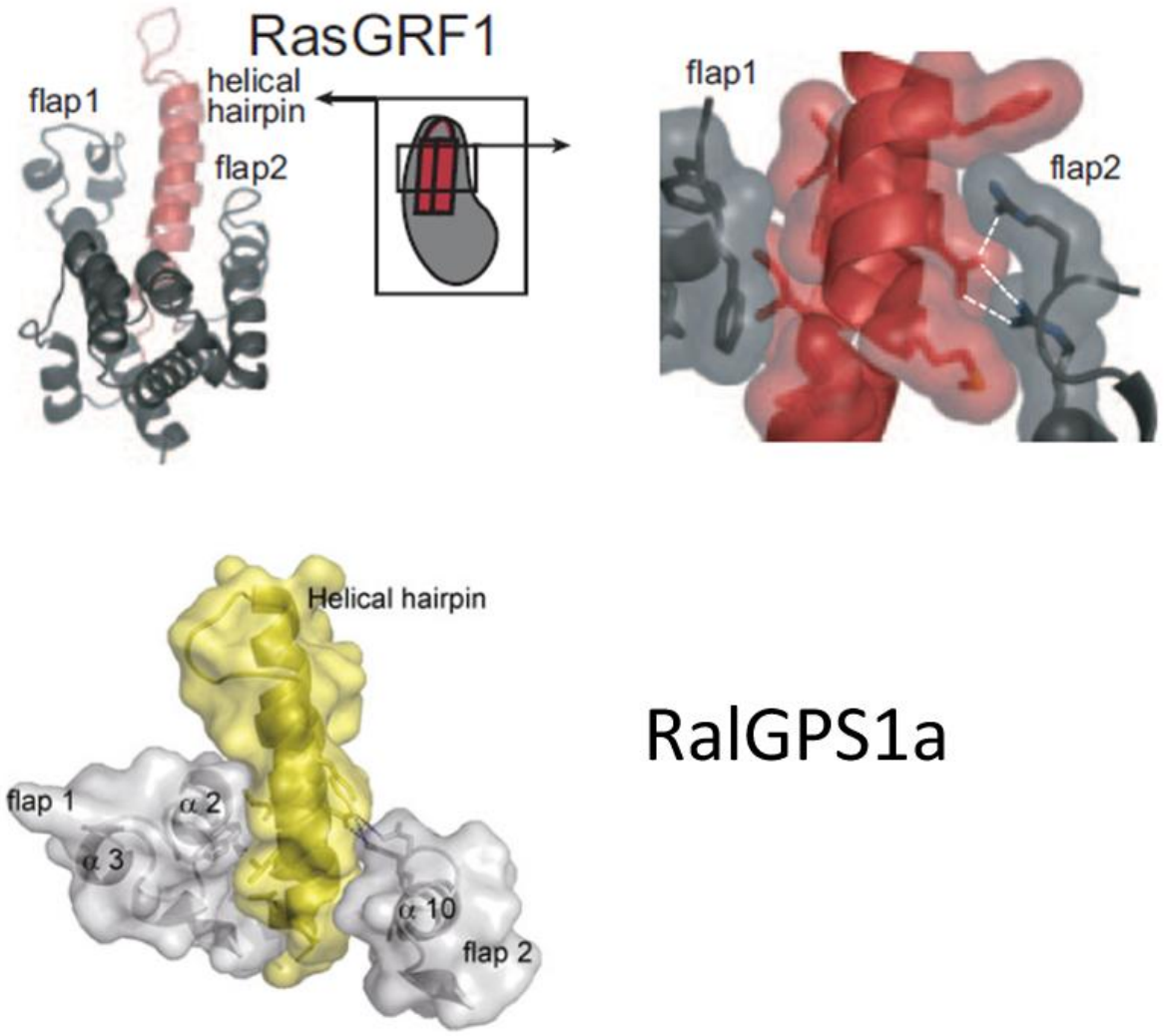

Fig 3.9 Flap buttressing of the Helical hairpin in RasGRF1 and RalGPS1a

RasGRF1 and RalGPS1a have flap regions which are tightly associated with the Helical hairpin of the Cdc25 domain, as compared to Sos1 (Fig 3.7) which has a Flap 2 region with a lager gap from its hairpin [100, 101].

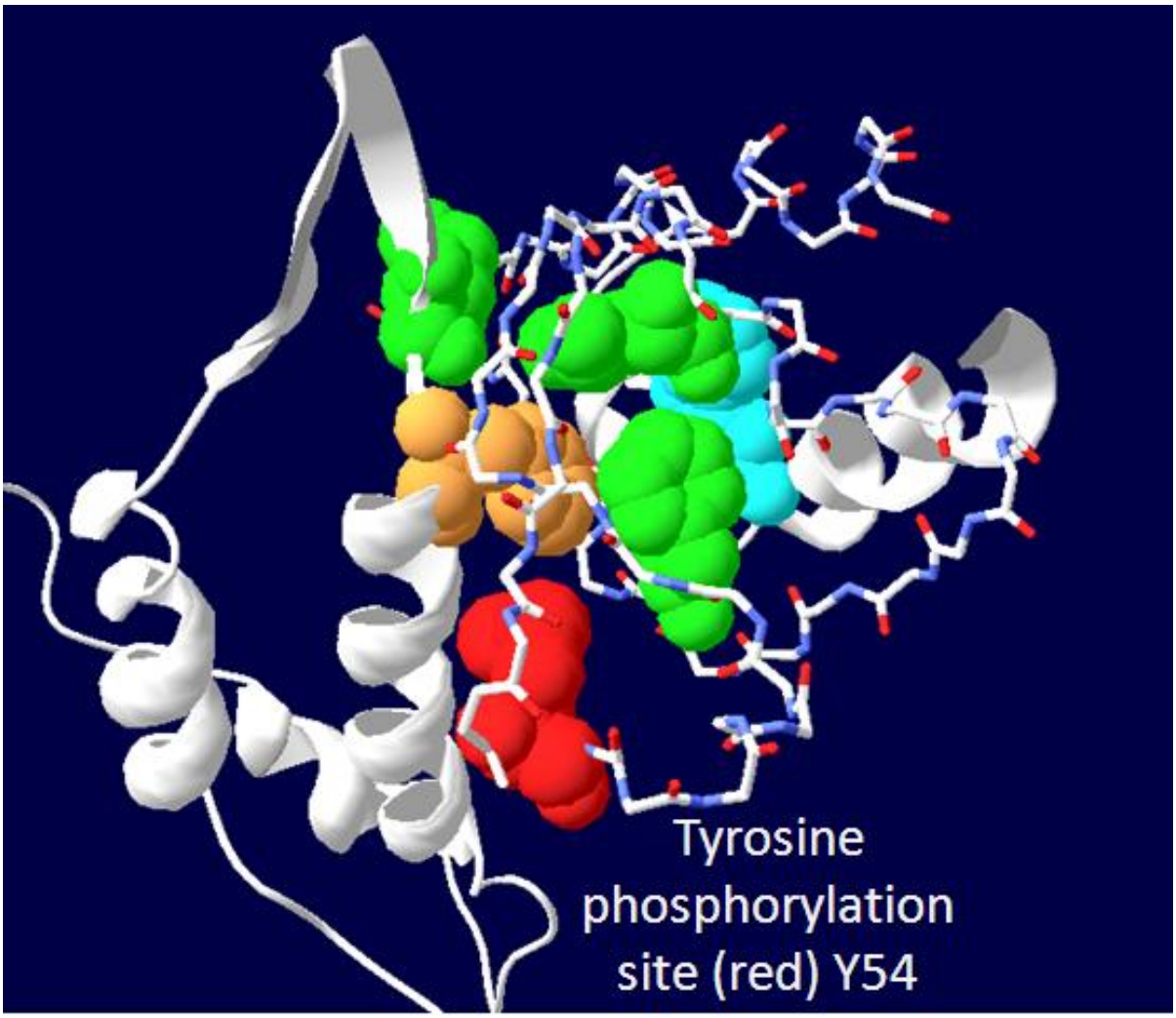

Fig 3.10 Mapping of the RalGDS tyrosine phosphorylation site Y54 to the Sos1 crystal structure.

The approximate location of the Y54 site found in RalGDS (highlighted in red) shows its proximity to the hydrophobic pocket at the center of the REM: Cdc25 association. The highlighted green Van der Waals force residues represent critical hydrophobic amino acids conserved between Sos1 and RalGDS. The highlighted beige residue represents a phenylalanine in Sos1 that is a tyrosine in RalGDS, both residues maintain the hydrophobic nature of the pocket. The highlighted in blue residue represents an identified mutation site in Rgl1.

3.2.2 Phosphorylation at Y752 uncouples RalGDS from Ras

Crystal structure analysis of the Y752 site suggested that phosphorylation there would disrupt RBD binding to Ras. To test this we began by making a phospho-mimetic mutation in the RBD (GST-Y752E RBD) and tested its ability to bind Ras. When compared to wildtype RBD we found that GST-Y752E RBD immobilized on glutathione beads was not able to pull down either H-Ras or K-Ras12V from transfected Cos-7 cells (Fig 3.11). These results confirmed to us that a charge shift similar to one seen with phosphorylation at Y752 severely blocks the ability of the RBD to bind to Ras.

To further study the biology of the Y752 site we generated a phospho specific antibody to this location. With this antibody we confirmed the mass spectroscopy analysis showing that c-Met co-transfection with RalGDS in Cos-7 cells generated phosphorylation at the Y752 site (Fig 3.12). In an attempt to identify a kinase downstream of c-Met signaling that could be mediating RalGDS phosphorylation, we tested an active Src kinase (SrcF527). Co-transfection of active Src with RalGDS generated robust tyrosine phosphorylation as determined by a total phospho-tyrosine antibody. Evidence of Src mediated phosphorylation at the Y752 site was seen as well but to a lesser degree than phosphorylation generated by c-Met (Fig 3.12). This suggests that Src or its family members could be mediating c-Met phosphorylation of RalGDS in the gastric cancer lines. We next treated Myc-RalGDS expressing KatoII cells with a Src kinase family inhibitor (PP2) and found that total tyrosine phosphorylation of RalGDS was greatly diminished (Fig 3.13). These results suggest that a majority of the tyrosine phosphorylation on RalGDS may be mediated by Src family kinases.

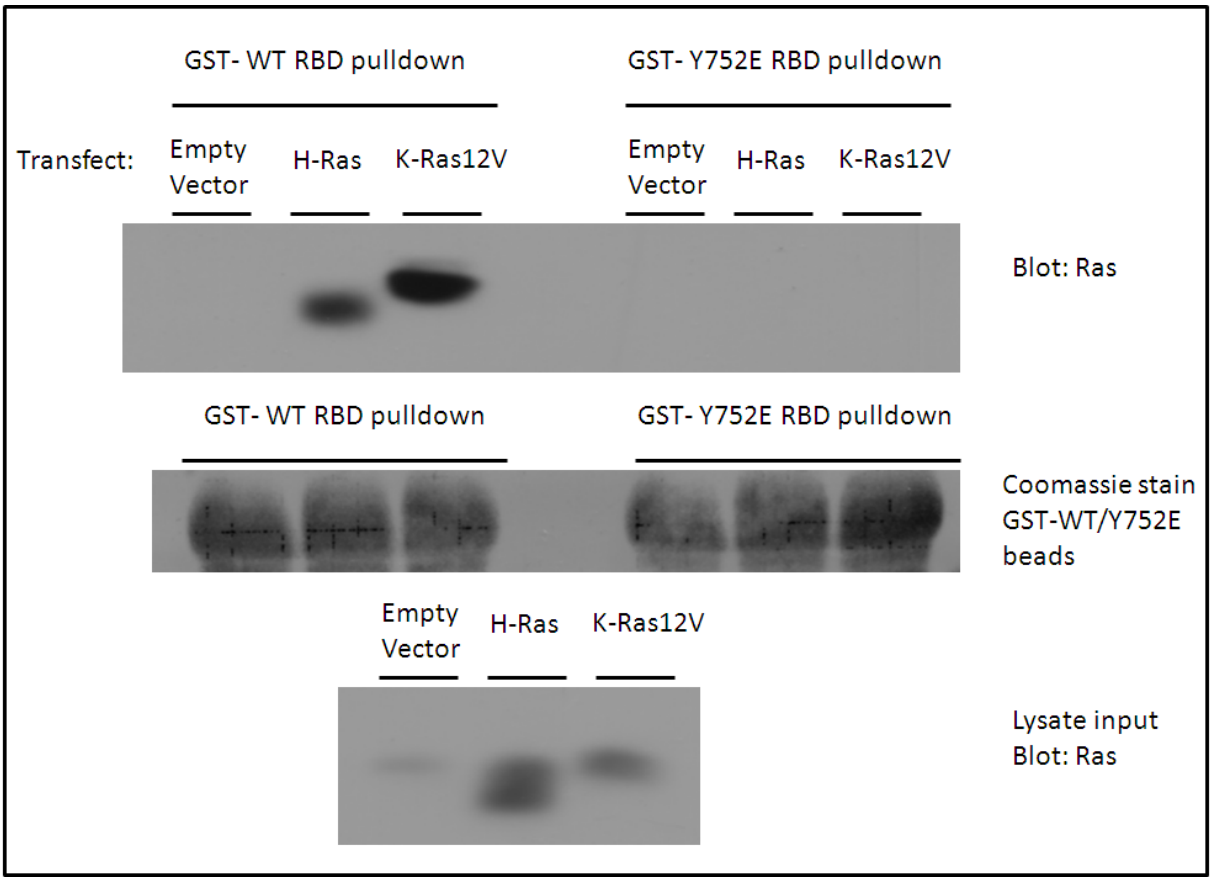

Fig 3.11 Y752E phosphomimetic mutation blocks RBD binding to Ras

GST-wildtype RBD and GST-Y752E RBD bound to glutathione agarose beads were tested for ability to bind exogenously expressed H-Ras and K-Ras12V. Lysate from Cos-7 cells expressing the Ras constructs was evenly divided and incubated with wildtype or Y752E RBD beads. Samples were run on a gel and blotted for Ras. Wildtype RBD was found to bind both H-Ras and K-Ras12V while Y752E RBD did not show binding to either Ras construct. GST-RBD protein from the beads was assessed by coomassie stain.

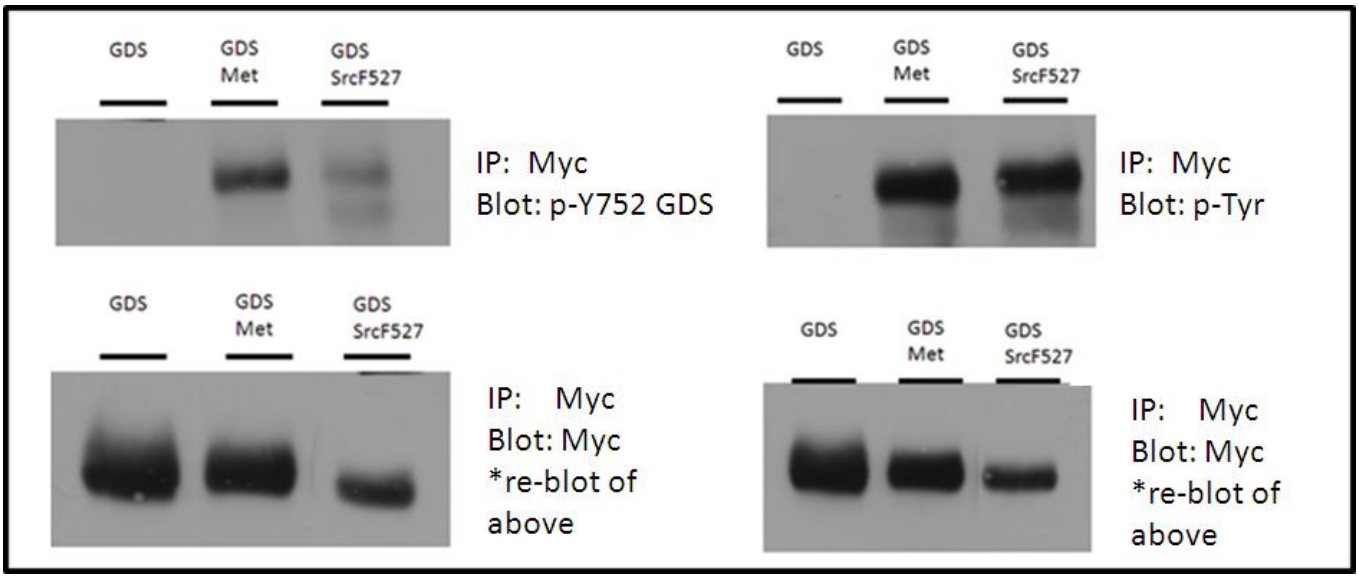

Fig 3.12 **Y752 phospho-specific antibody confirms c-Met and Src mediated phosphorylation**

Cos-7 cells were transfected with Myc-RalGDS alone or with C-Met or SrcF527 expression constructs. Cells were lysed and subject to Myc immuno-precipitation. Purified Myc-RalGDS was divided evenly and blotted with total phospho-tyrosine antibody or Y752 phospho-specific antibody. Cells co-transfected with c-Met or Src F527 resulted in RalGDS phosphorylation at the Y752 site.

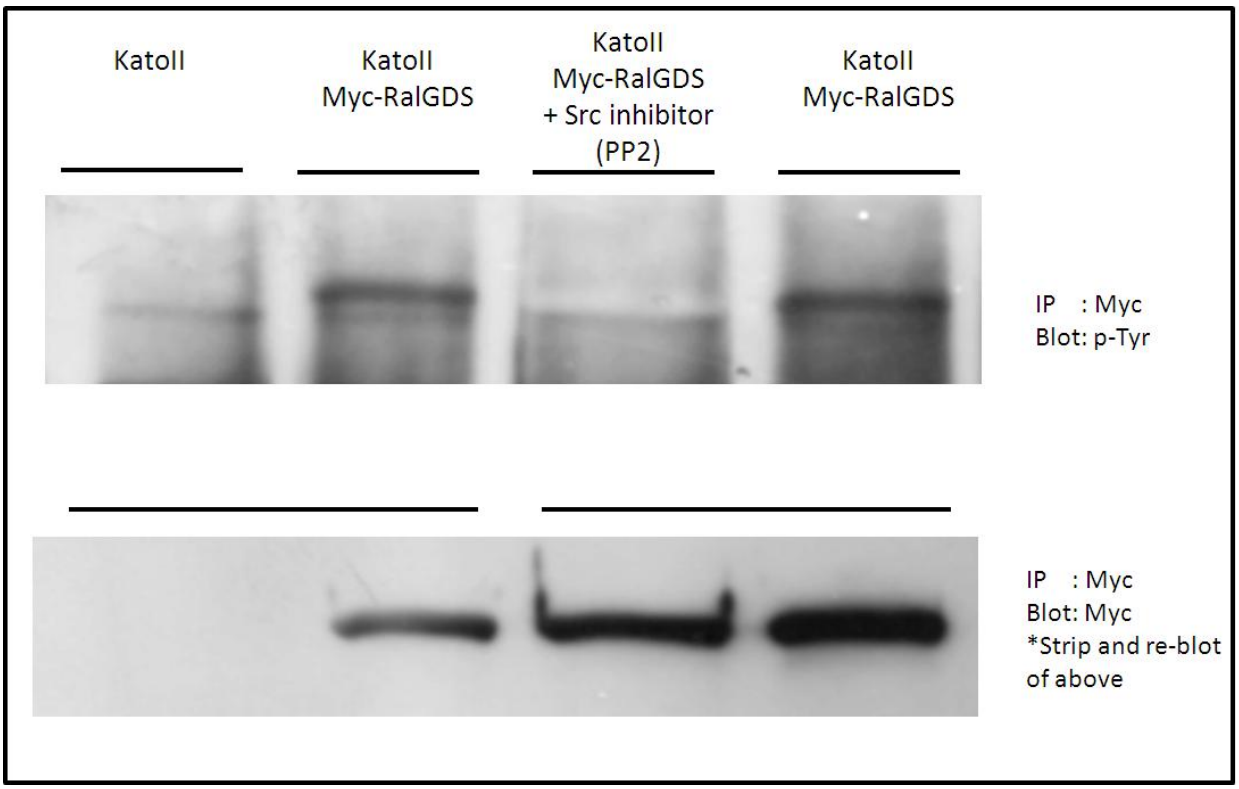

Fig 3.13 Src inhibitor blocks RalGDS phosphorylation

KatoII cells transfected with a Myc-RalGDS expression construct were treated with 10uM Src Kinase inhibitor PP2 (Calbiochem) for 4 hours, lysed, subject to Myc immuno precipitation, and blotted with a total phospho-tyrosine antibody. Phospho-tyrosine blots were stripped and re-blotted with Myc antibody to assess Myc-RalGDS pull down.

Next we tested if phosphorylation at the Y752 site blocked binding to Ras. To achieve this, we setup an experiment in which lysate from c-Met and Myc- RalGDS co-transfected Cos-7 cells was divided and subject to either Myc immunoprecipitation or GST-Ras pull down (diagramed in Fig 3.14). Myc pulled down both phosphorylated Y752 and non phospho-Y752 RalGDS. Because the Myc pull down is expected to show no preference between the two populations we can presume the amount of phosphorylated RalGDS represents the percent of phosphorylation for the given total amount of RalGDS (Fig 3.15). GST-Ras was unable to pull down detectable levels of Y752 phosphorylated RalGDS. At similar total amounts of RalGDS pulled down between Myc and GST-Ras a comparable percent of phospho-Y752 found in the Myc pull down is not seen in GST-Ras pull down (Fig 3.15). This indicates that Ras is unable to bind efficiently to the population of RalGDS that is Y752 phosphorylated.

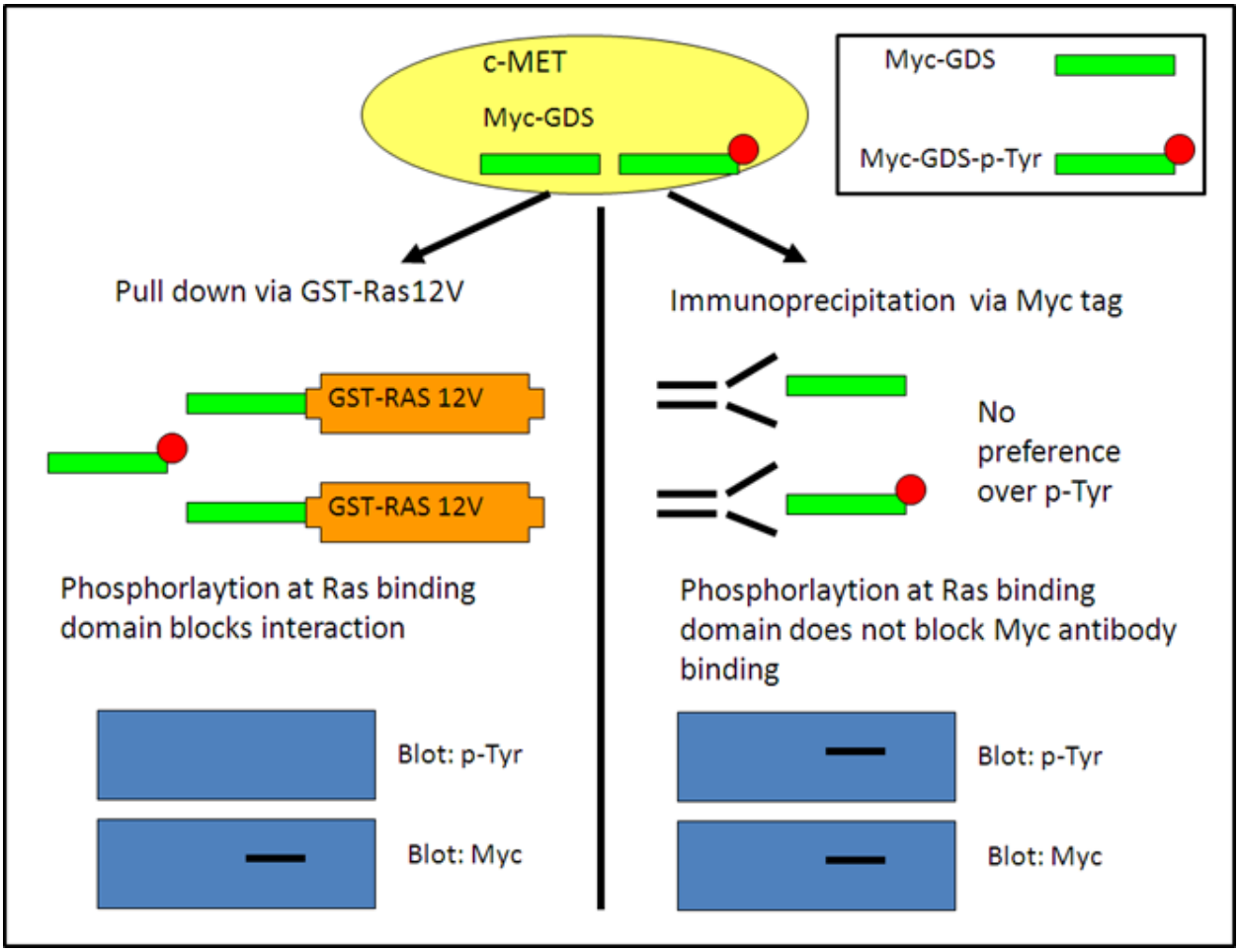

Fig 3.14 Assay schematic of GST-Ras vs. Myc pull down of RalGDS

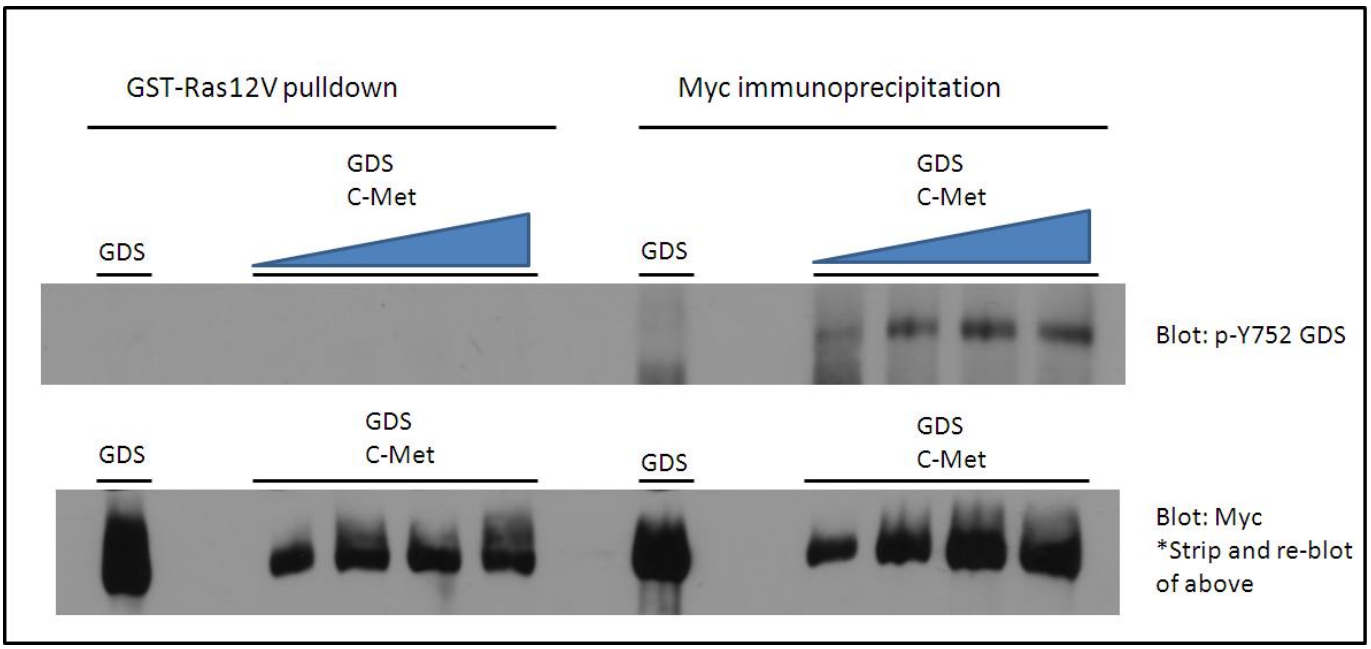

Fig 3.15 Phosphorylation at Y752 is incompatible with Ras binding

Assay was setup as diagramed in Fig 3.14. Increasing volumes from a single pool of Myc-RalGDS, c-Met co-transfected cell lysate was incubated for GST-Ras12V pull down or Myc immuno-precipitation. At similar amounts of RalGDS pulled down (as seen in the Myc re-blot) no Y752 phosphorylated protein was found in the Ras pulldown.

3.2.3 Ral activation is uncoupled from c-Met signaling in oncogene addicted gastric cancer cells.

Having shown c-Met mediated RalGDS uncoupling from Ras, we next assessed Ral activation in c-Met amplified gastric cancer lines MKN45 and KatoIII. Both lines have been used as models for c-Met oncogene addiction and test cells in the design of c-Met inhibitors. Studies in these cells have shown that, Ras and its effectors through Raf and AKT are activated while most other c-Met downstream pathways are inactive [16]. No characterization had been done

in regards to the Ral activation status of these cells. Our studies suggest that c-Met activation would uncouple and possibly inactivate RalGDS from active Ras, thus resulting in reduced Ral activation.

To test our hypothesis, we treated KatoIII and MKN45 cells with 1uM of c-Met inhibitor for 3 hours and then washed out the inhibitor to allow c-Met signaling to resume. These cells were then analyzed for Ral activation, AKT, and c-Met phosphorylation. After three hours of inhibition, c-Met and AKT phosphorylation were greatly decreased as compared to untreated cells (Fig 3.16). After three hours of inhibitor washout we saw an increase in AKT and c-Met phosphorylation, but we did not see an increase in Ral activation (Fig 3.16), even though c-MET has the capacity to acutely activate Ral in non-addicted cells [102]. These experiments were repeated multiple times, all with similar results.

We also noted that after 3 hours of inhibitor there was no decrease in Ral activation. In fact, a slight increase was usually observed, although we could not confirm that the result was statistically significant. A hypothesis for this phenomenon is that as c-Met is inhibited, RalGDS is no longer inhibited. If other signals are still activating Ras in these cells, we would expect to see an increase in Ral activation (diagramed in Fig 3.17).

These findings support our hypothesis that Ral activation is uncoupled from Ras signaling in c-Met addicted cancer cells. However, these observations could also be explained if c-MET were activating a RalGAP. In order to confirm that the effects are through RalGDS, we need to express a RalGDS protein in these cells that cannot be downregulated by tyrosine phosphorylation and show that restoration of c-Met signaling by inhibitor washout now leads to Ral activation. Unfortunately, we need to characterize the other tyrosine phosphorylation sites

and if they are involved in inhibition, a multiply mutated RalGDS must be used. This approach will be followed in the future.

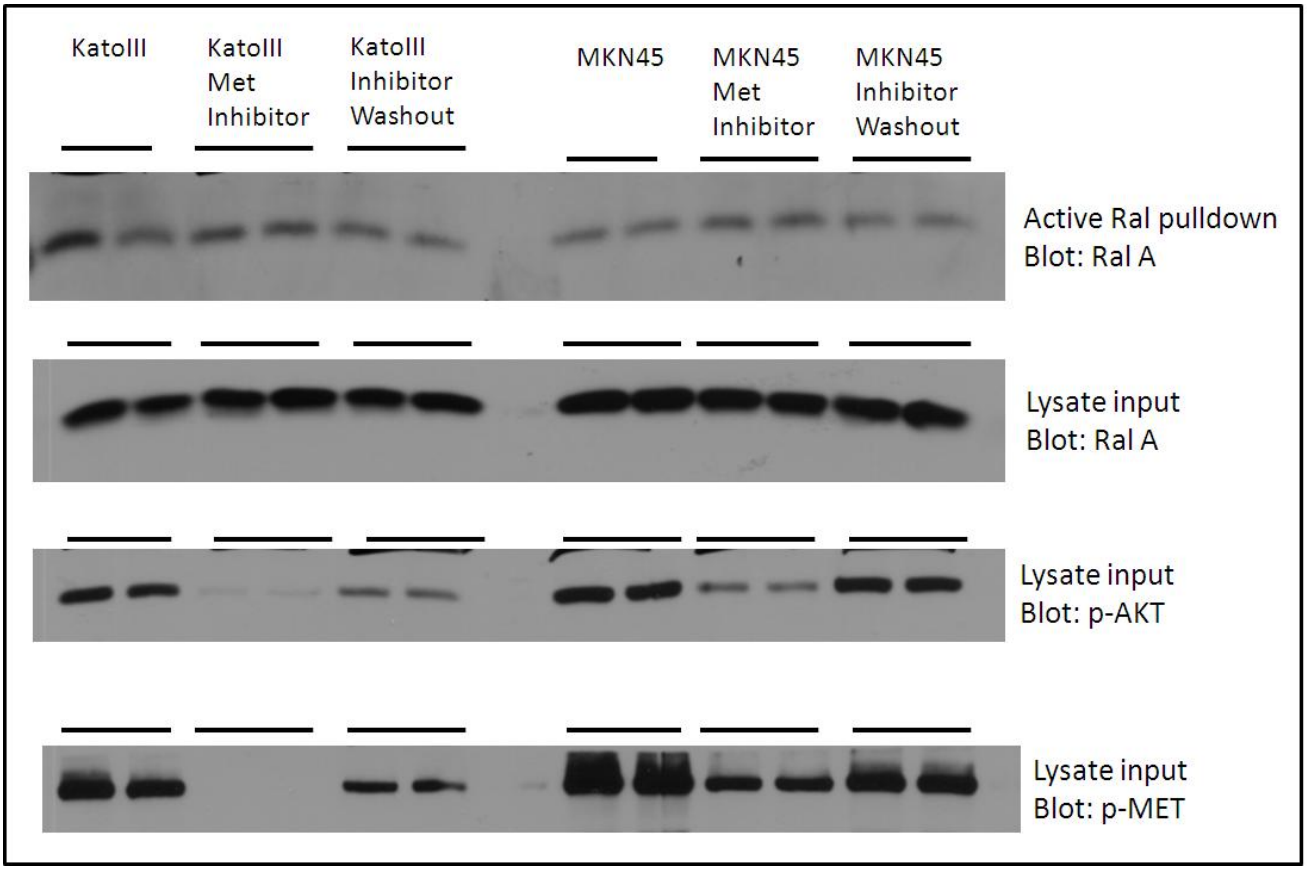

Fig 3.16 Ral activation is uncoupled from c-Met signaling in oncogene addicted gastric cancer cells.

KatoIII and MKN45 cell lines were incubated with 1uM Met inhibitor for 3 hours and then inhibitor washout for 3 hours. A second set of cells were also treaded with inhibitor during the 3 hour washout to give an idea of the level of inhibition the washout cells were recovering from. Cells were lysed and subject to active Ral pull down and blot with RalA antibody. Cell lysate was also blotted for phospho-AKT and phospho-MET to confirm efficacy of inhibition and wash out. Active Ral pull down shows no increase in Ral activation from c-Met recovery during washout.

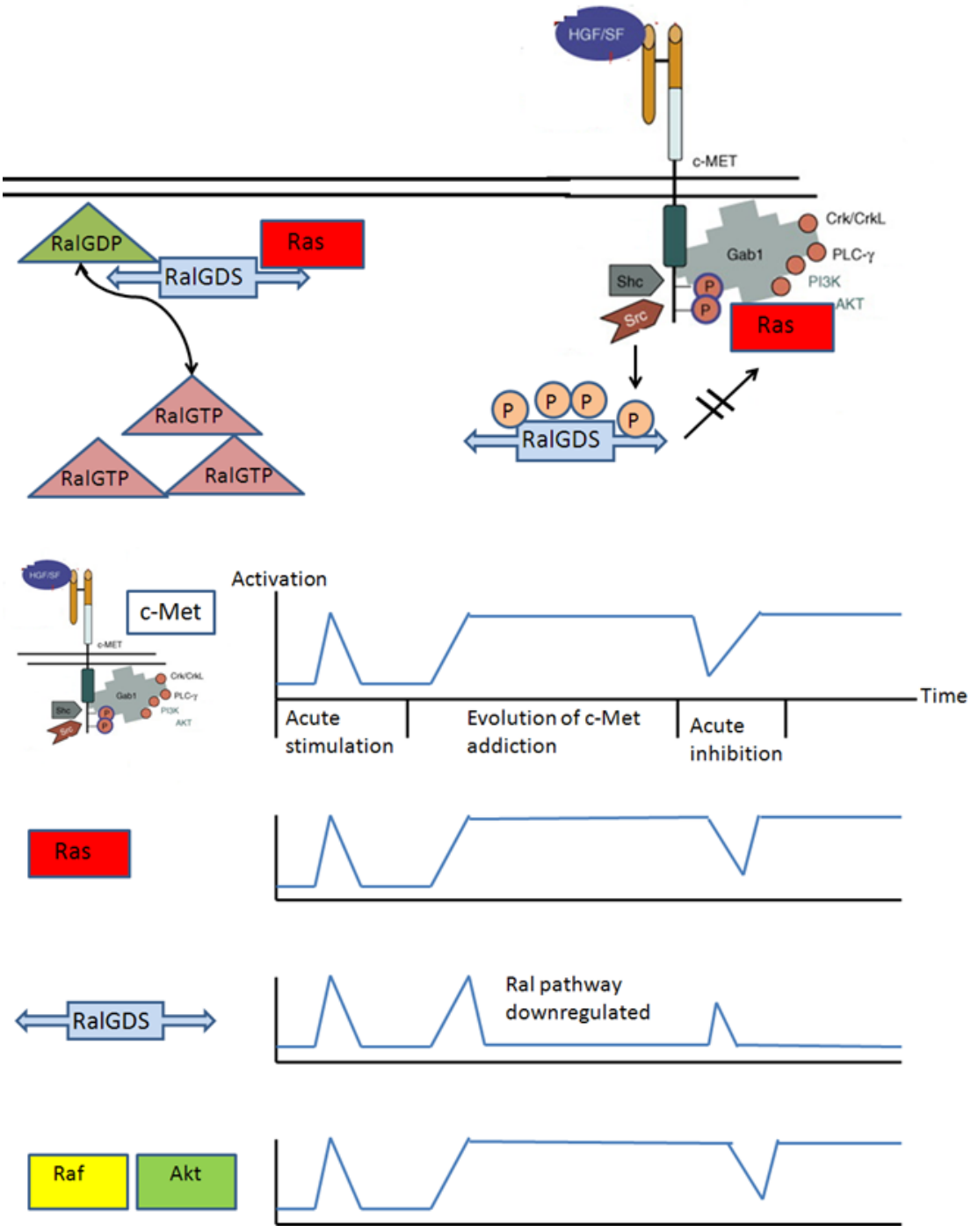

Fig 3.17 RalGDS regulation altered in c-Met addiction

c-Met signaling in normal cells has been shown to transiently activate Ras and subsequently Ral through RalGEFs. In c-Met oncogene addicted MKN45 and KatoIII cells we find that Ral activation is uncoupled from c-Met signaling through phosphorylation of RalGDS, possibly mediated through Src kinase.

3.3 Discussion

Under the theory of Oncogene addiction as cancers evolve, cells become dependent on key signaling pathways related to proliferation and pro-survival [96]. Identifying the initiators and mediators of these pathways is a key step in the development of targeted cancer therapeutics. Mutations or amplifications of the tyrosine kinase receptor c-Met has been found in a variety of cancers such as breast, lung, and gastric [16, 98, 103, 104]. c-Met addicted gastric cancers are often highlighted as prime examples of oncogene addiction because only a subset of the downstream pathways are sustained and required for cell survival. Labs have found introduction of mutationally active Ras or its effectors Raf or AKT could rescue growth arrest from c-Met inhibition in gastric cancer cell lines [16]. Active Raf or AKT alone could not rescue inhibited cells as efficiently as Ras suggesting a role for other effectors. Not mentioned in these studies was an analysis of RalGEFs so we initiated work to examine their role in c-Met oncogene addiction.

Our initial hypothesis was that Ral activation through RalGDS would be one of the Ras effector pathways kept on in c-Met addiction. Studies of Ras driven tumorigenisis in kidney cells found that constitutively active RalGEF could take the place of active Ras in maintaining anchorage independent growth [105]. Other work found RalGDS knockout mice had impaired tumor formation of Ras driven skin carcinomas from DMBA/TPA treatment [36]. Knockdown of Ral in HT-1080, J82 and SW-620 cancer cell lines inhibited their ability to form tumors in the flanks of immunocompromised mice [106]. In light of these studies it is provocative and potentially significant that RalGDS and subsequently Ral activation is actively down regulated in c-Met addicted cancer cells.

Our initial finding that RalGDS is tyrosine phosphorylated at multiple sites in response to c-Met signaling represents a first for the Ral family of exchange factors. There is currently no published evidence of any RalGEF being functionally tyrosine phosphorylated. Previous studies done in our lab found PKC is able to down regulate RalGDS activity through an unidentified serine/threonine phosphorylation in the protein's N-terminus [107]. There is also evidence that PKC may phosphorylate a C-terminal site in the RalGEF Rgl2 that in theory could uncouple Ras binding [34]. Our current studies are the first identification and functional characterization of RalGEF phosphorylation in a cancer setting.

Of the four c-Met mediated phosphorylation sites identified, Y752 was the first to be confirmed and characterized. Phosphorylation at this site resulted in uncoupling of RalGDS from active Ras. This marks a novel mechanism of regulation for the RalGEF family of Ras effectors. To the best of our knowledge this is also the first functional evidence of this direct mechanism of regulation in any Ras effector. The Y752 site is conserved throughout all RBD containing RalGEFs and is not found in most other RBD containing proteins. This fact suggests a means of uncoupling the entire Ral effector pathway at Ras activation complexes while not influencing other types of Ras effectors.

Phosphorylation at the three other identified sites map to regions of the protein that suggest they would have a negative effect on catalytic activity and Ras binding. Further studies are needed to confirm these biological effects. If verified for their believed effects, the generation of a RalGDS phosphorylation resistant mutant at all four sites is need to prove that c-Met is down regulating Ral activation through RalGDS and not activating a RalGAP.

The possible redundant mechanisms of down regulation suggest RalGDS inhibition in the c-Met amplified setting may be a result of selective pressure and not a happenstance occurrence. In c-Met addicted MKN45 and KatoIII cancer cells we found Ral activation to be uncoupled from the sustained c-Met activation. In normal cells acute c-Met activation from HGF has been documented to increase RalGTP levels [102]. Multiple attempts at stably expressing RalGDS or active Ral A in these gastric cancer cell lines were unsuccessful as compared to the stable expression of GFP using the same delivery vectors (data not shown). These findings suggest that Ral activation had a detrimental effect on c-Met addicted cells.

Studies by other labs found that Src inhibition blocked soft agar growth of MKN45 cells while not drastically effecting c-Met or AKT activation [99]. This led the authors to propose that a Src mediated pathway is essential for c-Met addicted cancers to be sustained. The specific mechanism this has yet to be identified. Our findings that Src mediates at least one phosphorylation site on RalGDS suggests that Ral inhibition may be a necessary function in c-Met addiction. If true then the targeted activation of the Ral pathway in these types of cancers may be a valuable therapeutic tool. This may seem counter intuitive since there have been studies highlighting the ability of activated Ral signaling to replace Ras activation in promoting anchorage independent growth [105]. Studies have also shown active RalA is needed for tumor formation in various cancer cell lines [106]. But recent work in our lab has shown RalA activation can have a negative effect on the invasiveness of Ras-induced human squamous cell carcinoma through the recycling of E-cadherin to the plasma membrane. Further work has also shown that the invasiveness of this type of carcinoma is driven in part by c-Met signaling through the constant secretion of HGF from surrounding stromal cells [108]. It is possible that down regulation

of Ral may be a necessary function in c-Met driven cancers and not other oncogene driven malignancies.

If activation of the Ral pathway does prove detrimental to c-Met addicted cancers, it would highlight a caveat to the theory of oncogene addiction. Current models suggest the upregulation of specific pro-survival and anti-apoptotic signaling pathways are the most important factors in addiction. With this in mind the inhibition of the addicted pathways has become the primary goal in developing treatments for such cancers. Unfortunately current targeted therapies are often plagued by the fact that cancers will evolve a compensating activation to the inhibited pathway [76, 78, 95]. In a more nuanced description of oncogene addiction, cancers may be equally dependent on the down regulation of specific pathways as it is on the upregulation of other pathways. With this in mind a combination approach where some pathways are reactivated while others are inhibited may prove highly effective in combating some cancers. Ral activation may be one such candidate for a combination with c-Met inhibitors in the treatment of c-Met addicted cancers.

3.4 Future directions

Further characterization of the Y52, Y463, and Y784 phosphorylation sites are necessary to gain a better understanding of their effects on RalGDS. Phospho-mimetic and resistant mutations will be made at these sites in the full length and domain specific expression constructs. The Y52 site which may affect REM: Cdc25 association will be tested for changes in association between the two domains using binding assays highlighted in Chapter 2. A full length protein with phospho-mimetic mutations to the Y52 or Y463 site will be tested for changes in exchange

activity. We hypothesize that the mutations will have a negative effect on exchange activity. The Y784 site will be tested for possible effects on Ras binding using similar experiments highlighted in this chapter in the characterization of the Y752 site.

The inability of c-Met to activate Ral in our studies if suggestive but not conclusive of RalGDS being uncoupled or inactivated. It remains possible that c-Met may be activating a RalGAP. There is only one known RalGAP complex which has been just recently identified [109, 110]. Characterizing the regulation of this protein complex is ongoing and may lend insight to what role if any c-Met has. To confirm c-Met inhibition of RalGDS we will generate a full length RalGDS with phospho-resistant tyrosine to phenylalanine mutations to all four identified phosphorylation sites. This mutant will be expressed in MKN45 and KatoIII cells and compared to cells expressing wildtype protein. We believe that the phospho-resistant mutant will show restored coupling of Ral activation to c-Met signaling, and with it some negative growth consequence for the cell.

Due to difficulties maintaining stable expression of both RalGDS and active RalA in c-Met addicted cells, an inducible system will be created to express active RalA. These cells will be tested in proliferation and soft agar growth assays for changes due to Ral activation. We suspect that Ral activation will have a detrimental effect on one or more of these processes, hence the phosphorylation mediated uncoupling of the pathway in the c-Met addicted cells. With these same experiments we will also follow up published work showing Src inhibition blocks soft agar growth of MKN45 cells. We have shown that Src mediates the phosphorylation of RalGDS and that Ral activation is blunted in these cells. It is possible the mechanism of Src's sustaining of growth is through Ral suppression. We will attempt to rescue MKN45 cells treated with Src inhibitor by expressing a dominant negative RalA. If Ral effector suppression is the

role of Src in c-Met addticted cells, the dominant negative construct will rescue the soft agar growth of inhibited cells.

Chapter 4: RalGDS associates with 14-3-3σ under oxidative stress

4.1 Introduction

Following initial observations of RalGDS phosphorylation described in Chapter 3, we postulated that the modification may mediate binding to other proteins. Having not yet identified the role of c-Met we used Pervanadate, a H_20_2 activated non-specific phosphatase inhibitor to generate phosphorylation on RalGDS. Further characterization of c-Met mediated phosphorylation did not identify new protein binding partners, but in the course of our studies we found that RalGDS bound to 14-3-3σ during oxidative stress from H_20_2 exposure.

14-3-3 proteins make up a diverse family of highly conserved small acidic proteins. The seven family members found in mammals are β, γ, ε, σ, ζ, τ and η. Often acting as homo or hetero dimers they bind to phosphoserine phosphothreonine sites on a vast array of proteins. The 14-3-3 proteins have been shown to act in various cell functions such as cell cycle control, apoptosis, cell migration, and transcriptional activation to name a few [111-113]. 14-3-3σ is unique from its other family members in it primarily forms homodimers. Early studies found 14-3-3σ to be involved with p53 regulation via Mdm2 binding and cell cycle arrest via CDC2 interaction [114]. 14-3-3σ levels were found to be decreased in a variety of cancers and over expressing the protein in some cancer cell lines reduced cell proliferation [115, 116]. Recent studies have begun to highlight various other roles for 14-3-3σ. The protein has been shown to be involved in the sequestering

of transcription factors FOXO1 and COP1[113, 117], mediating chemotherapy drug resistance [116], and inhibiting AKT [112].

The studies described in this chapter will go over some initial observations in characterizing the nature and role of 14-3-3σ binding to RalGDS.

4.2 Results

4.2.1 RalGDS associates with 14-3-3σ under oxidative stress

Early in our studies of RalGDS phosphorylation we hypothesized that the modification may facilitate binding to other proteins. As a robust albeit not specific means of generating RalGDS phosphorylation we used Pervanadate treatment. Pervanadate is a potent phosphatase inhibitor which is generated by H_20_2 incubation with NaVO4 (vanadate). Live cell inhibition with Pervanadate leads to the accumulation of phosphorylated proteins and activation of kinases which are normally inactive due to phosphatase activity [118, 119]. We treated Myc-RalGDS expressing MCF10A breast cells with the inhibitor, immunoprecipitated RalGDS, and looked for proteins that associated in treated vs. non-treated cells. These studies yielded one prominent 28KD protein which associated with RalGDS in treated cells (Fig 4.1). Mass spectroscopy analysis identified the protein as 14-3-3σ.

Follow-up experiments found that the association of 14-3-3σ was mediated by residual H202 used in the activation of Pervanadate. This conclusion was made after prolonged treatment of the Pervanadate inhibitor solution with catalase (a normal step in the activation protocol to eliminate H202) showed diminished 14-3-3σ association while still maintaining a high degree of

RalGDS phosphorylation (data not shown). When Myc-RalGDS expressing MCF10A cells were stimulated with 1mM H_20_2, prolonged catalase incubated Pervanadate, EGF, or insulin, only H_20_2 treatment induced robust 14-3-3σ binding (Fig 4.2).

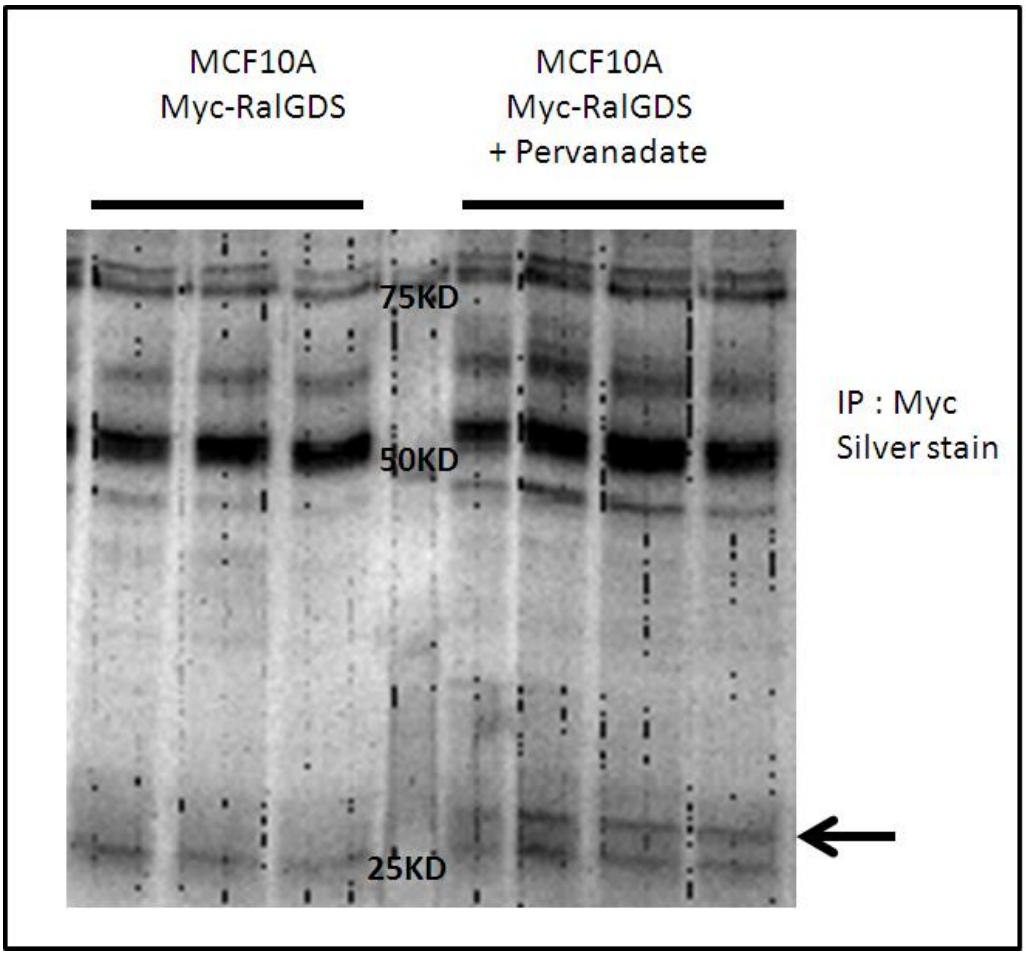

Fig 4.1 Pervanadate treatment causes RalGDS association to 14-3-3σ

MCF10A cells under growth conditions were stably expressing Myc-RalGDS were treated with H_20_2 activated Pervanadate for 10min. Treated and untreated cells were lysed, subject to Myc immunoprecipitation, gel electrophoresis, and silver stained. A prominent 28KD protein (arrow) was found to form a complex with RalGDS in treated cells. This protein was later identified as 14-3-3σ through mass spectroscopy analysis.

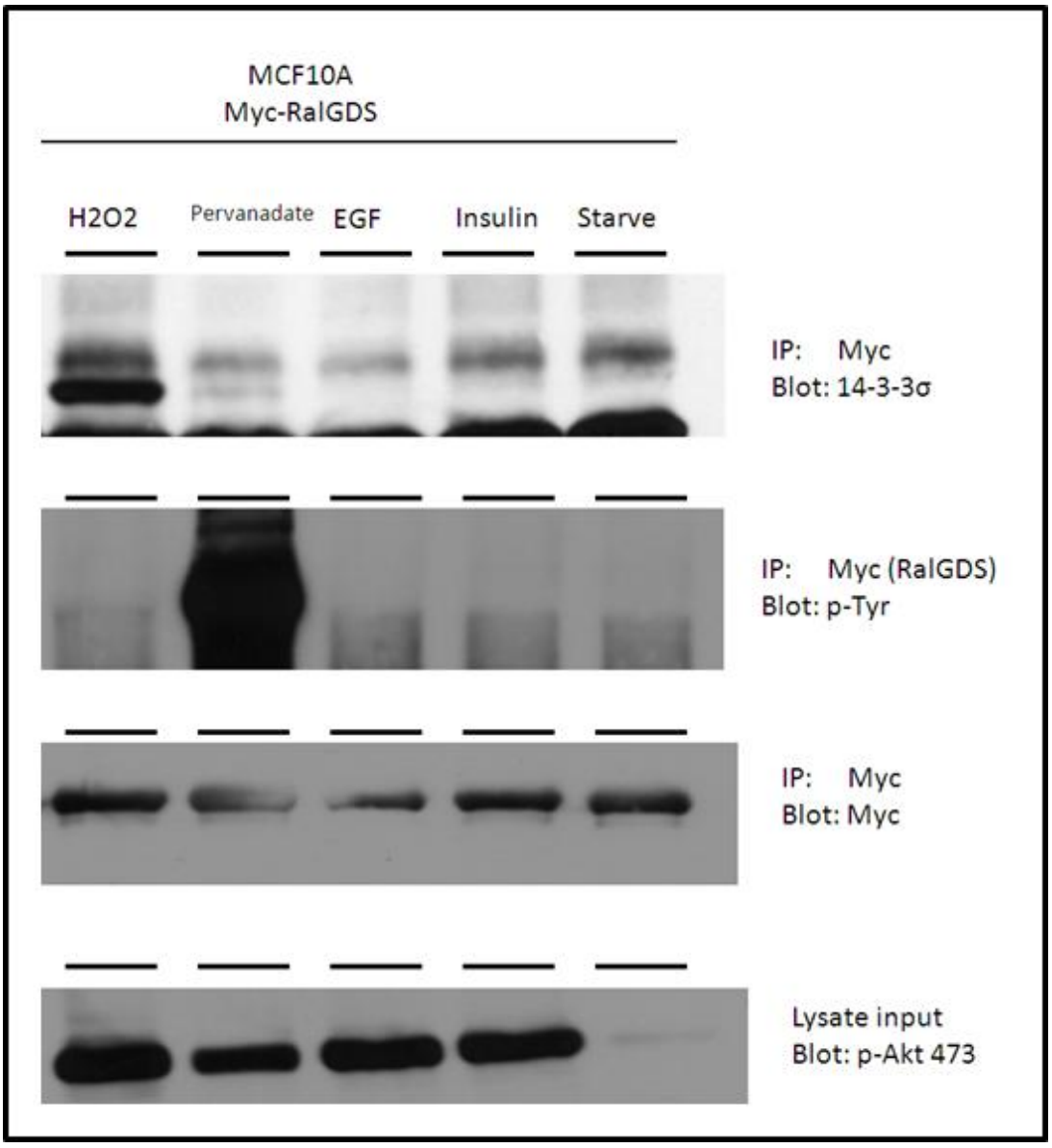

Fig 4.2 H202 stimulation causes 14-3-3σ association to RalGDS

MCF10A cells were serum starved overnight and stimulated for 10min with 1mM H202, prolonged catalyase incubated Pervanadate, EGF, or insulin. Cells were lysed, immunoprecipitatied with Myc antibody, and blotted for 14-3-3σ. Only cells treated with H202 showed robust association to 14-3-3σ. Pervanadate treated cells mediated tyrosine phosphorylation of RalGDS (as seen in p-Tyr blot of immunoprecipitated RalGDS), but this did not result in an increase in 14-3-3σ binding. p-Akt was assayed to confirm activation by the various stimulation agents.

4.2.2 14-3-3σ associates to the C-terminus of RalGDS

To define the region of RalGDS which binds to 14-3-3σ, we performed mapping studies using RalGDS deletion constructs. Four Myc tagged truncation constructs were made (1-586aa, 1-486aa, 301-852aa, and 486-852aa) and each was tested for association with exogenously expressed 14-3-3σ in Cos-7 cells. Progressive N-terminal truncations represented by the 301-852aa and 486-852aa constructs maintained the ability to bind 14-3-3σ. Progressive C-terminal truncations represented by 1-586aa (Ras binding domain truncation) and 1-486aa (RBD + catalytic hairpin truncation) showed diminished association to 14-3-3σ (Fig 4.3). These results show the 14-3-3σ binding site is located within a region of RalGDS, which encompasses the catalytic hairpin of the Cdc25 domain and the Ras binding domain. Binding of 14-3-3σ to this region may alter RalGDS binding to Ras or effect Ral exchange factor activity.

In the course of these mapping assays, Myc tagged Erk1 and Erk2 were also tested for the ability to bind 14-3-3σ. The two kinases were initially included as negative controls but we found Erk1 but not Erk2 bound to 14-3-3σ (Fig 4.3). This finding is interesting because 14-3-3σ has already been shown to bind Akt in an inhibitory manner [112]. The fact that 14-3-3σ can bind mediators of the three major Ras effector pathways suggests that it may play a key role in regulating Ras effector signaling.

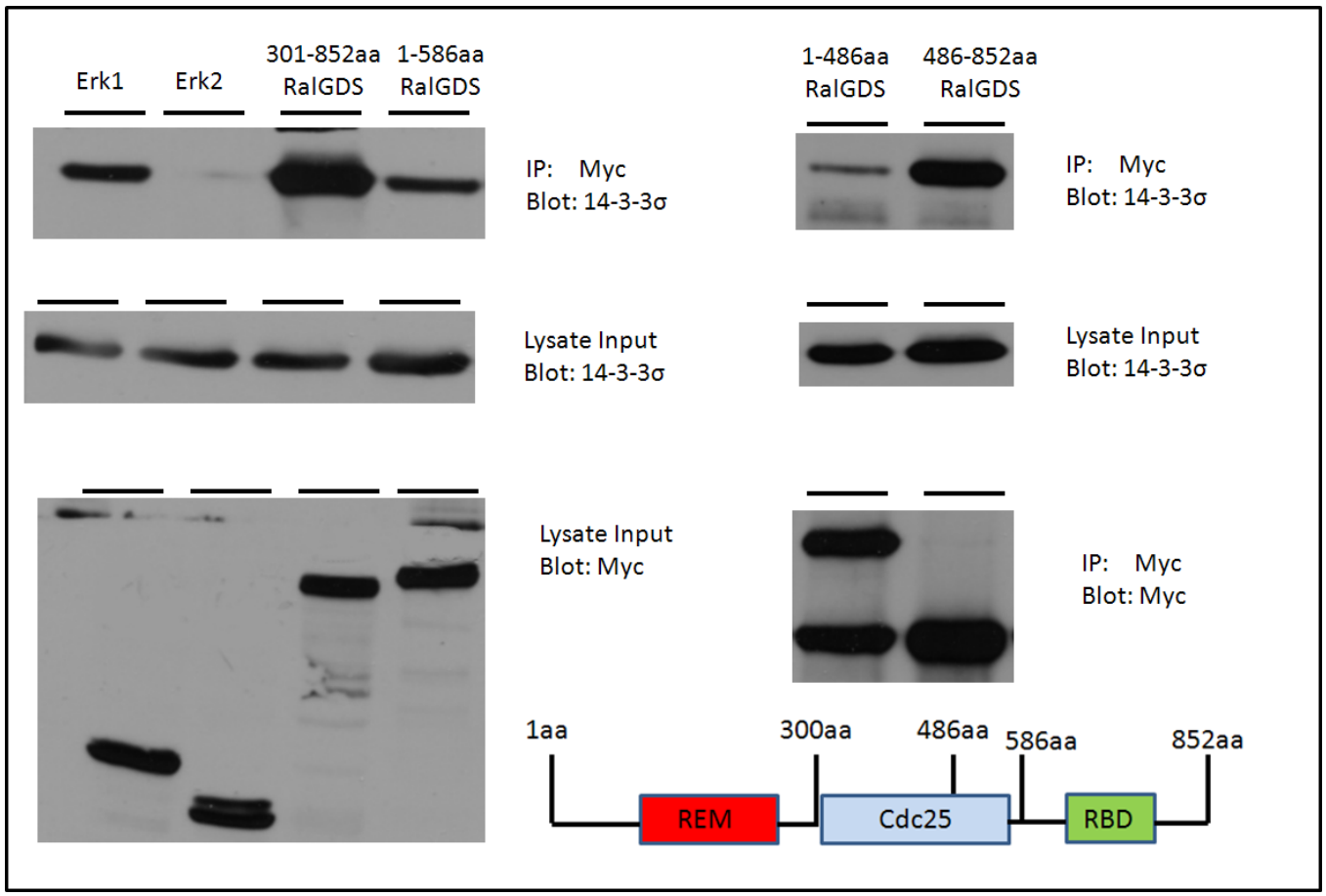

Fig 4.3 14-3-3σ associates to the C-terminus of RalGDS

Four Myc tagged RalGDS truncation constructs (1-586aa, 1-486aa, 301-852aa, and 486-852aa) were co-transfected with a 14-3-3σ construct in Cos-7 cells. Cells were lysed, immunoprecitated with Myc antibody, and immunoblotted with 14-3-3σ antibody. Truncation constructs 1-586aa and 1-486aa representing progressive C-terminal deletions of the Ras binding domain and Cdc25 domain showed diminished 14-3-3σ association. N-terminal deletion constructs 301-852aa and 486-852aa maintained robust binding to 14-3-3σ. Myc tagged Erk1 and Erk2 were initially included as negative controls but we found Erk1 but not Erk2 bound to 14-3-3σ.

4.2.3 14-3-3σ does not affect RalGDS exchange activity

To test if 14-3-3σ binding directly affects RalGDS exchange activity we expressed the two proteins alone or together in Cos-7 cells and measured changes in Ral activation. Results showed no difference in the amount of active Ral in cell expressing RalGDS with or without 14-3-3σ (Fig 4.4). These findings suggest that 14-3-3σ does not have a direct effect on RalGDS exchange activity. Although it remains possible that 14-3-3σ binding may have an effect on RalGDS ability to bind Ras or its localization in the cell. Either possibility could affect Ral activation by regulating the ability of RalGDS to localize to its substrate Ral proteins.

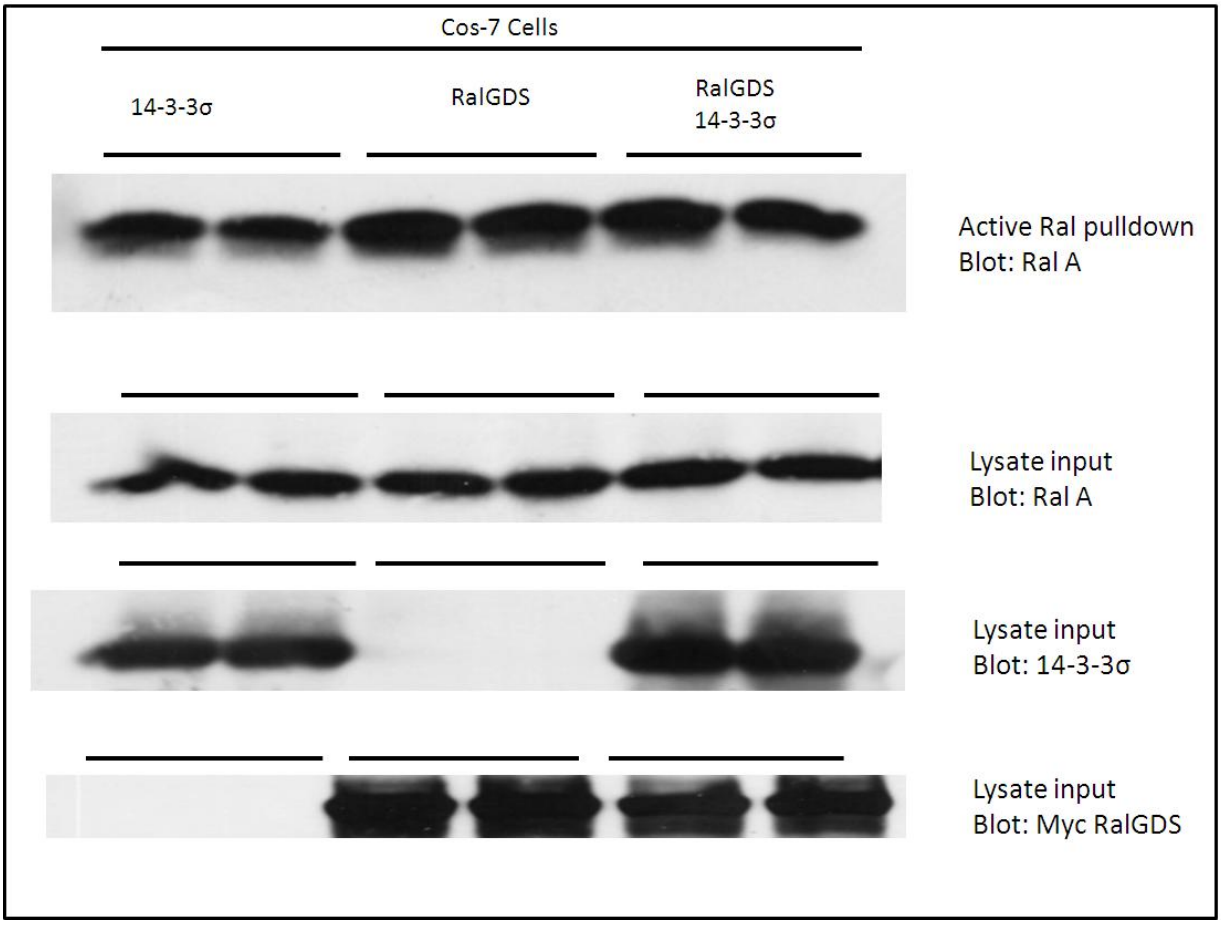

Fig 4.4 14-3-3σ does not affect RalGDS exchange activity

Cos-7 cells were transfected with expression constructs for 14-3-3σ, RalGDS, or both proteins. Cells were maintained in serum supplemented growth media and RalGTP levels were assayed via Western blot using a Ral pulldown assay. Cells expressing RalGDS with or without 14-3-3σ showed no difference in the amount of active Ral. Lower panels show exogenous expression of the transfected 14-3-3σ or RalGDS.

4.2.4 14-3-3σ localization at cell: cell contacts in MCF10A cells is disrupted by H_20_2 stimulation.

To date, 14-3-3σ has been primarily described as a cytosolic protein which functions in part through sequestering binding partners in the cytoplasm [120]. A recent study found 14-3-3σ to also be important in maintaining cell polarity in MDCK and MCF10A cells. Investigators found that when 14-3-3σ was knocked down, MCF10A cells lost the ability to grow as hollow mamospheres [121]. When we immunostained MCF10A cells for 14-3-3σ we found it to be primarily located at cell: cell interfaces. When MCF10A cells were exposed to oxidative stress through H_20_2 treatment, 14-3-3σ moved from the plasma membrane into the cytoplasm (Fig 4.5). RalGDS is primarily located in the cytoplasm unless recruited to the plasma membrane through binding to activated Ras. It is possible the binding of 14-3-3σ to RalGDS we observe in our studies occurs as a result of the co-localization of the two proteins in the cytoplasm after H_20_2 treatment.

The biological consequence of 14-3-3σ binding to RalGDS in MCF10A cells is not known. It is possible that 14-3-3σ in the cytoplasm acts to sequester RalGDS preventing its translocation to the plasma membrane to activate Ral. It is also possible that 14-3-3σ at the plasma membrane is able to block RalGDS association to Ras or drive RalGDS off active Ras as it moves to the cytoplasm in the case of H_20_2 stimulation. Either scenario would result in down regulating Ral activation.

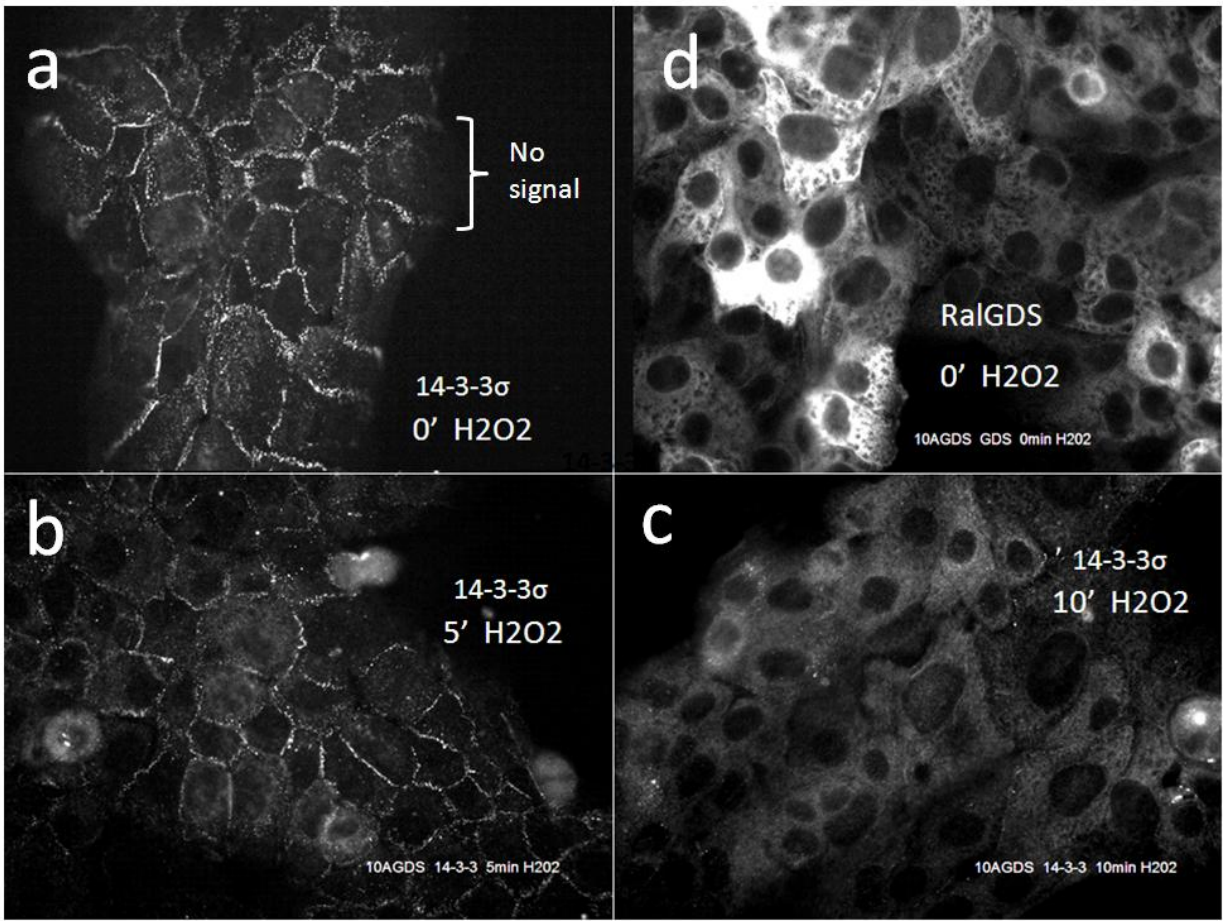

Fig 4.5 14-3-3σ localization at cell: cell contacts is disrupted by H202 stimulation.

MCF10A cells expressing Myc RalGDS were maintained in serum supplemented growth media and subjected to 0, 5, and 10 min incubation with 1mM H202. Cells were then fixed in acetone and immunostained with 14-3-3σ antibody (panel a,b, and c) or Myc antibody (d). Untreated cells have (a) 14-3-3σ primarily located at cell cell contacts and (d) Myc RalGDS located in the cytoplasm. 5 min H202 treatment (b) caused a slight decrease in 14-3-3σ staining at cell cell contacts, but by 10 min of treatment (c) a majority of 14-3-3σ staining was in the cytoplasm and no longer at the plasma membrane.

4.2.5 Oxidative stress modulates Ral activation

We next assayed the effects of H_20_2 treatment on Ral activation. Studies have shown reactive oxygen species (ROS) generated from H_20_2 treatment can activate various signal cascades downstream of growth factor receptors. Examples of activated signaling mediators include Ras, JNK/p38, MAPKs, PI-3K, and NF-κB [118, 119]. H202 has also been shown to stimulate Ral activation in NIH3T3 cells [122]. When we tested the effects of H202 treatment on MCF10A cells we found that Ral activation varied based on growth conditions. MCF10A cells maintained in serum supplemented media showed a decrease in active Ral in response to H_20_2 treatment (Fig 4.5). MCF10A cells that were serum starved overnight (similar to conditions of H_20_2 mediated Ral activation in NIH3T3 studies) showed Ral activation in response to H_20_2 treatment (Fig 4.6). Association of RalGDS to 14-3-3σ described earlier in this chapter was performed under both growth and starved conditions. No difference in binding was noted between the two conditions.

Under growth conditions we expect a basal level of Ras activation and subsequently RalGDS localization to the plasma membrane (Fig 4.8). H_20_2 treatment under these conditions show a decrease in Ral activation at the same time 14-3-3σ is moving from the membrane to the cytoplasm. These results are consistent with the hypothesis that 14-3-3σ may be driving RalGDS from the membrane thereby decreasing Ral activation. H_20_2 mediated activation of Akt is still occurring under growth conditions (Fig 4.5) so it is expected that Ras activation is occurring as well.

It is likely that under starvation conditions there is little active Ras to recruit RalGDS to the plasma membrane (Fig 4.7). When stimulated by H_20_2 Ras activation would lead to

recruitment of RalGDS to the membrane and subsequent activation of Ral. Under starvation conditions, 14-3-3σ in MCF10A cells is still located at the plasma membrane (data not shown). During the timing of H202 activation (5-10 minutes post stimulus), 14-3-3σ has moved to the cytoplasm. Because both RalGDS and 14-3-3σ are moving in opposite directions, at this time it is difficult to guess the role of 14-3-3σ in Ral activation. If 14-3-3σ acts by driving RalGDS from the plasma membrane it is possible that it is no longer present there by the time a population of Ras is activated to recruit RalGDS. If 14-3-3σ acts to sequester RalGDS in the cytoplasm, it is possible that some RalGDS has already been recruited to Ras before a significant amount of 14-3-3σ reaches the cytoplasm.

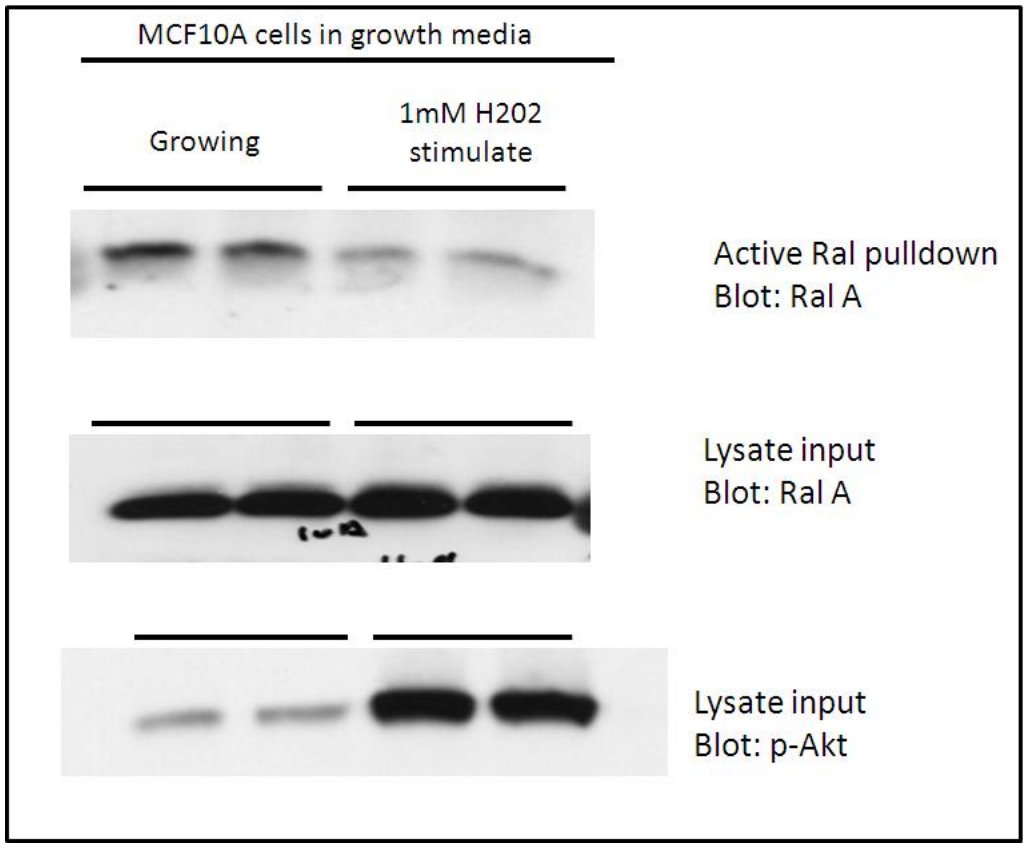

Fig 4.6 H_20_2 stimulation decreases active Ral in growing MCF10A cells

MCF10A cells maintained in serum supplemented growth media were treated for 10min with 1 mM H_20_2. RalGTP levels were assayed via Western blot using a Ral pulldown assay. Treated cells showed a decrease in active RalA in comparison to untreated cells. p-Akt was also assayed to confirm efficacy of H_20_2 stumulation.

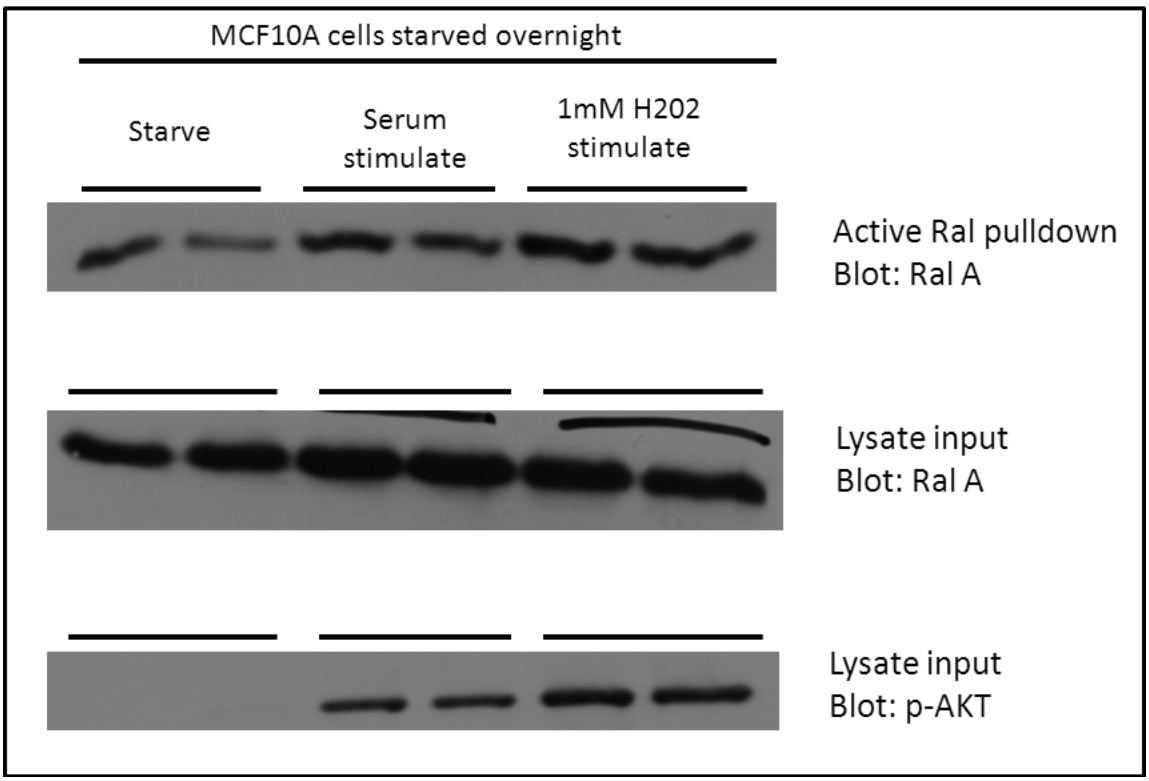

Fig 4.7 H_20_2 stimulation increases active Ral in starved MCF10A cells

MCF10A cells serum starved overnight were treated for 10min with 1 mM H_20_2 or serum supplemented media. RalGTP levels were assayed via Western blot using a Ral pulldown assay. Both H_20_2 and serum stimulated cells showed an increase in active RalA in comparison to untreated cells. p-Akt was also assayed to confirm efficacy of H_20_2 stimulation.

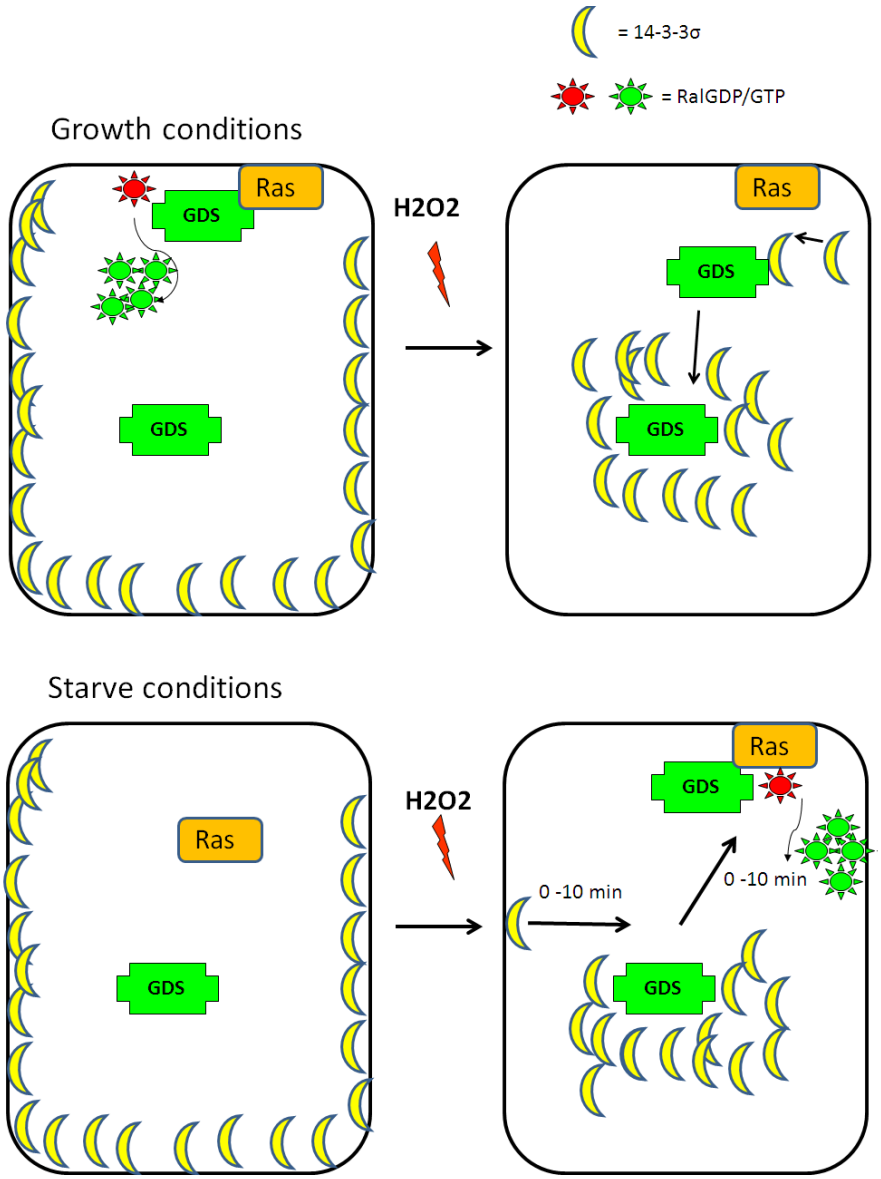

Fig 4.8 Proposed location of RalGDS in MCF10A cells in serum starved and growing conditions

4.2.6 14-3-3σ knock down does not affect H_20_2 mediated Ral inactivation.

To test if 14-3-3σ is mediating H_20_2 induced decrease in Ral activation under growing conditions we began by knocking down 14-3-3σ in MCF10A cells. A stable cell line was created using lentivirus delivered shRNA targeting 14-3-3σ. A pooled population of selected cells showed a 65% knockdown in 14-3-3σ (Fig 4.9). These cells were then subject to H_20_2 stimulation under growth conditions and assayed for Ral activation. The results of this assay showed no change in the ability of H_20_2 to decrease active Ral in growing cells (Fig 4.10). At this time these results would not support our hypothesis that H_20_2 suppresses RalGDS activity by 14-3-3σ driving RalGDS from the plasma membrane. However it is possible that 65% knockdown of 14-3-3σ may not be sufficient to prevent sequestering of RalGDS. Testing of other shRNA constructs are planned in order to generate a cell line with a higher percentage of knockdown. Once established these cells will be challenged with H_20_2 and assayed for effects on Ral activation.

It is possible that the effects of 14-3-3σ binding to RalGDS do not affect the protein in the manner we have proposed. 14-3-3σ has been shown to perform a variety of functions, a short list include protein localization, inhibition, scaffolding, and degradation [120, 123]. Any of these could be the purpose of the 14-3-3σ RalGDS interaction. Further study exploring these avenues will need to be planned if a more substantial knock down of 14-3-3σ does not alter H_20_2 mediated Ral activation in growing cells.

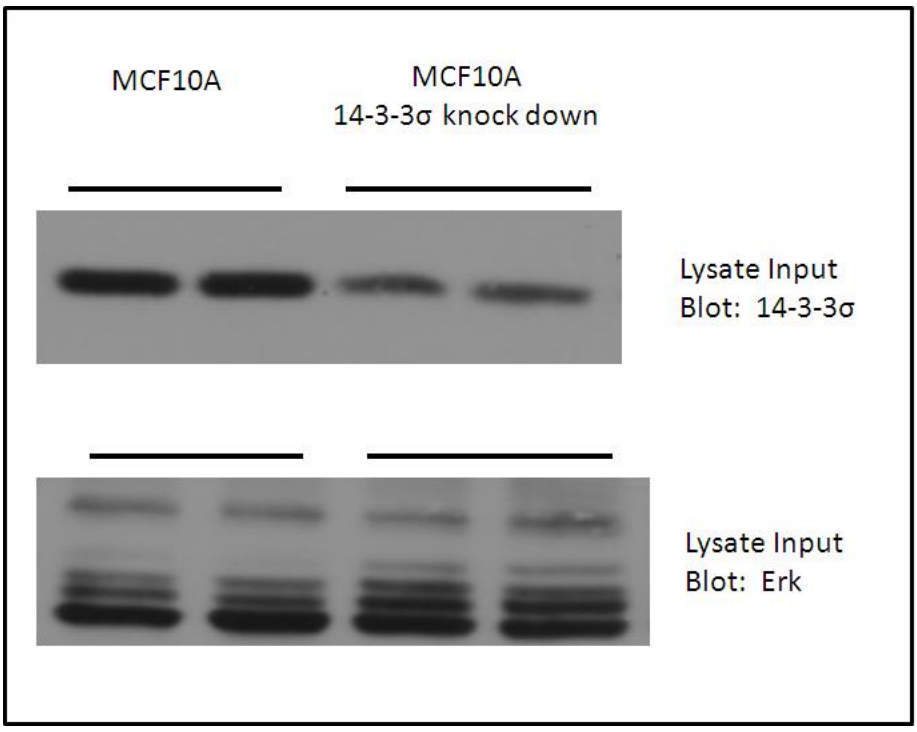

Fig 4.9 14-3-3σ knockdown in MCF10A cells

MCF10A cells were infected with lentivirus delivered shRNA targeting 14-3-3σ. Infected cells were drug selected and pooled to yield a cell line with ~65% 14-3-3σ knockdown. Knockdown and wildtype cells were Western blotted for 14-3-3σ to assess knockdown and total Erk was blotted as a loading control.

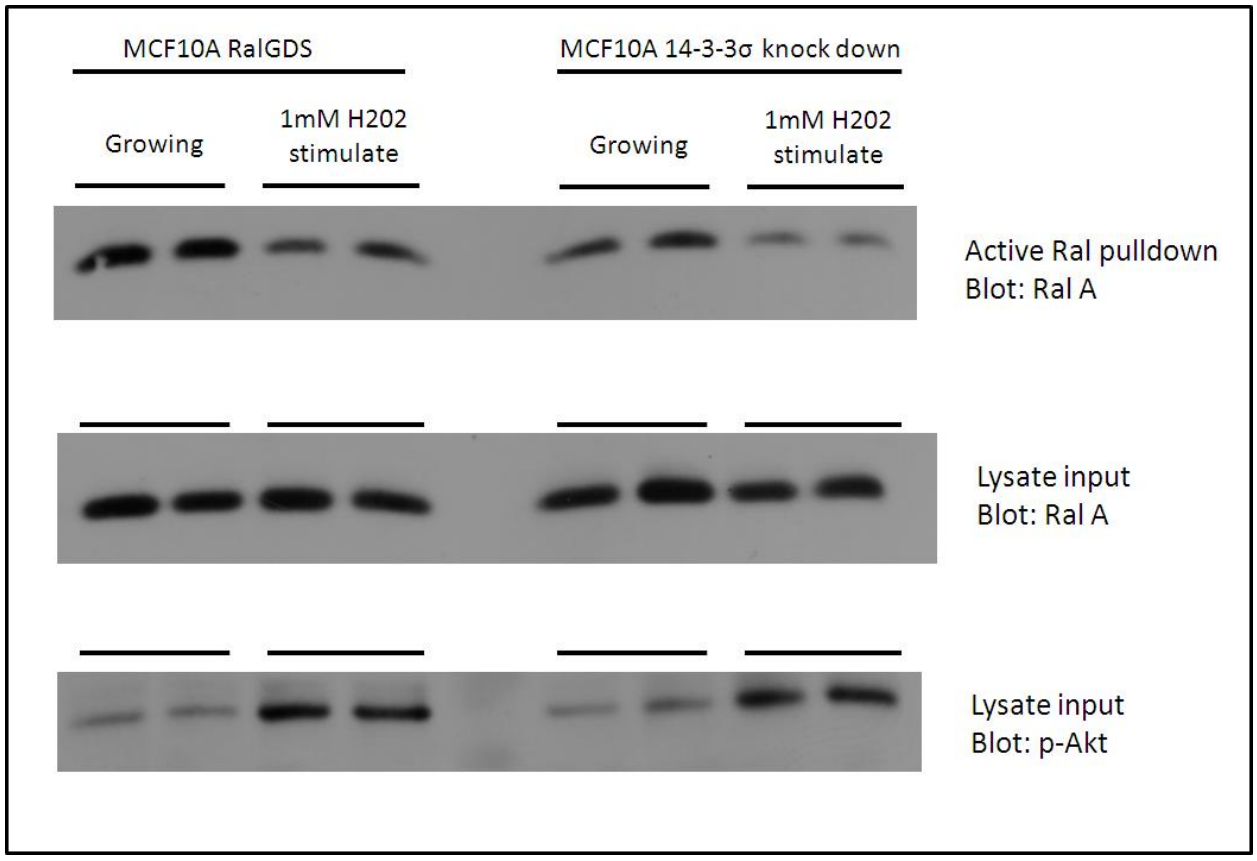

Fig 4.10 14-3-3σ knock down does not affect H_20_2 mediated Ral activation.

MCF10A RalGDS and 14-3-3σ knock down cells maintained in serum supplemented growth media were treated for 10min with 1 mM H_20_2. RalGTP levels were assayed via Western blot using a Ral pulldown assay. Both RalGDS and knockdown cells treated with H_20_2 showed a decrease in active RalA in comparison to untreated cells. p-Akt was also assayed to confirm efficacy of H_20_2 stumulation.

4.3 Discussion

The 14-3-3 family of proteins (β, γ, ε, σ, ζ, τ and η) are involved in a variety of cellular functions. Forming hetero/homo dimers they bind to phospho serine or threonine at consensus motifs R[SFYW]XpSXP or RX[SYFWTQAD]Xp(S/T)X[PLM] [111] . 14-3-3σ is unique from its family members in that it only forms homo dimers and the sequence at its C-terminus is highly divergent from other family members. 14-3-3σ has a role in a diverse range of cellular activities in both normal and cancer cells. Initially characterized as a breast epithelial cell marker, 14-3-3σ was by DNA damage through p53 [114]. Further work found that 14-3-3σ could bind p53 negative regulators Mdm2 and COP1 and block their activity through cytoplasmic sequestration. 14-3-3σ can also bind Cdc2/cyclin B1keeping it in the cytoplasm to prevent cell cycle progression. These observations lead investigators to analyze 14-3-3σ gene methylation and mRNA expression in a variety of cancer types. These studies found increased gene methylation and decreased mRNA expression in some breast, lung, and gastric cancers [115, 124, 125]. This suggested that down regulation of the protein may be important in cancer biology. Further studies highlight a more complex picture when it was found that actual protein levels of 14-3-3σ remained high in various cancers, despite low mRNA expression or high gene methylation [126, 127]. In some pancreatic cancers high expression was even correlated with poor patient prognosis [128].

Recent studies have found 14-3-3σ can be secreted to promote stromal fibroblasts to produce MMPs [129]. Within the cell, the protein has also been found to promote resistance of cancer cells to DNA damaging drugs. This resistance may be mediated by binding to Bax and Bad proteins to block apoptosis. In roles that may have anti-cancer effects, 14-3-3σ has also been found to inhibit Akt activity, promote cell polarity, and decrease the metastatic potential of some breast cancer cells [112].

H_20_2 is normally produced in cells by NADPH oxidase in response to growth factor signaling and is the precursor for superoxide which has been shown to inhibit protein phosphatases and activate a variety of signaling pathways [118, 119]. In our studies we found RalGDS bound 14-3-3σ after H_20_2 stimulation in MCF10A cells. Our initial hypothesis was that binding might directly affect the exchange activity of RalGDS. We found this not to be true when 14-3-3σ did not inhibit RalGDS in co-transfection experiments. This lead us to hypothesize binding may regulate localization of the protein. We found H_20_2 stimulation caused relocalization of 14-3-3σ from the plasma membrane to the cytoplasm. This movement suggested a few possible roles for RalGDS binding. In one scenario once localized to the cytoplasm, 14-3-3σ could prevent the exchange factor from moving to its target Ral proteins at the plasma membrane. In another possibility 14-3-3σ could bind active RalGDS at the membrane and drive it away from its substrate as it moves to the cytoplasm. Both have 14-3-3σ acting to decrease Ral activation through sequestering RalGDS.

Testing the effect of H_20_2 stimulation on Ral activation gave opposite results depending on the growth conditions of the cell. In starved MCF10A cells H_20_2 caused an increase in active Ral. Cells maintained in growth media showed a decrease in active Ral in response to H_20_2 treatment. It is unclear what role, if any 14-3-3σ may have in either condition. Regardless of growth conditions we found 14-3-3σ was localized to the plasma membrane and then moved to the cytoplasm after approximately 10 minutes of H_20_2 stimulation. The down regulation of Ral in growing cells fit our model of 14-3-3σ driving RalGDS from the membrane, but knocking down 14-3-3σ had no effect on H_20_2 mediated Ral decrease. It is possible that the degree of knockdown was insufficient to prevent RalGDS relocalization. More experiments are required to delineate how 14-3-3σ may regulate RalGDS.

Previous work in our lab found RalGDS mediated growth factor activation of Akt in MCF10A cells through the scaffolding protein Jip1 [35]. Other investigators have found 14-3-3σ binds and regulates Akt under conditions of drug mediated DNA damage. It is possible that 14-3-3σ may act in a manner similar to Jip1 to scaffold RalGDS to Akt. Studies have also found 14-3-3σ to act in preventing the degradation of its binding partner COP1. It is possible that the binding of 14-3-3σ to RalGDS serves a similar function.

Both RalGDS and 14-3-3σ have been shown to have important roles in cell signaling. It is provocative that the two proteins directly interact with each other. The elucidation of the biological consequence of this interaction will likely offer interesting new insights into their combined functions both in normal and cancer biology.

4.4 Future experiments

Mapping experiments suggested that 14-3-3σ may be binding to RalGDS in its Ras binding domain. To test if this association interferes with Ras binding we will assay the ability of GST-KRas12V to bind RalGDS from Cos-7 cells co-transfected with 14-3-3σ. If 14-3-3σ interferes with binding we would expect to see no protein associated with RalGDS bound to Ras12V beads. If 14-3-3σ does block Ras binding, this would suggest the nature of the association would be to inhibit Ral activation. Follow up experiments would test if 14-3-3σ overexpression could decrease Ral activation in the setting of constitutively activated Ras.

As mentioned in the previous section 14-3-3σ may be scaffolding Akt to RalGDS. To test this theory Akt and RalGDS will be expressed in Cos-7 cells with or without 14-3-3σ co-transfection. RalGDS will be immunoprecipitated and assayed for changes in complex

formation with Akt in the presence of 14-3-3σ. If the addition of 14-3-3σ increases Akt association to RalGDS, this would suggest that the complex formation may have a role in Akt activation.

Conclusion

In this thesis we described three major findings that expand the knowledge and understanding of the Ral exchange factor RalGDS. Our studies began with the investigation of structural interactions within the protein. Using a yeast two hybrid screen, we found early indications that RalGDS may use intra-molecular regulatory interactions found in other exchange factors such as Sos1 and EPAC2. Without the benefit of crystal structure data, it is sometimes difficult to glean the relevance of protein interactions and modifications we find in nature. Our characterization of RalGDS through binding assays allowed us to form an understanding about the nature of the N-terminal REM domain's role in regulating the catalytic activity of the Cdc25 domain. We found that the REM domain associates to the catalytic helical hairpin in the Cdc25 domain through a specific hydrophobic interaction. This association, much like one found in Sos1, gives a mechanistic understanding of how the full length protein is regulated and opens the door for later insights into the relevance of modifications found nature.

With our structural understanding, we proposed a mechanism for previous observations where the full deletion of the REM domain is shown to increase the catalytic activity of the protein. When a cancer associated mutation in the REM domain of RalGEF Rgl1 was identified, we proposed that it could affect the association between the REM and catalytic domain. Our studies found this to be true even though the catalytic activity of the protein was not changed. Later, we observed a c-Met mediated phosphorylation of a site in the REM domain of RalGDS. Again we were able to reference this site to information gained from our binding assays. Based on the charge consequence of phosphorylation, we believe the modification will negatively

impact the hydrophobic association between the REM domain and catalytic hairpin leading to decreased RalGDS exchange activity.

Our second major study identified and characterized the c-Met mediated phosphorylation of RalGDS at four sites throughout the protein. This discovery marks the first confirmed and characterized tyrosine phosphorylation of a RalGEF. One of the identified sites (Y752) mapped to the Ras binding domain of RalGDS. Phosphorylation at this site uncoupled RalGDS from Ras, suggesting the purpose of c-Met mediated phosphorylation was to down regulate the Ral pathway. To the best of our knowledge this is also the first functional evidence of Ras effector uncoupling through direct phosphorylation of a Ras association domain. The Y752 site is conserved among all other known RBD containing RalGEFs and is not found in most other Ras effectors. This suggests a means of selective uncoupling the entire Ral effector pathway at Ras activation complexes, while not influencing other types of Ras effectors.

Phosphorylation at the three other identified sites mapped to regions of RalGDS that suggest they would have a negative effect on catalytic activity and Ras binding. When we assayed c-Met addicted cancer cell lines, Ral activation was indeed uncoupled from c-Met activation. Suppression of Ral activation in the c-Met addicted setting is a provocative finding, considering Ral activation has been shown to be an essential element in many oncogenic processes. Multiple attempts at stably expressing RalGDS or active Ral A in two c-Met addicted gastric cancer lines were unsuccessful, as compared to the stable expression of GFP. These findings suggest that Ral activation may have a detrimental effect on c-Met addicted cells.

If activation of the Ral pathway were detrimental to c-Met addicted cancers, it would be an intersting caveat to the theory of oncogene addiction. Current models suggest the

upregulation of specific pro-survival and anti-apoptotic signaling pathways are the most important factors in addiction. In a more nuanced description of the theory, cancers may be equally dependent on the down regulation of specific pathways as it is on the upregulation of other pathways. With this in mind a combination approach where some pathways are reactivated while others are inhibited may prove highly effective in combating some cancers. Ral activation may be one such candidate for a combination with c-Met inhibitors in the treatment of c-Met addicted cancers.

In our final study we identified the novel interaction between 14-3-3σ and RalGDS in response to H_20_2 stimulation. The 14-3-3 family of proteins regulate a variety of cellular processes. 14-3-3σ in particular is unique from its family members in sequence and preference in acting as a homodimer. Its regulation of numerous pathways important to cancer biology have made 14-3-3σ the topic of intense study. Our initial observations suggest 14-3-3σ is binding RalGDS in or near its Ras binding domain. Relocalization of 14-3-3σ from the plasma membrane to cytoplasm in response to H_20_2 in MCF10A cells suggest that it's binding to RalGDS may act to sequester it from its upstream activators or downstream substrates. Both RalGDS and 14-3-3σ have been shown to have important roles in cell signaling. It is thought-provoking that the two proteins have now been shown to directly interact with each other. The elucidation of the biological consequence of this interaction will likely offer interesting new insights into their combined functions both in normal and cancer biology.

Taken together we have expanded the body of knowledge on RalGDS in terms of structure, function, and regulation. Our studies have identified novel interactions and modes of regulation that have opened the door for many future studies. The greater understanding of

RalGEFs and their roles in the cancer will hopefully aid in the eventual development of new treatments for disease.

Materials and Methods

M.1 Cell lines

Cos-7 cells were cultured in DMEM media with 10% Fe-bovine calf serum supplemented with glutamine and antibiotics.

MCF10A immortalized breast epithelium cells were cultured in DMEM/F12 supplemented with 10% FBS, 8 μg/ml insulin, 29 ng/ml epidermal growth factor and 500 ng/ml hydrocortisone.

MKN45 and KatoII/III cell were cultured in RPMI-1640 medium (Gibco, Grand Island, NY) with 10% fetal bovine serum (Gibco), 100 μg/mL penicillin, and 100 μg/mL streptomycin, 180mg/l glucose.

293FT Lentivirus producing cells were isolated from a fast-growing clone of human embryonic kidney 293 cells (293F) and subsequently transfected with SV40 Large T Antigen. 293FT cells were obtained from Invitrogen and were maintained in sodium pyruvate free DMEM supplemented with 10% FBS, 1% Pen-Strep, 1% non-essential amino acids, 1% L-glutamine, and 500 μg/ml G418.

M.2 Transfection and Infection

Cos-7 and 293FT cells were transfected with DNA using Lipofectamine 2000 transfection reagent.

Lentivirus Transduction Protocol

Day 1: Plate continuous cells dishes **Day 2:** Rinse cells, and add back normal growth medium. Add 1000x polybrene. Try 3 different MOI; stock virus is 10e6 particles/200 ul = 5000 particles/ul. **Day 3** Rinse off virus and replace with normal growth cell media. 48 hours post transduction cells can undergo analysis and/or proceed with puromycin selection. There may be too few cells for qPCR or WB analysis at this step. **Day 4** Add selection (1ug/mL Puromycin), and split cells into either 10 cm or T75 flasks containing selection.

M.3 Immunoprecipitations, pulldowns, and Western blotting

Cells were washed two times with ice-cold phosphate-buffered saline and then lysed on ice for 5 min with 1 ml lysis buffer (100 mM Tris, pH 7.5, 1% NP-40, 130 mM NaCl, 1 mM Na3VO4, 5 mM MgCl2, 1 mM EDTA, and 10 mM NaF) supplemented with Complete, EDTA-free protease inhibitor . Whole cell lysates were cleared by centrifugation for 10 min at 13,000 × g. Lysates were incubated with 4 μg of the indicated antibody for 2 h at 4°C, and then protein A/G beads were added for 2 h at 4°C to precipitate the antibody. Beads were washed three times in lysis buffer and then resuspended in 2X SDS sample buffer. The reaction products were washed with lysis buffer, and the immune complexes were resolved by sodium dodecyl sulfate–polyacrylamide gel electrophoresis (SDS-PAGE). The proteins were electrotransferred to membranes.

For immunoblotting, membranes were blocked in TBS with 3% skim milk or 2% BSA, and incubated overnight with primary antibodies: 14–3–3σ (1:2000; Santa Cruz Biotechnologies); myc (1:2000), p-Tyr (1:2000), p-Akt473(1:2000), p-Met(1:2000) . Later, membranes were washed and then treated by 1 h of incubation with HRP-conjugated mouse, rabbit, and goat secondary antibodies (1:10000 in TBS). Blots were developed with enhanced chemiluminescence

M.4 Phospho-specific Antibody

RalGDS Y752 rabbit antibody was developed by Proteintech Group Inc. Order #MU000826. Two rabbits were tested for antibody production. Only Rabbit #2 produced functional and specific antibody. Antibody is used at 1:75 dilution for western blot. Serum, matrix and peptide are in store age for 2nd antibody purification if needed.

M.5 RalGDS Expression Vectors

Full-length and truncation constructs of wild-type mouse RalGDS were isolated from a mouse cDNA library by PCR with primers to incorporate flanking restriction sites: ie. RalGDS, BamHI and EcoRI. These fragments were then subcloned or recombined into the pBabe puro retrovirus expression vector, pEntr4 no ccDB (686-1) (Addgene), pLenti CMV Puro DEST (w118-1) (Addgene), pJ3M (Myc tag vector), or pJ3H (HA tag vector which adds an in-frame sequence to encode an N-terminal hemagglutinin (HA) epitope tag sequence).

M.6 Mutagenesis

To generate point mutations in RalGDS, site-specific mutagenesis by PCR was used. Primers overlapping the mutation site were created as described in the QuikChange manual (Stratagene), incubated with a supercoiled vector wild-type RalGDS, and subjected to PCR to amplify the entire vector. Template DNA was destroyed by incubation with 1 µl *Dpn*I enzyme for 1 hour, and the entire reaction was run on a 0.8% TAE-agarose gel for 30 minutes. The non-supercoiled product was extracted using the QiaQuick Gel Extraction Kit (Qiagen). The purified product contained nicked DNA from the PCR and was ligated with T4 DNA Ligase (New England Biolabs) before transformation into DH5α *E. coli*.

Transfection-grade DNA was prepared with the HiSpeed Plasmid Midi Kit

M.7 Immunofluorescence (IF)

Cells grown on cover slips washed 2X PBS and were fixed for 2-3 min at -20deg in cold acetone (methanol was not as effective for 14-3-3 membrane staining), (OPTIONAL may hurt 14-3-3 stiaing) permeabilized for 10 min in 0.5% Triton X-100 in PBS, followed by washes of in PBS. Blocking was performed with IF buffer (PBS, 0.1% BSA, 0.2% Triton X-100, 0.05% Tween-20) plus 2% BSA for 1 h followed by overnight of incubation at 4 deg in primary antibodies diluted in IF buffer. Cells were washed in IF buffer and incubated in a humidified chamber with the appropriate Alexa-fluor-conjugated secondary antibodies (1:1000; Molecular Probes) diluted in IF buffer for 1hr min at 4 deg. The nuclei were counterstained with 4′,6-diamidino-2-phenylindole (DAPI) (Jackson Laboratories) for 5 min.

M.8 Fluorescent imaging

Fluorescence of cells on coverslips was observed on a Nikon Eclipse 80i microscope with 2X, 4X, 10X, 20X and 40X objectives. Black-and-white fluorescent micrographs were acquired with a SPOT-RT Slider camera (Diagnostic Instruments) and post-processed (colorized) with SPOT Advanced software version 4.6. Within a single experiment, all fluorescent exposures were specified manually and were the same for all samples. Any post-processing steps, such as background correction, were performed linearly and to all applicable images in that experiment. Fluorescence of live cells (e.g. GFP) was observed on a Nikon Eclipse TE2000-S inverted microscope with 10X and 20X objectives. Black-and-white fluorescent micrographs were acquired with a SPOT RT KE camera (Diagnostic Instruments) and post-processed (colorized)

with SPOT Advanced software version 4.5. Within a single experiment, all fluorescent exposures were specified manually and were the same for all samples. Any post-processing steps, such as background correction, were performed linearly and to all applicable images in that experiment.

M.9 RalA Activation Assay

Cells were lysed in cold lysis buffer consisting of, 50 mM Tris, pH 7.5, 1% NP-40, 130 mM NaCl, 1 mM Na3VO4, 10% glycerol, 5 mM $MgCl_2$, and protease inhibitor mix, After removal of insoluble materials, the lysate was incubated with glutathione beads that were conjugated to glutathione S-transferase-fused Sec5-RBD protein and incubated on an orbiter for 30 min at 4 deg to allow GTP-bound RalA to bind to the beads. Beads were washed with lysis buffer, and bound proteins and lysate were subjected to immunoblot analysis. All procedures were carried out at 4 °C unless otherwise specified.

********Important in this assay is to not saturate Sec5 beads with Ral when doing the assay, multiple lysate concentrations should be tested with physiological controls (starved/stimulated) to gauge the dynamic range of activation. GTP gamma S is not a good positive control as it gives a non physiological activation. Assays for RalB will require more lysate as the concentration of this protein is usually much lower in cells. ********

M.10 GST- fusion protein expression and purification

For Sec5 RBD and RalGDS RBD consructs

1. Inoculate one colony of each bacterial strain expressing each construct (GST alone, GST fusion proteins) into individual 5-ml aliquots of LB broth containing appropriate antibiotic selection. Grow overnight at 37°C with shaking.

2. Inoculate 1 liter of LB containing the antibiotic selection with the 5-ml overnight culture from Step 1.

3. Grow the cultures at 37°C with shaking to an OD_{600} of 0.5-1.0 (this should take 3-6 hr).

4. Induce expression of the protein by adding IPTG to a final concentration of 0.1 mM.

5. Incubate the cultures for an additional 3-4 hours at 37°C with shaking.

6. Centrifuge the bacterial culture at 3500*g* for 20 minutes at 4°C.

7. Discard the supernatant. Wash bacteria 3X in 50mM Tris pH 7.4, 150mM NaCl, (2mM MgCl2 of Sec5, 2mM EDTA for GST RBD). Pellets can be frozen at this point

8. Resuspend the pellet in lysis buffer.

9. Sonicate the bacterial suspension on ice, in short 10-second bursts alternated with 10 seconds of resting on ice. Three cycles of sonication are usually sufficient.

10. Centrifuge the lysate at 12,000*g* for 15 minutes at 4°C.

11. Transfer the supernatant to a fresh tube.

12. Add slurry of glutathione-Sepharose beads in PBS lysis buffer.

13. Incubate for overnight minutes at 4°C, rotating the tube end over end to ensure mixing.

14. Centrifuge the samples at 750*g* for 1 minute at 4°C to pellet the beads. Remove the supernatant.

15. Wash the beads in ice-cold lysis buffer with protease inhibitors.

16. Centrifuge the samples at 750*g* for 1 minute at 4°C to pellet the beads. Remove the supernatant.

17. Wash the beads in ice-cold lysis buffer with protease inhibitors.

18. Centrifuge the samples again at 750*g* for 1 minute at 4°C to pellet the beads. Remove the supernatant. Samples may be tested for quality of the prep.

The fusion protein can be stored on the beads at 4°C at this stage. This is appropriate if the protein is to be labeled or used in a GST pull-down experiment. Add 10% glycerol and azide for storage. The method of storage must be determined empirically. For example, a protein to be used subsequently in an enzymatic assay may require specific handling as compared to a protein to be used in a protein-protein interaction study. Most proteins can be stored for short periods of time at 4°C. In general, freeze-thaw cycles should be avoided. After prolonged storage, it is important to run an SDS-polyacrylamide gel to check the integrity of the protein

19. Run the samples from the eluates containing protein on an SDS-polyacrylamide gel and stain with Coomassie blue dye

The GST moiety is 26 kDa; therefore, add 26 kDa to determine the predicted molecular weight (MW) of the fusion protein.

M.11 MS/MS analysis

Myc-RalGDS expressing MCF10A cells treated with 1mM H_20_2 for 10 min were used in 14-3-3 identification studies. Myc-RalGDS , c-Met co-transfected Cos-7 cells were used in identification of p-Tyr RalGDS sites. Cells were lysed and subject to myc immunoprecipitation as described above. Samples were prepared from SDS-PAGE gels, stained with Collidial blue (Invitrogen), and excised for mass spectrometry sequencing and phosphorylated tyrosine site mapping. Gel pieces were digested overnight with modified trypsin (Promega) at 37°C (pH 8.3). Peptides were extracted and analyzed by data-dependent microcapillary liquid chromatography–MS/MS (LC-MS/MS) with both linear ion trap (Thermo Scientific) and a high-resolution/mass accuracy hybrid linear ion trap LTQ Orbitrap XL mass spectrometer (Thermo Scientific) coupled to an EASY-nLC nanoflow HPLC (Proxeon Biosystems). MS/MS spectra acquired through collision-induced dissociation (CID) were searched against the reversed and concatenated Swiss-Prot protein database (version 55.8, UniProt) with a fixed modification for carbamidomethylation (+57.0293) and variable modifications for oxidation (+15.9949) and ubiquitination (+114.10, GG tag) using the Sequest algorithm in Proteomics Browser Software (Thermo Scientific). Peptides RalGDS and 14-3-3 were identified by database scoring, and peptides modified by tyrosine were validated manually to be sure that all ions were consistent with the modified residue; additional validation was performed with GraphMod software in Proteomics Browser Software (Thermo Scientific). The peptide false discovery rate (FDR) was less than 1.5% based on reversed database hits.

M.12 Crystal structure analysis

RalGDS RBD:Ras, Sos1, and RasGRF1 structure pdb files were downloaded from http://www.rcsb.org. Structures were analyzed using Swiss PDB-viewer and images highlighting domains of interaction were processed using PDB-viewer tools.

M.13 Sequence alignment and analysis

RalGEFs and RBD containing proteins were identified using the Protein Knowledge database http://www.uniprot.org/. Protein sequences were aligned and pair-wise homology calculated using the ClustalW2 general purpose multiple sequence alignment program for DNA or proteins. http://www.ebi.ac.uk/Tools/msa/clustalw2/

***Mouse RalGDS sequence used for alignment was Accession ID Q03385 ***

M.14 Inhibitors

Pervanadate : 0.1 mM sodium orthovanadate (NaVo3) and 3 mM H_20_2 were incubated at room temperature in cell culture media for 15 min. Catalase is then added to the media for 10 minutes to inactive H_20_2, over time Pervanadate will also become inactivated. Pervanadate treatement from 5-15min is effective in inhibiting tyrosine phosphatases.

PP2: Src family kinase inhibitor (Calbiochem) was used at 10nM for 4hr in gastric cancer cell lines.

Met Kinase inhibitor II : Met inhibitor (Calbiochem) was used at 2nM for 1-4hr in gastric cancer sell lines.

Bibliography

1. Pratilas, C. A. & Solit, D. B. Targeting the mitogen-activated protein kinase pathway: physiological feedback and drug response. *Clin. Cancer Res.* **16**, 3329-3334 (2010).

2. Ye, X. & Carew, T. J. Small G protein signaling in neuronal plasticity and memory formation: the specific role of ras family proteins. *Neuron* **68**, 340-361 (2010).

3. Vigil, D., Cherfils, J., Rossman, K. L. & Der, C. J. Ras superfamily GEFs and GAPs: validated and tractable targets for cancer therapy? *Nat. Rev. Cancer.* **10**, 842-857 (2010).

4. Wennerberg, K., Rossman, K. L. & Der, C. J. The Ras superfamily at a glance. *J. Cell. Sci.* **118**, 843-846 (2005).

5. Boguski, M. S. & McCormick, F. Proteins regulating Ras and its relatives. *Nature* **366**, 643-654 (1993).

6. McCormick, F. Ras-related proteins in signal transduction and growth control. *Mol. Reprod. Dev.* **42**, 500-506 (1995).

7. Seabra, M. C. & Wasmeier, C. Controlling the location and activation of Rab GTPases. *Curr. Opin. Cell Biol.* **16**, 451-457 (2004).

8. Channing J. Der. in ***RAS family GTPases*** (Springer press, 2006).

9. Colicelli, J. Human RAS superfamily proteins and related GTPases. *Sci. STKE* **2004**, RE13 (2004).

10. Cox, A. D. & Der, C. J. Ras family signaling: therapeutic targeting. *Cancer. Biol. Ther.* **1**, 599-606 (2002).

11. Skolnik, E. Y. *et al*. The function of GRB2 in linking the insulin receptor to Ras signaling pathways. *Science* **260**, 1953-1955 (1993).

12. Margolis, B. & Skolnik, E. Y. Activation of Ras by receptor tyrosine kinases. *J. Am. Soc. Nephrol.* **5**, 1288-1299 (1994).

13. Bos, J. L. Ras Oncogenes in Human Cancer: a Review. *Cancer Res.* **49**, 4682-4689 (1989).

14. da Cunha Santos, G., Saieg, M. A., Geddie, W. & Leighl, N. EGFR gene status in cytological samples of nonsmall cell lung carcinoma: Controversies and opportunities. *Cancer. Cytopathol.* **119**, 80-91 (2011).

15. Gutierrez, C. & Schiff, R. HER2: biology, detection, and clinical implications. *Arch. Pathol. Lab. Med.* **135**, 55-62 (2011).

16. Bertotti, A. *et al*. Only a subset of Met-activated pathways are required to sustain oncogene addiction. *Sci. Signal.* **2**, er11 (2009).

17. Blum, R., Cox, A. D. & Kloog, Y. Inhibitors of chronically active ras: potential for treatment of human malignancies. *Recent. Pat. Anticancer Drug Discov.* **3**, 31-47 (2008).

18. Montagut, C. & Settleman, J. Targeting the RAF-MEK-ERK pathway in cancer therapy. *Cancer Lett.* **283**, 125-134 (2009).

19. Rotblat, B., Ehrlich, M., Haklai, R. & Kloog, Y. The Ras inhibitor farnesylthiosalicylic acid (Salirasib) disrupts the spatiotemporal localization of active Ras: a potential treatment for cancer. *Methods Enzymol.* **439**, 467-489 (2008).

20. Repasky, G. A., Chenette, E. J. & Der, C. J. Renewing the conspiracy theory debate: does Raf function alone to mediate Ras oncogenesis? *Trends Cell Biol.* **14**, 639-647 (2004).

21. Kyriakis, J. M. *et al*. Raf-1 activates MAP kinase-kinase. *Nature* **358**, 417-421 (1992).

22. Weber, C. K. *et al*. Mitogenic signaling of Ras is regulated by differential interaction with Raf isozymes. *Oncogene* **19**, 169-176 (2000).

23. Cleary, J. M. & Shapiro, G. I. Development of phosphoinositide-3 kinase pathway inhibitors for advanced cancer. *Curr. Oncol. Rep.* **12**, 87-94 (2010).

24. Manning, B. D. & Cantley, L. C. AKT/PKB signaling: navigating downstream. *Cell* **129**, 1261-1274 (2007).

25. Hernandez-Munoz, I., Malumbres, M., Leonardi, P. & Pellicer, A. The Rgr oncogene (homologous to RalGDS) induces transformation and gene expression by activating Ras, Ral and Rho mediated pathways. *Oncogene* **19**, 2745-2757 (2000).

26. Rebhun, J. F., Chen, H. & Quilliam, L. A. Identification and characterization of a new family of guanine nucleotide exchange factors for the ras-related GTPase Ral. *J. Biol. Chem.* **275**, 13406-13410 (2000).

27. Freedman, T. S. *et al*. A Ras-induced conformational switch in the Ras activator Son of sevenless. *Proc. Natl. Acad. Sci. U. S. A.* **103**, 16692-16697 (2006).

28. Ferro, E. & Trabalzini, L. RalGDS family members couple Ras to Ral signalling and that's not all. *Cell. Signal.* **22**, 1804-1810 (2010).

29. Bhattacharya, M. *et al*. Beta-arrestins regulate a Ral-GDS Ral effector pathway that mediates cytoskeletal reorganization. *Nat. Cell Biol.* **4**, 547-555 (2002).

30. Ryu, C. H. *et al*. The merlin tumor suppressor interacts with Ral guanine nucleotide dissociation stimulator and inhibits its activity. *Oncogene* **24**, 5355-5364 (2005).

31. Tian, X., Rusanescu, G., Hou, W., Schaffhausen, B. & Feig, L. A. PDK1 mediates growth factor-induced Ral-GEF activation by a kinase-independent mechanism. *EMBO J.* **21**, 1327-1338 (2002).

32. Rusanescu, G., Gotoh, T., Tian, X. & Feig, L. A. Regulation of Ras signaling specificity by protein kinase C. *Mol. Cell. Biol.* **21**, 2650-2658 (2001).

33. Rondaij, M. G. *et al*. Guanine exchange factor RalGDS mediates exocytosis of Weibel-Palade bodies from endothelial cells. *Blood* **112**, 56-63 (2008).

34. Ferro, E. *et al*. G-protein binding features and regulation of the RalGDS family member, RGL2. *Biochem. J.* **415**, 145-154 (2008).

35. Hao, Y., Wong, R. & Feig, L. A. RalGDS couples growth factor signaling to Akt activation. *Mol. Cell. Biol.* **28**, 2851-2859 (2008).

36. Gonzalez-Garcia, A. *et al*. RalGDS is required for tumor formation in a model of skin carcinogenesis. *Cancer. Cell.* **7**, 219-226 (2005).

37. de Ruiter, N. D., Wolthuis, R. M., van Dam, H., Burgering, B. M. & Bos, J. L. Ras-dependent regulation of c-Jun phosphorylation is mediated by the Ral guanine nucleotide exchange factor-Ral pathway. *Mol. Cell. Biol.* **20**, 8480-8488 (2000).

38. Yin, J. *et al*. Activation of the RalGEF/Ral pathway promotes prostate cancer metastasis to bone. *Mol. Cell. Biol.* **27**, 7538-7550 (2007).

39. Sjoblom, T. *et al*. The consensus coding sequences of human breast and colorectal cancers. *Science* **314**, 268-274 (2006).

40. Vigil, D. *et al*. Aberrant overexpression of the Rgl2 Ral small GTPase-specific guanine nucleotide exchange factor promotes pancreatic cancer growth through Ral-dependent and Ral-independent mechanisms. *J. Biol. Chem.* **285**, 34729-34740 (2010).

41. Shirakawa, R. *et al*. Tuberous sclerosis tumor suppressor complex-like complexes act as GTPase-activating proteins for Ral GTPases. *J. Biol. Chem.* **284**, 21580-21588 (2009).

42. Chen, X. W. *et al*. A Ral GAP complex links PI 3-kinase/Akt signaling to RalA activation in insulin action. *Mol. Biol. Cell* **22**, 141-152 (2011).

43. Emkey, R., Freedman, S. & Feig, L. A. Characterization of a GTPase-activating protein for the Ras-related Ral protein. *J. Biol. Chem.* **266**, 9703-9706 (1991).

44. Falsetti, S. C. *et al*. Geranylgeranyltransferase I inhibitors target RalB to inhibit anchorage-dependent growth and induce apoptosis and RalA to inhibit anchorage-independent growth. *Mol. Cell. Biol.* **27**, 8003-8014 (2007).

45. Shipitsin, M. & Feig, L. A. RalA but not RalB enhances polarized delivery of membrane proteins to the basolateral surface of epithelial cells. *Mol. Cell. Biol.* **24**, 5746-5756 (2004).

46. Cascone, I. *et al*. Distinct roles of RalA and RalB in the progression of cytokinesis are supported by distinct RalGEFs. *EMBO J.* **27**, 2375-2387 (2008).

47. Lalli, G. & Hall, A. Ral GTPases regulate neurite branching through GAP-43 and the exocyst complex. *J. Cell Biol.* **171**, 857-869 (2005).

48. Corrotte, M. *et al*. Ral isoforms are implicated in Fc gamma R-mediated phagocytosis: activation of phospholipase D by RalA. *J. Immunol.* **185**, 2942-2950 (2010).

49. Bodemann, B. O. *et al*. RalB and the exocyst mediate the cellular starvation response by direct activation of autophagosome assembly. *Cell* **144**, 253-267 (2011).

50. Rosse, C. *et al*. RalB mobilizes the exocyst to drive cell migration. *Mol. Cell. Biol.* **26**, 727-734 (2006).

51. Lim, K. H. *et al*. Activation of RalA is critical for Ras-induced tumorigenesis of human cells. *Cancer. Cell.* **7**, 533-545 (2005).

52. Lim, K. H. *et al*. Activation of RalA is critical for Ras-induced tumorigenesis of human cells. *Cancer. Cell.* **7**, 533-545 (2005).

53. Chien, Y. & White, M. A. RAL GTPases are linchpin modulators of human tumour-cell proliferation and survival. *EMBO Rep.* **4**, 800-806 (2003).

54. Chien, Y. *et al*. RalB GTPase-mediated activation of the IkappaB family kinase TBK1 couples innate immune signaling to tumor cell survival. *Cell* **127**, 157-170 (2006).

55. Lim, K. H. *et al*. Divergent roles for RalA and RalB in malignant growth of human pancreatic carcinoma cells. *Curr. Biol.* **16**, 2385-2394 (2006).

56. Sowalsky, A. G., Alt-Holland, A., Shamis, Y., Garlick, J. A. & Feig, L. A. RalA suppresses early stages of Ras-induced squamous cell carcinoma progression. *Oncogene* **29**, 45-55 (2010).

57. Sowalsky, A. G., Alt-Holland, A., Shamis, Y., Garlick, J. A. & Feig, L. A. RalA function in dermal fibroblasts is required for the progression of squamous cell carcinoma of the skin. *Cancer Res.* **71**, 758-767 (2011).

58. Yamaguchi, A., Urano, T., Goi, T. & Feig, L. A. An Eps homology (EH) domain protein that binds to the Ral-GTPase target, RalBP1. *J. Biol. Chem.* **272**, 31230-31234 (1997).

59. Cantor, S. B., Urano, T. & Feig, L. A. Identification and characterization of Ral-binding protein 1, a potential downstream target of Ral GTPases. *Mol. Cell. Biol.* **15**, 4578-4584 (1995).

60. Boissel, L. *et al*. Recruitment of Cdc42 through the GAP domain of RLIP participates in remodeling of the actin cytoskeleton and is involved in Xenopus gastrulation. *Dev. Biol.* **312**, 331-343 (2007).

61. Yamaguchi, A., Urano, T., Goi, T. & Feig, L. A. An Eps homology (EH) domain protein that binds to the Ral-GTPase target, RalBP1. *J. Biol. Chem.* **272**, 31230-31234 (1997).

62. Cullis, D. N., Philip, B., Baleja, J. D. & Feig, L. A. Rab11-FIP2, an adaptor protein connecting cellular components involved in internalization and recycling of epidermal growth factor receptors. *J. Biol. Chem.* **277**, 49158-49166 (2002).

63. Panner, A. *et al*. mTOR-independent translational control of the extrinsic cell death pathway by RalA. *Mol. Cell. Biol.* **26**, 7345-7357 (2006).

64. Moskalenko, S. *et al*. The exocyst is a Ral effector complex. *Nat. Cell Biol.* **4**, 66-72 (2002).

65. Shipitsin, M. & Feig, L. A. RalA but not RalB enhances polarized delivery of membrane proteins to the basolateral surface of epithelial cells. *Mol. Cell. Biol.* **24**, 5746-5756 (2004).

66. Rosse, C. *et al*. RalB mobilizes the exocyst to drive cell migration. *Mol. Cell. Biol.* **26**, 727-734 (2006).

67. Frankel, P. *et al*. RalA interacts with ZONAB in a cell density-dependent manner and regulates its transcriptional activity. *EMBO J.* **24**, 54-62 (2005).

68. Balda, M. S. & Matter, K. The tight junction protein ZO-1 and an interacting transcription factor regulate ErbB-2 expression. *EMBO J.* **19**, 2024-2033 (2000).

69. Georgiadis, A. *et al*. The tight junction associated signalling proteins ZO-1 and ZONAB regulate retinal pigment epithelium homeostasis in mice. *PLoS One* **5**, e15730 (2010).

70. D'Souza-Schorey, C., Li, G., Colombo, M. I. & Stahl, P. D. A regulatory role for ARF6 in receptor-mediated endocytosis. *Science* **267**, 1175-1178 (1995).

71. Peng, X. & Frohman, M. A. Mammalian Phospholipase D Physiological and Pathological Roles. *Acta Physiol. (Oxf)* (2011).

72. Saito, M. *et al*. Expression of phospholipase D2 in human colorectal carcinoma. *Oncol. Rep.* **18**, 1329-1334 (2007).

73. Zheng, Y. *et al*. Phospholipase D couples survival and migration signals in stress response of human cancer cells. *J. Biol. Chem.* **281**, 15862-15868 (2006).

74. Trusolino, L., Bertotti, A. & Comoglio, P. M. MET signalling: principles and functions in development, organ regeneration and cancer. *Nat. Rev. Mol. Cell Biol.* **11**, 834-848 (2010).

75. Pennacchietti, S. *et al*. Hypoxia promotes invasive growth by transcriptional activation of the met protooncogene. *Cancer. Cell.* **3**, 347-361 (2003).

76. Cepero, V. *et al*. MET and KRAS gene amplification mediates acquired resistance to MET tyrosine kinase inhibitors. *Cancer Res.* **70**, 7580-7590 (2010).

77. Dua, R., Zhang, J., Parry, G. & Penuel, E. Detection of hepatocyte growth factor (HGF) ligand-c-MET receptor activation in formalin-fixed paraffin embedded specimens by a novel proximity assay. *PLoS One* **6**, e15932 (2011).

78. Qi, J. *et al*. Multiple mutations and bypass mechanisms can contribute to development of acquired resistance to MET inhibitors. *Cancer Res.* **71**, 1081-1091 (2011).

79. Hruban, R. H. *et al*. K-ras oncogene activation in adenocarcinoma of the human pancreas. A study of 82 carcinomas using a combination of mutant-enriched polymerase chain reaction analysis and allele-specific oligonucleotide hybridization. *Am. J. Pathol.* **143**, 545-554 (1993).

80. Salhab, N., Jones, D. J., Bos, J. L., Kinsella, A. & Schofield, P. F. Detection of ras gene alterations and ras proteins in colorectal cancer. *Dis. Colon Rectum* **32**, 659-664 (1989).

81. van der Schroeff, J. G., Evers, L. M., Boot, A. J. & Bos, J. L. Ras oncogene mutations in basal cell carcinomas and squamous cell carcinomas of human skin. *J. Invest. Dermatol.* **94**, 423-425 (1990).

82. Agrawal, A. G. & Somani, R. R. Farnesyltransferase inhibitor as anticancer agent. *Mini Rev. Med. Chem.* **9**, 638-652 (2009).

83. Caponigro, F. Farnesyl transferase inhibitors: a major breakthrough in anticancer therapy? Naples, 12 April 2002. *Anticancer Drugs* **13**, 891-897 (2002).

84. Gureasko, J. *et al*. Role of the histone domain in the autoinhibition and activation of the Ras activator Son of Sevenless. *Proc. Natl. Acad. Sci. U. S. A.* **107**, 3430-3435 (2010).

85. Yadav, K. K. & Bar-Sagi, D. Allosteric gating of Son of sevenless activity by the histone domain. *Proc. Natl. Acad. Sci. U. S. A.* **107**, 3436-3440 (2010).

86. Freedman, T. S. *et al*. A Ras-induced conformational switch in the Ras activator Son of sevenless. *Proc. Natl. Acad. Sci. U. S. A.* **103**, 16692-16697 (2006).

87. Schiller, M. R. *et al*. Regulation of RhoGEF activity by intramolecular and intermolecular SH3 domain interactions. *J. Biol. Chem.* **281**, 18774-18786 (2006).

88. Yohe, M. E. *et al*. Auto-inhibition of the Dbl family protein Tim by an N-terminal helical motif. *J. Biol. Chem.* **282**, 13813-13823 (2007).

89. Tian, X., Rusanescu, G., Hou, W., Schaffhausen, B. & Feig, L. A. PDK1 mediates growth factor-induced Ral-GEF activation by a kinase-independent mechanism. *EMBO J.* **21**, 1327-1338 (2002).

90. Huang, L., Hofer, F., Martin, G. S. & Kim, S. H. Structural basis for the interaction of Ras with RalGDS. *Nat. Struct. Biol.* **5**, 422-426 (1998).

91. Livingstone, C. D. & Barton, G. J. Protein sequence alignments: a strategy for the hierarchical analysis of residue conservation. *Comput. Appl. Biosci.* **9**, 745-756 (1993).

92. Hall, B. E., Yang, S. S., Boriack-Sjodin, P. A., Kuriyan, J. & Bar-Sagi, D. Structure-based mutagenesis reveals distinct functions for Ras switch 1 and switch 2 in Sos-catalyzed guanine nucleotide exchange. *J. Biol. Chem.* **276**, 27629-27637 (2001).

93. Callahan, R. & Hurvitz, S. Human epidermal growth factor receptor-2-positive breast cancer: Current management of early, advanced, and recurrent disease. *Curr. Opin. Obstet. Gynecol.* **23**, 37-43 (2011).

94. Traish, A. M. & Morgentaler, A. Epidermal growth factor receptor expression escapes androgen regulation in prostate cancer: a potential molecular switch for tumour growth. *Br. J. Cancer* **101**, 1949-1956 (2009).

95. Metzger-Filho, O., Moulin, C. & Awada, A. Molecular targeted therapy in prevalent tumors: learning from the past and future perspectives. *Curr. Clin. Pharmacol.* **5**, 166-177 (2010).

96. Yan, W., Zhang, W. & Jiang, T. Oncogene addiction in gliomas: Implications for molecular targeted therapy. *J. Exp. Clin. Cancer Res.* **30**, 58 (2011).

97. Rehman, F. L., Lord, C. J. & Ashworth, A. Synthetic lethal approaches to breast cancer therapy. *Nat. Rev. Clin. Oncol.* **7**, 718-724 (2010).

98. Torti, D. *et al*. A preclinical algorithm of soluble surrogate biomarkers that correlates with therapeutic inhibition of the MET oncogene in gastric tumors. *Int. J. Cancer* (2011).

99. Bertotti, A. *et al*. Inhibition of Src impairs the growth of met-addicted gastric tumors. *Clin. Cancer Res.* **16**, 3933-3943 (2010).

100. Freedman, T. S. *et al*. A Ras-induced conformational switch in the Ras activator Son of sevenless. *Proc. Natl. Acad. Sci. U. S. A.* **103**, 16692-16697 (2006).

101. Peng, W. *et al*. Structural study of the Cdc25 domain from Ral-specific guanine-nucleotide exchange factor RalGPS1a. *Protein Cell.* **2**, 308-319 (2011).

102. Suzuki, J., Yamazaki, Y., Li, G., Kaziro, Y. & Koide, H. Involvement of Ras and Ral in chemotactic migration of skeletal myoblasts. *Mol. Cell. Biol.* **20**, 4658-4665 (2000).

103. Ma, P. C. & Salgia, R. Novel targets for therapeutic agents in small cell lung cancer. *J. Natl. Compr. Canc Netw.* **2**, 165-172 (2004).

104. Eder, J. P., Vande Woude, G. F., Boerner, S. A. & LoRusso, P. M. Novel therapeutic inhibitors of the c-Met signaling pathway in cancer. *Clin. Cancer Res.* **15**, 2207-2214 (2009).

105. Mizumoto, Y. *et al*. Creation of tumorigenic human endometrial epithelial cells with intact chromosomes by introducing defined genetic elements. *Oncogene* **25**, 5673-5682 (2006).

106. Lim, K. H. *et al*. Activation of RalA is critical for Ras-induced tumorigenesis of human cells. *Cancer. Cell.* **7**, 533-545 (2005).

107. Tian, X., Rusanescu, G., Hou, W., Schaffhausen, B. & Feig, L. A. PDK1 mediates growth factor-induced Ral-GEF activation by a kinase-independent mechanism. *EMBO J.* **21**, 1327-1338 (2002).

108. Sowalsky, A. G., Alt-Holland, A., Shamis, Y., Garlick, J. A. & Feig, L. A. RalA function in dermal fibroblasts is required for the progression of squamous cell carcinoma of the skin. *Cancer Res.* **71**, 758-767 (2011).

109. Chen, X. W. *et al*. A Ral GAP complex links PI 3-kinase/Akt signaling to RalA activation in insulin action. *Mol. Biol. Cell* **22**, 141-152 (2011).

110. Shirakawa, R. *et al*. Tuberous sclerosis tumor suppressor complex-like complexes act as GTPase-activating proteins for Ral GTPases. *J. Biol. Chem.* **284**, 21580-21588 (2009).

111. Li, Z., Liu, J. Y. & Zhang, J. T. 14-3-3sigma, the Double-Edged Sword of Human Cancers. *Am. J. Transl. Res.* **1**, 326-340 (2009).

112. Yang, H. *et al*. DNA damage-induced protein 14-3-3 sigma inhibits protein kinase B/Akt activation and suppresses Akt-activated cancer. *Cancer Res.* **66**, 3096-3105 (2006).

113. Su, C. H. *et al*. Nuclear export regulation of COP1 by 14-3-3sigma in response to DNA damage. *Mol. Cancer.* **9**, 243 (2010).

114. Hermeking, H. *et al*. 14-3-3 sigma is a p53-regulated inhibitor of G2/M progression. *Mol. Cell* **1**, 3-11 (1997).

115. Umbricht, C. B. *et al*. Hypermethylation of 14-3-3 sigma (stratifin) is an early event in breast cancer. *Oncogene* **20**, 3348-3353 (2001).

116. Liu, Y., Liu, H., Han, B. & Zhang, J. T. Identification of 14-3-3sigma as a contributor to drug resistance in human breast cancer cells using functional proteomic analysis. *Cancer Res.* **66**, 3248-3255 (2006).

117. Su, Y. W. *et al*. 14-3-3sigma regulates B-cell homeostasis through stabilization of FOXO1. *Proc. Natl. Acad. Sci. U. S. A.* **108**, 1555-1560 (2011).

118. Finkel, T. Oxidant signals and oxidative stress. *Curr. Opin. Cell Biol.* **15**, 247-254 (2003).

119. Reiland, J. *et al*. Pervanadate activation of intracellular kinases leads to tyrosine phosphorylation and shedding of syndecan-1. *Biochem. J.* **319 (Pt 1)**, 39-47 (1996).

120. Morrison, D. K. The 14-3-3 proteins: integrators of diverse signaling cues that impact cell fate and cancer development. *Trends Cell Biol.* **19**, 16-23 (2009).

121. Ling, C., Zuo, D., Xue, B., Muthuswamy, S. & Muller, W. J. A novel role for 14-3-3sigma in regulating epithelial cell polarity. *Genes Dev.* **24**, 947-956 (2010).

122. Essers, M. A. *et al*. FOXO transcription factor activation by oxidative stress mediated by the small GTPase Ral and JNK. *EMBO J.* **23**, 4802-4812 (2004).

123. Muslin, A. J. & Xing, H. 14-3-3 Proteins: Regulation of Subcellular Localization by Molecular Interference. *Cell. Signal.* **12**, 703-709 (2000).

124. Aprelikova, O., Pace, A. J., Fang, B., Koller, B. H. & Liu, E. T. BRCA1 is a selective co-activator of 14-3-3 sigma gene transcription in mouse embryonic stem cells. *J. Biol. Chem.* **276**, 25647-25650 (2001).

125. Simpson, P. T. *et al*. Distribution and significance of 14-3-3sigma, a novel myoepithelial marker, in normal, benign, and malignant breast tissue. *J. Pathol.* **202**, 274-285 (2004).

126. Yang, H., Zhao, R. & Lee, M. H. 14-3-3sigma, a P53 Regulator, Suppresses Tumor Growth of Nasopharyngeal Carcinoma. *Mol. Cancer. Ther.* **5**, 253-260 (2006).

127. Han, B., Xie, H., Chen, Q. & Zhang, J. T. Sensitizing hormone-refractory prostate cancer cells to drug treatment by targeting 14-3-3sigma. *Mol. Cancer. Ther.* **5**, 903-912 (2006).

128. Logsdon, C. D. *et al*. Molecular profiling of pancreatic adenocarcinoma and chronic pancreatitis identifies multiple genes differentially regulated in pancreatic cancer. *Cancer Res.* **63**, 2649-2657 (2003).

129. Carr, M., Chavez-Munoz, C., Lai, A. & Ghahary, A. Dermal fibroblasts influence the expression profile of 14-3-3 proteins in human keratinocytes. *Mol. Cell. Biochem.* (2011).